

PHOSPHATE ORE PRE-REACTION WITH ACIDIC PROCESS WATER

A Thesis

Presented in Fulfillment of the Requirements for the

Degree of Master of Science

with a

Major in Chemical Engineering

in the

College of Graduate Studies

University of Idaho

by

Theodore Warner

Major Professor: Vivek Utgikar, Ph.D.

Committee Members: Haiyan Zhao, Ph.D., Maxine Dakins, Ph.D.

Department Administrator: Eric Aston, Ph.D.

August 2016

## AUTHORIZATION TO SUBMIT THESIS

This thesis of Theodore Warner, submitted for the degree of Master of Science with a Major in Chemical Engineering and titled “Phosphate Ore Pre-Reaction with Acidic Process Water,” has been reviewed in final form. Permission, as indicated by the signatures and dates below is now granted to submit final copies for the College of Graduate Studies for approval.

Major Professor: \_\_\_\_\_ Date: \_\_\_\_\_  
Vivek Utgikar, Ph.D.

Committee Members: \_\_\_\_\_ Date: \_\_\_\_\_  
Haiyan Zhao, Ph.D.

\_\_\_\_\_ Date: \_\_\_\_\_  
Maxine Dakins, Ph.D.

Department Administrator: \_\_\_\_\_ Date: \_\_\_\_\_  
Eric Aston, Ph.D.

## ABSTRACT

This study evaluated the use of phospho-gypsum pond water to pre-react phosphate ore associated with phosphoric acid production via the wet process. The objective was to improve phosphate recovery and aid in the management of pond water inventory. The non-catalytic heterogeneous solid-liquid reaction kinetics were examined associated with carbonate in the ore and the acidic phosphate, fluoride and sulfate present in pond water. Additionally, the sedimentation and dewatering characteristics of phosphate ore slurry were evaluated to determine the feasibility of recovering neutralized pond water and returning ore slurry back to an acceptable solids concentration ready for acidulation with sulfuric acid. The reaction kinetics between acidic process water and phosphate ore exhibited zero and first order reaction behavior and Arrhenius temperature dependence. Additionally a mixture of hydro-cyclones, gravity thickening and centrifugation proved to be feasible options for separating neutralized process water effluent and re-concentrating phosphate ore slurry.

## ACKNOWLEDGEMENTS

I would like to thank my direct supervisor, Trisha Arave, for her ongoing support and allowing me to conduct this research in conjunction with my day to day work activities; my major professor Vivek Utgikar for his guidance through the Chemical Engineering Master's Program; my committee members Haiyan Zhao and Maxine Dakins and most importantly my family and friends for their patience and support over the last few years.

## TABLE OF CONTENTS

AUTHORIZATION TO SUBMIT THESIS.....	ii
ABSTRACT .....	iii
ACKNOWLEDGEMENTS.....	iv
TABLE OF CONTENTS .....	v
LIST OF TABLES.....	vii
LIST OF FIGURES .....	viii
CHAPTER 1: INTRODUCTION.....	1
PHOSPHORIC ACID PRODUCTION VIA THE WET PROCESS .....	1
FLUORAPATITE & THE BENEFICIATION PROCESS .....	2
THE WET PROCESS.....	3
PHOSHPO-GYPSUM & BYPRODUCT HANDLING SYSTEMS .....	8
PAP WATER BALANCE & POND WATER.....	11
CHAPTER 2: HYPOTHESIS & OBJECTIVES .....	14
ORE PRE-REACTION PROCESS OVERVIEW .....	14
REACTION KINETICS .....	15
ORE SLURRY DEWATERING .....	19
CHAPTER 3: LITERATURE REVIEW .....	20
CARBONATE REMOVAL .....	20
POND WATER MANAGEMENT & TREATMENT .....	22
PHOSPHATE DEWATERING.....	23
LITERATURE REVIEW CONCLUSIONS .....	24
CHAPTER 4: MATERIALS & METHODS .....	25
BENCH SCALE BATCH TESTS .....	25
CONSTANT VOLUME BATCH REACTOR.....	25
HYDRO-CYCLONE TEST WORK .....	28
HYDRO-CYCLONE OVERFLOW SEDIMENTATION TEST WORK.....	30
PILOT TESTING .....	32
PROCESS EQUIPMENT .....	32
MISCELLANEOUS DEWATERING TEST WORK.....	34
ANALYTICAL TECHNIQUES.....	35
CHAPTER 5: REACTION KINETIC RESULTS & DISCUSSION .....	39

P <sub>2</sub> O <sub>5</sub> EVALUATION.....	39
EXPLANATION OF TIME DELAY & REACTION INTERMEDIATE SOLUBILITY .....	50
SO <sub>4</sub> EVALUATION .....	54
POND WATER EVALUATION .....	57
REACTOR DESIGN CONSIDERATION.....	62
CONCLUSIONS .....	62
CHAPTER 6: DEWATERING RESULTS & DISCUSSION.....	64
HYDRO-CYCLONE TEST WORK .....	64
HYDRO-CYCLONE OVERFLOW SEDIMENTATION TEST WORK.....	67
THICKENER FEED DILUTION.....	72
SETTLING SYSTEM DESIGN.....	74
CHAPTER 7: PILOT TESTING RESULTS & DISCUSSION .....	75
LAB PILOT .....	76
PLANT PILOT .....	79
MISCELLANEOUS DEWATERING .....	81
DEWATERING SCREENS .....	81
DECANTER CENTRIFUGE .....	83
CHAPTER 8: SUMMARY & CONCLUSIONS .....	85
SUMMARY.....	85
CONCLUSIONS & RECOMMENDATIONS FOR FUTURE WORK .....	86
REFERENCES .....	87

## LIST OF TABLES

Table 1 - Beneficiation Plant Product Ore Chemical Composition.....	3
Table 2 - Gypsum Process Water Chemical Composition.....	10
Table 3 - Bench Scale Test Parameters .....	26
Table 4 - Bench Scale Test Dosing Parameters .....	27
Table 5 - Lab Scale Hydro-Cyclone Test Matrix.....	29
Table 6 - Settling Test Matrix.....	31
Table 7 - Lab Scale Pilot Process Equipment List.....	33
Table 8 - Reaction Time Delay.....	41
Table 9 - Arrhenius Temperature Dependence for $P_2O_5$ w/Limestone & Phosphate Ore .....	49
Table 10 - Reaction Order, Solubility and Salts Formed.....	51
Table 11 - Predicted Liquid Phase Analysis for CSTR .....	62
Table 12 - Cyclone Overflow Slurry Characteristics.....	67
Table 13 - Settling Test Supernatant Water Quality .....	68
Table 14 - Final Bed Compaction and Weight % Solids .....	69
Table 15 - Settling Test Results with Feed Dilution & Polymer .....	74
Table 16 - Pilot Testing Nominal Design Capacities.....	75
Table 17 - Lab Pilot Feed/Product Analysis and Mass Balance .....	76
Table 18 - Continuous Lab Pilot Stream Analysis .....	77
Table 19 - Lab Pilot Cyclone Achieved Solids & Recoveries.....	78
Table 20 - Lab Pilot Thickener Achieved Solids & Recoveries .....	78
Table 21 - Plant Pilot Process Feed and Product Water Analysis .....	80
Table 22 - Continuous Plant Pilot Stream Analysis.....	80
Table 23 - Plant Pilot Cyclone Achieved Solids and Recoveries .....	81
Table 24 - Plant Pilot Thickener Achieved Solids and Recoveries .....	81
Table 25 - Reactor Product Dewatering Screen Performance .....	83
Table 26 - Hydro-Cyclone Underflow Dewatering Screen Performance .....	83
Table 27 - Decanter Centrifuge Dewatering Test Results .....	84

## LIST OF FIGURES

Figure 1 - General Phosphoric Acid Production & Downstream Process Flow Sheet .....	5
Figure 2 - Di-Hydrate Wet Process Phosphoric Acid Production .....	6
Figure 3 - Phosphoric Acid Plant Cooling Water System Process Schematic.....	7
Figure 4 - Phosphoric Acid Plant Gypsum Handling System Process Schematic.....	9
Figure 5 - Phosphoric Acid Plant Water Balance Process Schematic .....	12
Figure 6 - Fluid-Particle Reaction Models for Unchanging Particle Size from Levenspiels Chemical Reaction Engineering 3rd Edition.....	16
Figure 7 - Constant Volume Batch Reactor.....	25
Figure 8 - Batch Reactor Schematic .....	25
Figure 9 - Lab Centrifuge .....	27
Figure 10 - Sample after Centrifuging.....	27
Figure 11 - Vacuum Filtration Apparatus.....	28
Figure 12 - Vacuum Filtration of Supernatant.....	28
Figure 13 - Hydro-Cyclone Batch Test Equipment Schematic .....	30
Figure 14 - Sedimentation Cylinders .....	31
Figure 15 - Continuous Pilot Process Schematic.....	32
Figure 16 - Lab Pilot Process Equipment .....	33
Figure 17 - Plant Pilot Process Equipment .....	34
Figure 18 - Dewatering Screen .....	35
Figure 19 - Decanter Centrifuge .....	35
Figure 20 - Rigaku XRF Analyzer.....	36
Figure 21 - Perkin Elmer ICP .....	36
Figure 22 - Thermo/Orion Fluoride Probe.....	36
Figure 23 - Malvern Particle Size Analyzer .....	37
Figure 24 - Lamotte NTU Meter.....	37
Figure 25 - 75°F P <sub>2</sub> O <sub>5</sub> Solution Concentration & pH vs. Time w/Limestone.....	40
Figure 26 - 100°F P <sub>2</sub> O <sub>5</sub> Solution Concentration & pH vs. Time w/Limestone.....	40
Figure 27 - 120°F P <sub>2</sub> O <sub>5</sub> Solution Concentration & pH vs. Time w/Limestone.....	41
Figure 28 – 75°F P <sub>2</sub> O <sub>5</sub> Solution Concentration vs. Time w/Ore (2 <sup>nd</sup> Proton).....	42
Figure 29 - 100°F P <sub>2</sub> O <sub>5</sub> Solution Concentration vs. Time w/Ore (2 <sup>nd</sup> Proton).....	42
Figure 30 - 120°F P <sub>2</sub> O <sub>5</sub> Solution Concentration vs. Time w/Ore (2 <sup>nd</sup> Proton).....	43
Figure 31 - 75°F P <sub>2</sub> O <sub>5</sub> Solution Concentration vs. Time w/Ore (1 <sup>st</sup> Proton) .....	43

Figure 32 - 100°F P <sub>2</sub> O <sub>5</sub> Solution Concentration vs. Time w/Ore (1 <sup>st</sup> Proton) .....	44
Figure 33 - 120°F P <sub>2</sub> O <sub>5</sub> Solution Concentration vs. Time w/Ore (1 <sup>st</sup> Proton).....	44
Figure 34 - P <sub>2</sub> O <sub>5</sub> w/Limestone Natural Log of Concentration vs Time .....	47
Figure 35 - P <sub>2</sub> O <sub>5</sub> w/Ore (2 <sup>nd</sup> Proton) Natural Log of Concentration vs Time .....	47
Figure 36 - P <sub>2</sub> O <sub>5</sub> w/Limestone Arrhenius Temperature Dependence .....	49
Figure 37 - P <sub>2</sub> O <sub>5</sub> w/Ore Arrhenius Temperature Dependence (2 <sup>nd</sup> Proton) .....	49
Figure 38 - P <sub>2</sub> O <sub>5</sub> w/Ore Arrhenius Temperature Dependence (1 <sup>st</sup> Proton).....	50
Figure 39 - Proton Dissociation for Phosphoric Acid.....	53
Figure 40 - SO <sub>4</sub> Solution Concentration & pH vs Time w/Limestone (Low Concentration).....	55
Figure 41 - SO <sub>4</sub> Solution Concentration & pH vs Time w/Ore (Low Concentration).....	55
Figure 42 - SO <sub>4</sub> Solution Concentration & pH vs Time w/Limestone (High Concentration) .....	56
Figure 43 - SO <sub>4</sub> Solution Concentration & pH vs Time w/Ore (High Concentration) .....	56
Figure 44 - SO <sub>4</sub> Natural Log of pH Predicted Concentration vs Time .....	57
Figure 45 - Pond Water P <sub>2</sub> O <sub>5</sub> Concentration & pH vs Time w/Limestone.....	58
Figure 46 - Pond Water P <sub>2</sub> O <sub>5</sub> Concentration & pH vs Time w/Ore.....	58
Figure 47 - Pond Water SO <sub>4</sub> Concentration vs Time w/Limestone .....	59
Figure 48 - Pond Water SO <sub>4</sub> Concentration vs Time w/Ore.....	59
Figure 49 - Pond Water F Concentration & pH vs Time w/Limestone .....	60
Figure 50 - Pond Water F Concentration & pH vs Time w/Ore .....	60
Figure 51 - Pre/Post Reaction Histogram PSD .....	61
Figure 52 - Pre/Post Reaction Cumulative PSD .....	62
Figure 53 - Krebs Hydro-Cyclone Underflow Solids Recovery Performance .....	65
Figure 54 - Krebs Hydro-Cyclone Underflow Solids Performance.....	65
Figure 55 - Krebs Hydro-Cyclone Performance Curves @ 28 PSIG .....	66
Figure 56 - Krebs Hydro-Cyclone Cut Away (Arterburn, 1982).....	66
Figure 57 - Hydro-Cyclone Spray vs Rope Discharge (GN Solids Control, 2016).....	67
Figure 58 - Hydro-Cyclone Overflow Particle Size Distribution .....	68
Figure 59 - Settling Test Supernatant NTU's.....	69
Figure 60 - Settling Test Solid-Liquid Interface Position.....	70
Figure 61 - No Floc @ 60 min.....	70
Figure 62 - No Floc @ 24 hrs .....	70
Figure 63 - Anionic @ 60 min.....	71
Figure 64 - Anionic @ 24 hrs .....	71
Figure 65 - Cationic @ 75 min .....	71

Figure 66 - Cationic @ 24 hrs .....	71
Figure 67 - An & Cat @ 40 min .....	72
Figure 68 - An & Cat @ 24 hrs .....	72
Figure 69 - Flux Settling Curve .....	73
Figure 70 - Ore Pre-Reaction Pilot Flowsheet.....	75
Figure 71 - Lab Pilot Conical Thickener .....	78
Figure 72 - Plant Pilot Thickener Feed Well .....	79
Figure 73 - Plant Pilot Thickener Rake .....	79
Figure 74 - Dewatering Screen Side View .....	82
Figure 75 - Dewatering Screen Solids Discharge .....	82

## CHAPTER 1: INTRODUCTION

The management of phospho-gypsum pond water is an ongoing issue for phosphoric acid producers who deal with onsite stacking of the industry byproduct, phospho-gypsum. This chapter presents the background of the phosphoric acid/phosphate based fertilizer process to provide context for the study of pre-reacting phosphate ore with phospho-gypsum pond water.

### PHOSPHORIC ACID PRODUCTION VIA THE WET PROCESS

Phosphate fertilizer demand is set by the pace of the global agricultural economy and world demand for food. The key raw material for all phosphate based fertilizers derived from phosphoric acid is phosphate rock. The manufacturing process of phosphoric acid results in a number of environmental challenges or concerns in the form of air, water and solid waste. Particulates from cooling towers and gaseous fluorides released during the reaction and concentration steps are the main source of emissions from the process (EFMA, 2000). Fluoride is an environmental concern for vegetation since it can accumulate in certain plant species. Phospho-gypsum disposal, a by-product of the manufacturing process, is probably the largest environmental issue as a result of the following:

- Transport/process pond water acidity
- Dissolved metals
- Radionuclides

Each constituent is in very low concentrations but the large quantity of low toxicity material makes it regulated by EPA under the Bevill amendment which allows producers to stack the material on site. The Bevill amendment is part of the Resource Conservation and Recovery Act (RCRA) which outlines regulations for the management of hazardous waste. 'Waste' covered by Bevill is typically generated in large quantities but believed to be less hazardous to human health than hazardous waste as defined by RCRA (EPA, 2016). Currently the use of lining systems and water recycle systems are the most common methods of protecting the surrounding environment from phospho-gypsum handling systems. However, there are a number of constraints around the quality and quantity of phospho-gypsum transport water that can be returned to the process. If these requirements cannot be met and all

of the water cannot be returned to the process there are a number of costly treatment alternatives. These include but are not limited to the following (Siemens, 2009):

- Evaporation
- Single Liming
- Double Liming
- Double Liming followed by Reverse Osmosis
- Hauling Water off site
- Deep Well Injection
- Reverse Osmosis

However, the production process of phosphate based fertilizers begins with the mining of phosphate rock which occurs before many of these environmental challenges are encountered.

#### FLUORAPATITE & THE BENEFICIATION PROCESS

Phosphate ore is a fluorapatite made up mainly of calcium phosphate ( $\text{Ca}_3(\text{PO}_4)_2$ ), typically 55-65% depending on ore quality, along with a variety of other impurities. Throughout the world, mined phosphate is primarily used as a feedstock for the production of phosphoric acid which can be converted into a variety of phosphate based liquid and solid fertilizers.

In the Western United States, a number of open pit phosphate mines are in operation for the purpose of generating high quality phosphate ore for use in the production of phosphoric acid. Some of the largest in the area are operated along the Idaho, Wyoming and Utah borders and currently produce up to 2,000,000 tons per year (TPY) of phosphate ore. Once mined, the ore is beneficiated in order to upgrade the overall quality and remove low grade gangue minerals and impurities. A number of beneficiation techniques exist such as thermal beneficiation, flotation or gravity separation. The beneficiation plant is typically located very near to the mine and the process is highly dictated by the quality of the ore.

Thermal beneficiation is a possible method for upgrading much of the high Btu (British thermal unit) ore present in the Western US but many environmental challenges exist with permitting such a process, not to mention they are also very capital intensive to construct. As a result, the preferred beneficiation technique is either flotation or gravity

separation. The first step in either of these processes involves crushing the ore using a combination of rod mills and ball mills to achieve the appropriate size fraction. Fine particles, clays and other impurities are then removed using various combinations of classifiers, hydro-cyclones, screens and/or flotation. The resulting product of the milling process is typically a phosphate ore slurry with a mean particle size in the 100-150  $\mu\text{m}$  range ready for further processing (Becker, 1989; Nielson, 1987). Typical chemical composition of the mill product used in this study is shown in Table 1.

Table 1 - Beneficiation Plant Product Ore Chemical Composition

Constituent	Content
P <sub>2</sub> O <sub>5</sub>	26.9%
Al <sub>2</sub> O <sub>3</sub>	1.8%
F	2.7%
CaO	42.5%
Fe <sub>2</sub> O <sub>3</sub>	0.7%
MgO	0.4%
SiO <sub>2</sub>	12.9%
Na <sub>2</sub> O	0.5%
K <sub>2</sub> O	0.5%
Btu	435
% Solids	65.1%
SG	1.71
Bulk Density	2.82

Due to the proximity of utilities, truck and rail access to markets, the downstream phosphoric acid plants are located long distances from the mine and beneficiation plants. The most common method of transporting the product slurry from the beneficiation plant to the phosphoric acid plant is via pipeline using very large positive displacement pumps.

## THE WET PROCESS

Before the phosphate nutrient can be utilized by plants, it must be converted to a readily available form. One of the first steps in this process is the generation of phosphoric acid by reaction of the phosphate ore with sulfuric acid. The preferred and most common

method of phosphoric acid production is via the Di-Hydrate (DH) Wet Process method. In this method sulfuric acid is reacted with phosphate ore in the Phosphoric Acid Plant (PAP).

In wet process phosphoric acid production Di-Hydrate refers to the amount of water associated with the gypsum ( $\text{CaSO}_4 \cdot 2\text{H}_2\text{O}$ ) produced in the digester, in this case 2 moles of water are attached to the gypsum. In Hemi-Hydrate (HH) production of phosphoric acid only  $\frac{1}{2}$  mole of water is associated with the gypsum. The HH process is beneficial from an energy standpoint due to the production of higher strength Filter Grade Acid (FGA) but requires a tighter window of operational control and is less forgiving to operate than the industry preferred DH process.

For 1,250 TPD of  $\text{P}_2\text{O}_5$  production, approximately 4,000 TPD of sulfuric acid, 100% concentration basis, is needed for acidulation of the phosphate ore. The sulfuric acid is commonly produced on site via the “contact” process where elemental sulfur is burned to form  $\text{SO}_2$ , converted to  $\text{SO}_3$  and then absorbed in water to form sulfuric acid product.



*Sulfur + Oxygen → Sulfur Dioxide*



*Sulfur Dioxide + Oxygen → Sulfur Trioxide*



*Sulfur Trioxide + Water → Sulfuric Acid*

A majority of the phosphoric acid produced at these facilities is primarily reacted with anhydrous ammonia to produce a variety of both liquid and dry ammonium phosphate fertilizers for agricultural use. The balance of phosphoric acid is sold for a variety of industrial purposes or is used for the production of animal feed products also manufactured on site. On average, processing facilities in the Western US produce upwards of ~ 400,000 TPY of  $\text{P}_2\text{O}_5$  and generate over one million tons of finished product which is mainly comprised of ammonium phosphate fertilizers. The general flow sheet for a phosphoric acid production facility is shown in Figure 1. The three number nomenclature for finished product refers to the

N-P-K formulation which indicates the percentage of N, P<sub>2</sub>O<sub>5</sub> and K<sub>2</sub>O present. In products where a 4<sup>th</sup> number is shown this refers to the percentage of S.

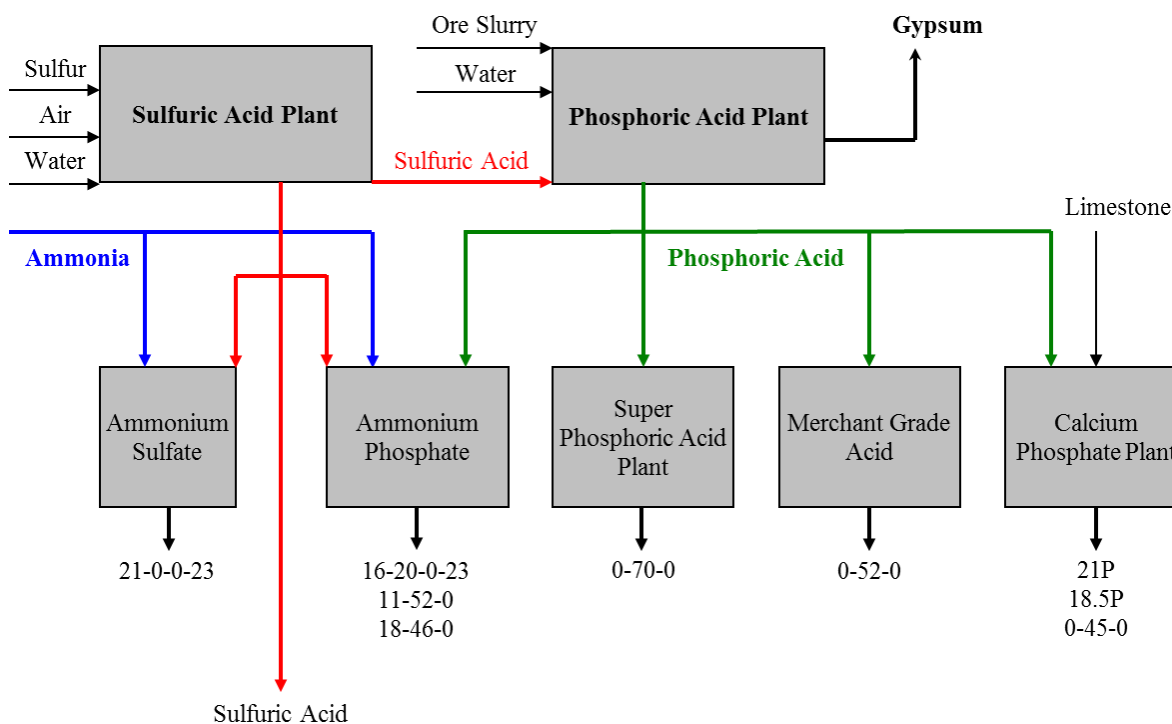
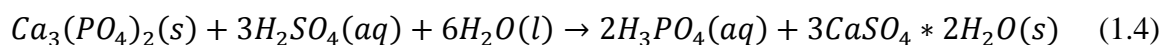


Figure 1 - General Phosphoric Acid Production & Downstream Process Flow Sheet

A simplified version of the general process chemistry for the production of phosphoric acid is shown in Equation 1.4; here phosphoric acid is the product and gypsum is the byproduct. Although not shown, there are also several complex side reactions that occur with impurities present in the ore matrix. In the phosphoric acid industry, the term phosphogypsum is typically used when referring to the gypsum byproduct. This is mainly due to the number of impurities present which typically end up in the solid phase during the reaction. Figure 2 is a depiction of a general process flow sheet for a DH plant attack and filtration sections.



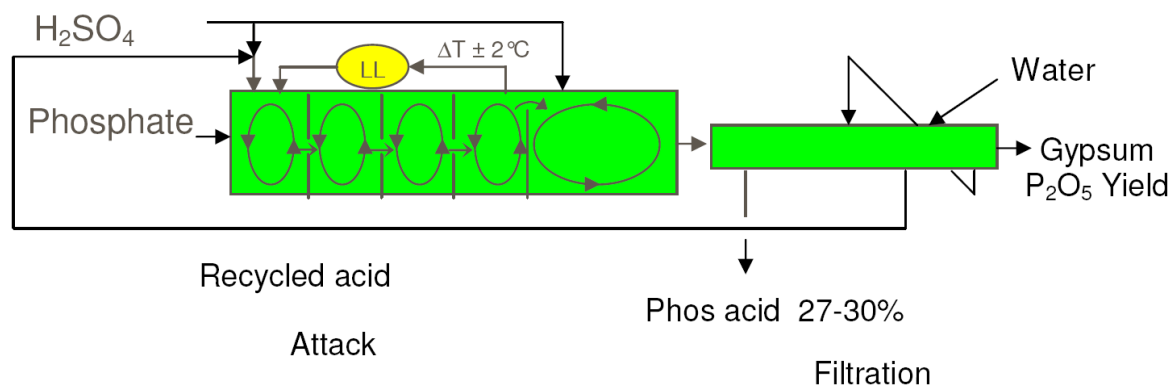


Figure 2 - Di-Hydrate Wet Process Phosphoric Acid Production

The phosphate content of this reaction is measured in the form of  $P_2O_5$ , which is simply a form of measurement used by the agriculture industry. To convert between phosphoric acid concentration and  $P_2O_5$  content the following equation is used.



The resulting products of the phosphate ore reaction with sulfuric acid are heat, phosphoric acid, also referred to as phos-acid, and phospho-gypsum solids. In order to dissipate the large amount of heat generated by the exothermic reaction and control the reaction temperature, a large volume of reactor slurry is circulated through vacuum flash coolers to evaporate water. The water is condensed in barometric condensers where a large volume of cooling water is circulated to maintain vacuum. The cooling water reports to a hot pit before being pumped to cooling towers where evaporative cooling lowers the water temperature before it is pumped back to the barometric condensers. Large diameter piping is used in the flash coolers to reduce gas velocity and minimize pressure drop, but despite careful design considerations there is a small degree of carryover from the reactor slurry to the condensate water. The carryover is primarily in the form of  $P_2O_5$ ,  $SO_4$  and  $F^1$  ( $H_3PO_4$ ,  $H_2SO_4$  and  $HF$ ) which contribute to the acidity of the process water circulating through the

<sup>1</sup> Industry standard to refer to phosphoric, sulfuric and hydrofluoric acid in the ion specific form without the use of charges

barometric condensers. The concentrations are relatively low, however, their presence contributes to a pH of less than 2 and the general scaling nature of this process water. Additionally, environmental regulations limit where blow down water from this process water circuit can be discharged and/or reused within the plant, which has an impact on the overall PAP water balance. Ultimately any blow down from this system ends up reporting to the gypsum handling system. A depiction of the PAP cooling water system is shown in Figure 3.

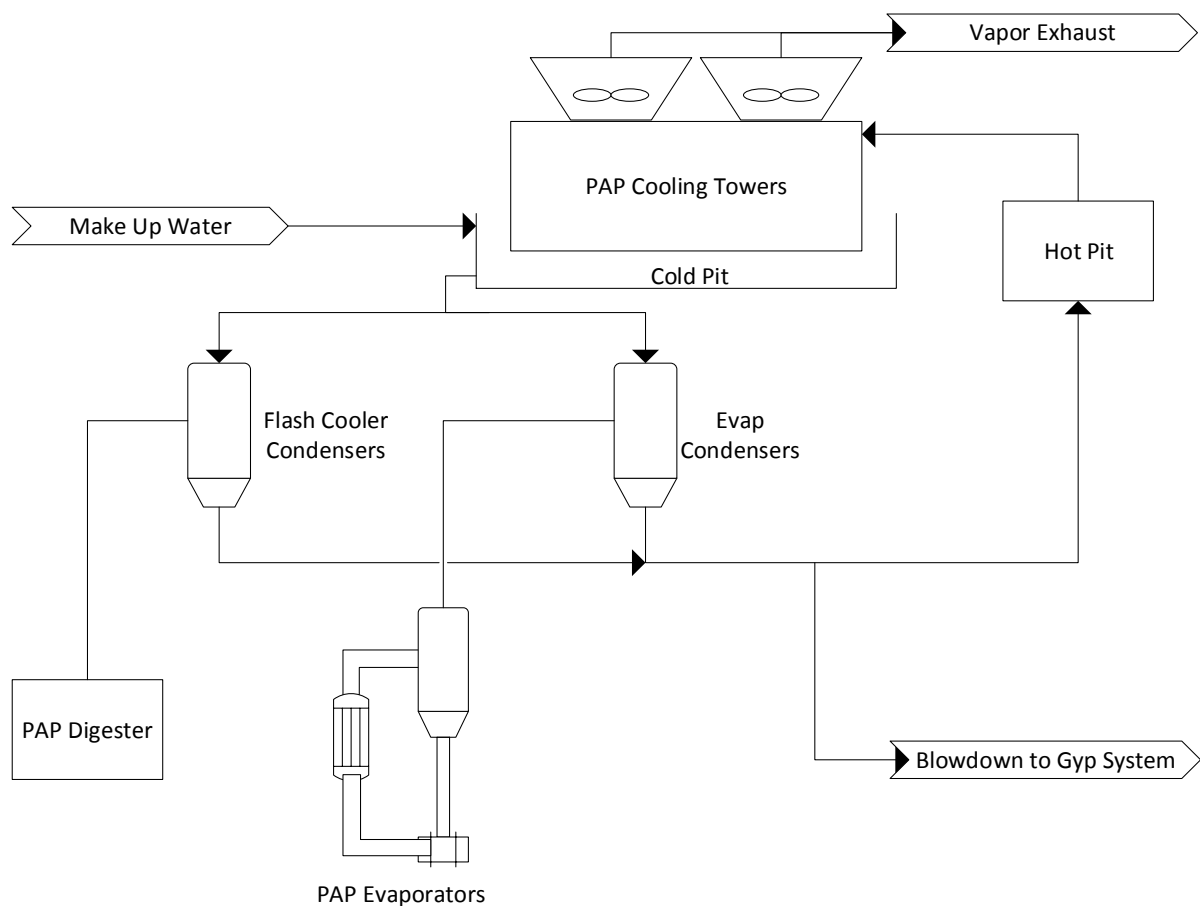


Figure 3 - Phosphoric Acid Plant Cooling Water System Process Schematic

Excess carbonate in the phosphate ore poses a number of problems in the phosphoric acid plant. Primarily, it can have a limiting impact on vacuum flash coolers performance and the overall digestion process. The evolution of  $\text{CO}_2$  causes excess foaming in the reaction vessels, which can result in increased carryover to the condenser water if the foam is not broken up or controlled (Prayon, 2011).



With sedimentary rock present in much of the Western US, this problem can be exacerbated due to the organic matter present in high Btu ore. The organics actually stabilize the foam, making control of this issue even more difficult. A variety of anti-foam agents exist made from oil fatty acids, oleic acids or silicones in combination with a surfactant (Partin, 2005). Many defoamer manufactures claim they can control surface foaming and reduce entrained gas in the slurry but these reagents add to production cost and are often times less than effective.

On a per ton basis, the presence of carbonate also increases the amount of sulfuric acid required to produce phosphoric acid due to the side reaction with carbonate as shown above in Equation 1.6. However, a small quantity of carbonate in the ore is viewed as a benefit since it is believed to chemically grind and break up the rock during the reaction. This increases the surface area and speed of reaction and reduces the possibility of coating the phosphate rock with gypsum. Coating the rock can result in co-crystallized losses where unreacted rock is tied up in the gypsum lattice causing an increase in Water Insoluble (WIS) P<sub>2</sub>O<sub>5</sub> losses (Theys, 2003). Ore with 3 to 5% CO<sub>2</sub> content is viewed as desirable since it can potentially increase rock reactivity.

#### PHOSHPO-GYPSUM & BYPRODUCT HANDLING SYSTEMS

Solids generation is a normal part of the phosphoric acid process and for each ton of P<sub>2</sub>O<sub>5</sub> produced, ~5 tons of gypsum is generated. Before the phosphoric acid reaches a form usable for downstream processing the phospho-gypsum solids generated during the reaction step must be removed. A common method for separation of the gypsum solids from the phosphoric acid is belt filtration. Alternatively, other equipment such as tilting pan or table filters can be used to separate the solids. A general schematic of the gypsum handling system is shown in Figure 4.

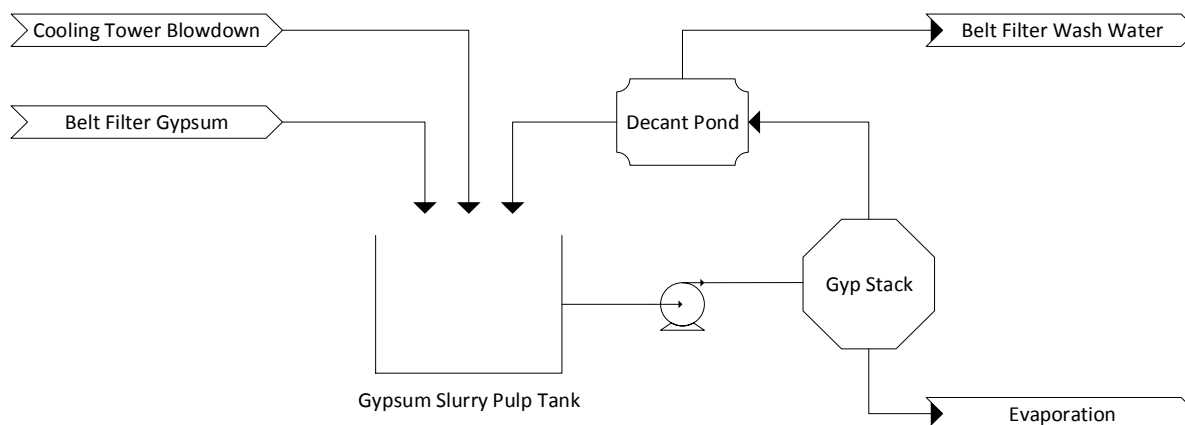


Figure 4 - Phosphoric Acid Plant Gypsum Handling System Process Schematic

In belt filtration, the slurry is discharged onto a moving belt filter under vacuum. The gypsum crystals, in the 50-70  $\mu\text{m}$  range, compact on the filter cloth and form a lattice structure for the acid to filter through. Typically the filter is comprised of 4 sections. In the first section, Filter Grade Phosphoric Acid (FGA) at ~26-28%  $\text{P}_2\text{O}_5$  is separated for downstream processing. In the final three wash sections residual phosphoric is rinsed from the filter cake to minimize mechanical losses of water soluble  $\text{P}_2\text{O}_5$ . Warm process water containing trace amounts of  $\text{P}_2\text{O}_5$  is introduced on the 4<sup>th</sup> and final section and fed counter-currently back to the previous section. The wash water collected on the 2<sup>nd</sup> section is then recycled back to the PAP digester to recover the  $\text{P}_2\text{O}_5$ . Fresh water would increase wash efficiency of the cake but because of water balance constraints this is not an industry accepted practice. The “dry” cake discharged off the end of the belt filters is then re-slurried using process water and pumped to the gyp stack. On average the dry cake contains ~0.5%  $\text{P}_2\text{O}_5$  and is ~35% moisture by weight. The  $\text{P}_2\text{O}_5$  remaining in the cake is a combined result of water soluble (mechanical) and water insoluble (chemical) losses that occur during the filtration and reaction steps, respectively.

Similar to the process water circulating through the barometric condensers, the process water from the gypsum handling system is also acidic and is primarily in the form of  $\text{P}_2\text{O}_5$ ,  $\text{SO}_4$  and F. Much of the acidity is a result of the mechanical losses occurring on the belt filter which transfer to the gypsum handling system. The chemical composition of the gypsum process water is shown in Table 2.

Table 2 - Gypsum Process Water Chemical Composition

Constituent	Content
P <sub>2</sub> O <sub>5</sub>	1.47%
F	0.83%
SO <sub>4</sub>	0.44%
Ca	0.18%
Al	143 ppm
Cd	1.9 ppm
Cr	10.4 ppm
Cu	0.8 ppm
Fe	103 ppm
Mg	191 ppm
Ni	2.9 ppm
V	12.2 ppm
Zn	24.5 ppm
K	337 ppm
Na	868 ppm
Si	2097 ppm

Due to environmental regulations the gypsum cannot be sold as a byproduct and is stacked on site, which is standard practice in the U.S. Phosphate Industry. All U.S. phosphate producers currently employ the “wet” stacking method of phospho-gypsum solids on site. This involves pumping the phospho-gypsum slurry into a large open area contained by dikes and allowing the solids to settle over time. Once settling is complete the water is decanted from the settling pond and re-used to slurry the dry cake coming off the belt filters. The pond section is then dried and the dikes around the perimeter are built up to a higher elevation with the existing gypsum. Once this step is complete the process is then repeated, and the height of the gyp stack slowly grows over time. In order to accommodate the continuous flow of gypsum slurry and avoid interrupting production the stacks are divided into multiple sections so that the filling, settling, drying and dike building can be systematically rotated from one section to the next.

As a result of the gypsum system pH, residual impurities, radiation, etc., there are a number of environmental concerns and regulations associated with stack management. Seepage of pond water into the surrounding environment is a primary concern and has been dealt with through the use of liners and/or shallow extraction wells near the base of the stacks.

Both reduce the possibility of impurities making their way into surrounding groundwater, rivers, lakes or streams which could cause potential contamination. As a result, regulators have mandated that all gyp-stacks currently in operation must now have a liner installed which has a serious impact on plant water balance. Water seepage which once accounted for a large portion of plant water is no longer possible.

Other concerns include the inevitable closure and remediation of a gyp stack. The stack life is finite since size is regulated, this requires proper remediation steps to be taken. Any residual pond water must be treated and stacks must be capped to avoid future runoff and/or environmental impact to the surroundings.

#### PAP WATER BALANCE & POND WATER

Water balance is an integral part of the PAP process. The water balance links the various processes within the PAP together and without proper control of the water balance, the system becomes unstable and disrupts efficient operation. In order to illustrate the interdependencies of each system, a depiction of the PAP water balance is shown in Figure 5. This is essentially a combination of the cooling water and gypsum handling systems shown previously. Water from the process and system washes reports to one of three final locations:

1. Water contained within the phosphoric acid products
2. Water evaporated at the PAP cooling towers
3. Water reporting to the gypsum stack (Pond Water)
  - a. Gypsum Pore/Crystallization/Seepage
  - b. Evaporation

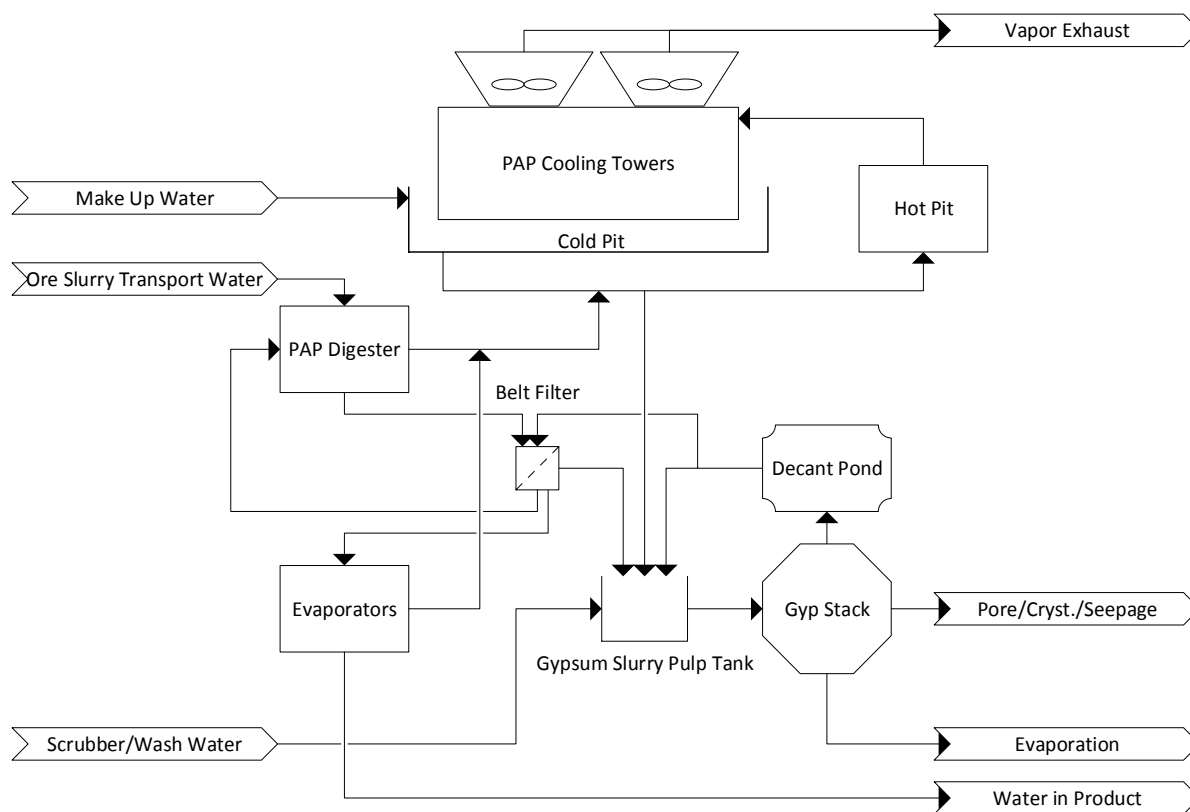


Figure 5 - Phosphoric Acid Plant Water Balance Process Schematic

The plant water balance impacts each process section and what occurs in one system will impact the others. The major connection between the various processes is the cooling tower and the gypsum stack. The cooling system impacts most of the operating processes. The blow down from the cooling tower reports to the gypsum thickener and eventually to the gypsum stack. The decant water from the gypsum stack returns to the PAP cooling tower and is circulated back to the other processes.

Overall most water used in the PAP system eventually reports to the gypsum handling system. Therefore, excessive water use will create water balance issues at the gypsum thickeners requiring greater quantities of transport/dilution water for gypsum fluidization to the gypsum stack. This could lead to gypsum stack instability and potential of gypsum stack failure that would be a severe environmental catastrophe.

Evaporation, pore water, gypsum water of formation and seepage all aid in reducing water inventory on the stack. However, with a lined stack seepage is no longer possible. Precipitation and PAP blow down cause an increase in stack pond water inventory. If the

system is not in balance and the water cannot be returned to the PAP plant, some method of treatment must be employed to neutralize the acidity of the pond water before it can be properly disposed of. Potential treatment options such as lime and/or limestone addition or reverse osmosis have been successfully implemented in the past but these systems can be extremely costly and very difficult to operate.

This study evaluates the use of an alternative method – ore pre-reaction – where excess carbonate (i.e. limestone) in the phosphate ore is utilized to neutralize the acidity of pond water. This process could be beneficial towards maintaining pond water inventories within manageable volumes and protection of the surrounding area from a potential system breach and an adverse environmental release to the surrounding area. The research hypothesis and objectives are stated in Chapter 2, a literature review is presented in Chapter 3, testing materials and methods are reviewed in Chapter 4, testing results are discussed in Chapters 5 through 7, and conclusions and recommendations for future work are presented in Chapter 8.

## CHAPTER 2: HYPOTHESIS & OBJECTIVES

### ORE PRE-REACTION PROCESS OVERVIEW

Pond water balance in phosphoric acid plants varies geographically from one location to the next and is heavily dependent on climate conditions as well as general plant process operating procedures, which can also vary considerably from one organization to the next. As a result there is a limited amount of literature available pertaining to pond water system management. The chemistry of these systems is fairly well understood, however, there is little information which discusses phosphoric acid processes where pond water balance is a concern and treatment options are needed in order to reduce the quantity of pond water in the system. The few exceptions where treatment literature is available primarily include liming (i.e. treatment with lime or limestone) and/or reverse osmosis (RO). Liming can be somewhat cost effective but  $P_2O_5$  losses and sludge disposal are a big downside and RO systems are very expensive to install and operate.

For facilities that handle phosphate ore delivered to the plant in a slurry form as opposed to dry solids, pond water balance can be much more of a challenge. As a result, the scenario where ore is delivered as a slurry will be the focus of this paper. This study evaluates an alternative treatment option to liming; instead carbonate present in the phosphate ore is utilized to neutralize the acidity present in excess volumes of pond water. This has the potential to aid with system water balance and maintain pond water quantities within reasonable levels.

The acidity of the phospho-gypsum pond water, which is assumed to be in the form of phosphoric acid, sulfuric acid and hydrofluoric acid, can be used to pre-react phosphate ore. This has the concomitant benefit of removing alkalinity before the ore is sent to the PAP digester in addition to neutralization of pond water acidity. The alkalinity of the ore, which is primarily in the form of calcium carbonate as well as calcium magnesium carbonate (dolomite), will convert a majority of acidic species to insoluble forms: calcium phosphate, calcium sulfate, and calcium fluoride, respectively. As a result this process could be beneficial towards the following:

1. Increased overall  $P_2O_5$  recovery
2. Reduction in sulfuric acid consumption needed to acidulate phosphate ore in PAP

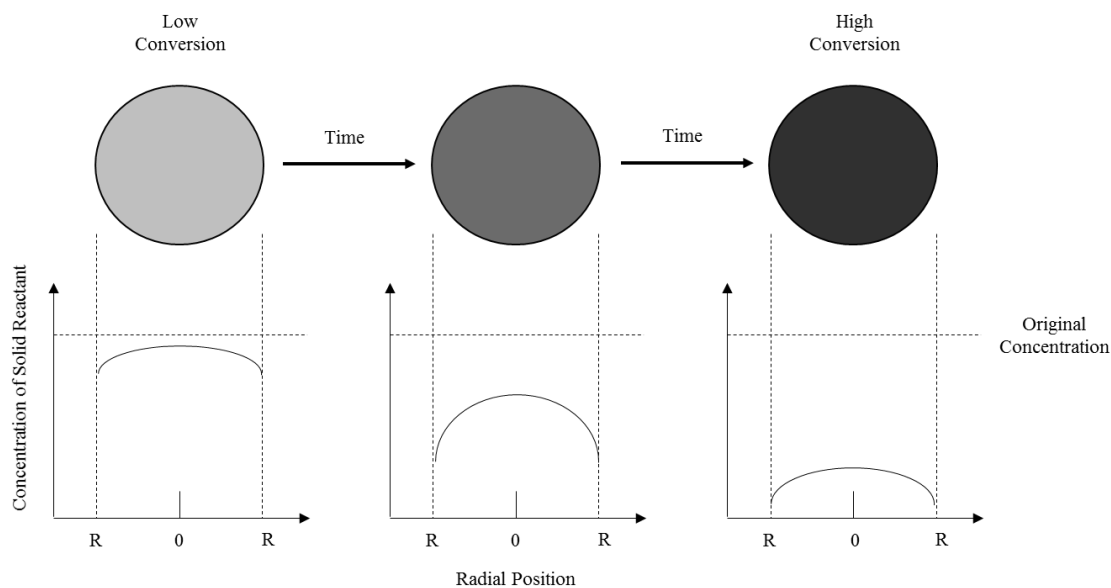
3. Fluoride is converted to a solid form lowering the liquid phase equilibrium concentrations in pond water and reducing potential for emissions
4. Gas loading on the digester flash coolers is reduced
5. Digester foaming is reduced

The downside of this process, however, is that the volume of pond water added dilutes the ore slurry to a solids concentration unsuitable for digester feed. Therefore a method must be employed to dewater the ore slurry to an acceptable concentration before it is sent to the PAP Digester. The objective of this study are twofold:

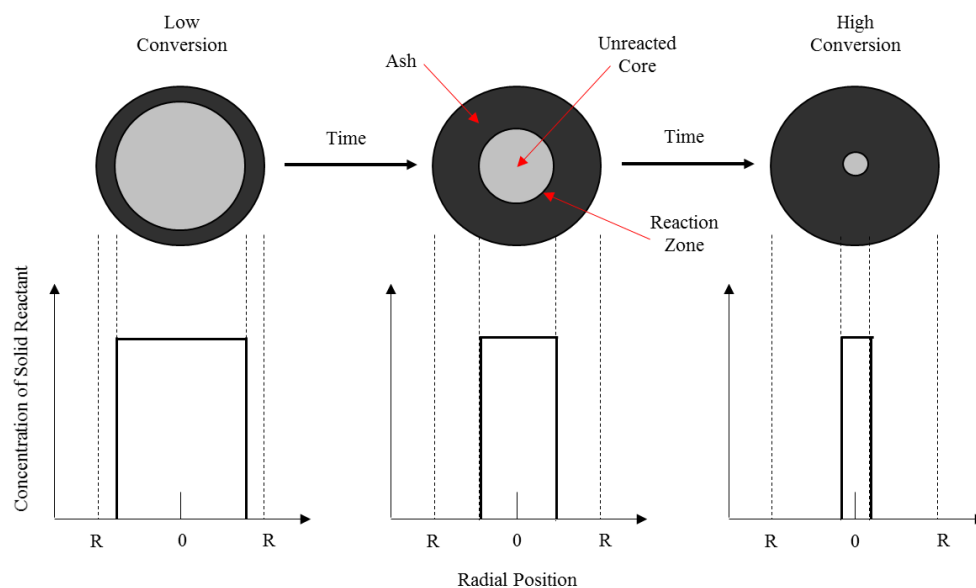
1. To evaluate the reaction kinetics associated with neutralizing the acidity of the pond water, and,
2. To develop and test a conceptual dewatering process capable of returning the phosphate ore slurry to an acceptable solids content after the dilution from adding pond water.

## REACTION KINETICS

Ore pre-reaction is a non-catalytic heterogeneous fluid-particle reaction. In this scenario a liquid comes in contact with a solid particle, reacts with it, and then transforms into a product. When the solid particle remains unchanged in size it will either follow the 'progressive conversion' or 'unreacted core' model as shown below in Figure 6 (Levenspiel, 1999).



### Progressive Conversion Model



### Unreacted Core Model

Figure 6 - Fluid-Particle Reaction Models for Unchanging Particle Size from Levenspiels Chemical Reaction Engineering 3rd Edition

Comparing both models in real situations the unreacted or shrinking core model (SCM) is believed to be the most accurate representation of the phenomena occurring when

the particle size remains unchanged. For the SCM one of following three is likely to be the rate limiting step that reasonably represents the rate of reaction:

1. Diffusion through the liquid film
2. Diffusion through the non-porous ash layer
3. Chemical reaction

Due to an abundance of pond water surrounding the solid particle and continuous agitation it is believed that mass transfer through the liquid film will be a non-limiting factor in the overall rate of reaction. The solids formed by neutralizing the acid may coat the outside of the ore particle in which case diffusion through the non-porous ash layer model may apply. However, test conditions in this study will ensure a high level of mixing is employed in order to eliminate external mass transfer resistance. Equation 2.1 represents the Crank-Ginstling-Brounshtein model where mass transfer across a nonporous product layer controls the reaction rate (Grenman, Tapio, & Murzin, 2011). Here ‘ $\alpha$ ’ is conversion of the solid reactant and  $g(\alpha) = kt$ , where ‘ $k$ ’ is the rate constant and ‘ $t$ ’ is time.

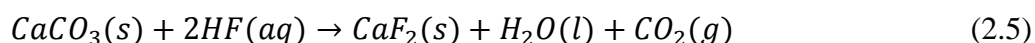
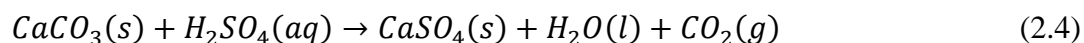
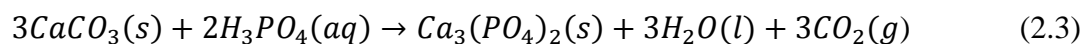
$$g(\alpha) = 1 - \frac{2}{3}\alpha - (1 - \alpha)^{2/3} \quad (2.1)$$

However, the ore only contains ~ 4.5% CO<sub>2</sub> in the form of carbonate and we are looking at reducing this concentration by 1 to 1.5% by pre-reacting the ore so the potential for solids formation is negligible in comparison to the amount of solid ore particles present on the order of 400:1. Therefore, the ore pre-reaction process should be most accurately represented by the ‘chemical reaction’ SCM shown in Equation 2.2. In this model the reaction kinetics are two-thirds-order and there is three dimensional advance of the reaction interface.

$$g(\alpha) = 1 - (1 - \alpha)^{1/3} \quad (2.2)$$

Although this model applies to the solid phase reactant and we must ensure that we have an accurate representation of the rate law for each of the liquid phase components. The three primary chemical reactions which occur during the pre-reaction process are shown below in

Equations 2.3-2.5. These take place simultaneously but will be evaluated individually in order to determine the mechanism for each reaction.



From experimental rate law data for each of the individual reactions, an overall rate law will be established by combining the simultaneous reactions. Here each reaction is in the form shown in Equation 2.6.



So the rate law can be expressed as

$$R = k[A]^m[B]^n \quad (2.7)$$

For the rate law 'R' the reaction order 'm' and 'n' can be found experimentally for each component as well as the rate constant 'k.' Once rate constants are determined at various temperatures, the constants in the Arrhenius temperature relationship represented by Equation 2.8 will be determined. In this equation 'A' is the pre-exponential factor, 'E<sub>a</sub>' is the activation energy, 'T' is the temperature and 'R' is the universal gas constant.

$$k(T) = Ae^{-E/RT} \quad (2.8)$$

Since carbonate is not the primary component in the phosphate ore, typically ranging from 3 to 5% by mass, simplistic vs complex kinetics will also be evaluated using limestone and phosphate ore to determine how impurities in the ore impact the overall reaction kinetics. It is expected that the reaction will take place at a much slower rate with phosphate ore since impurities will likely impede availability of carbonate and limit overall surface area compared

to pure limestone. Understanding reaction kinetics is an important factor in process design and the appropriate sizing of ore pre-reaction system equipment.

## ORE SLURRY DEWATERING

In the manufacturing of phosphoric acid via the wet process feed of phosphate rock to the reactor in a slurry form is a requirement and it is preferential that the solids concentration be no less than 68% solids by weight (Becker, 1989). Ideally 70% if possible, anything beyond this solids range and the rheology characteristics of the slurry will change to the point where it is no longer possible to pump. The higher end is preferred because it helps with plant water balance and  $P_2O_5$  recoveries by allowing more wash water, in this case pond water, to be brought onto the final wash section of the filters. Typically, phosphate ore is transferred from the beneficiation plant to the PAP plant at ~62% solids and then gravity-thickened to 68%+ before it is sent to the digester. The inherent issue with the ore pre-reaction process is that the amount of pond water added to the incoming pipeline ore could dilute the slurry down to 25 to 35% solids depending on operating conditions. This is unacceptable for PAP digester feed so some method of dewatering must be employed. This study evaluates multiple avenues for dewatering the slurry and generating a clean filtrate/supernatant which includes:

- 1) Hydro-cyclone in combination with gravity thickening
- 2) Hydro-cyclone in combination with dewatering screen and gravity thickening
- 3) Centrifuge

This list is not meant to be all inclusive, but only an evaluation of some common methods effectively employed in industry with material that has similar particle size distribution. The goal is to determine viability and any impacts to performance as a result of pre-reacting the ore.

Chapter 3 is a literature review of previous works and/or topics relevant to phosphate ore carbonate, solid-liquid reaction kinetics, pond water management and phosphate ore sedimentation/dewatering behavior.

## CHAPTER 3: LITERATURE REVIEW

### CARBONATE REMOVAL

It is well understood that increased levels of carbonate in the ore along with other organic impurities increase the foaming and carry over in the phosphoric acid digesters causing processing problems during acidulation. According to Prayon the foaming caused by CO<sub>2</sub> generation is worsened by the presence of organic material in sedimentary rock which actually stabilizes the foam making it more difficult to manage (Prayon, 2011).

Although according to Prayon the presence of carbonate also reduces of the impact of gypsum buildup and creates micro-agitation near the particle. This reduces coating effects during the PAP acidulations step and is viewed as a positive effect of having carbonate in the ore. In They's paper 'Influence of the rock impurities on the phosphoric acid process, products and some downstream uses,' he claims that when carbonate reacts and releases CO<sub>2</sub> it "chemically" grinds the phosphate rock during the reaction and increases reaction speed (Theys, 2003). As a result a small amount carbonate is believed to be desirable. However, both argue that the negative processing impacts associated with excessive carbonate far outweigh any benefits.

Olanipekun in his study 'Kinetics of Dissolution of Phosphorite in Acid Mixtures' found that the reaction of sulfuric acid follows the shrinking core model where the rate is controlled by the diffusion through ash layer (Olanipekun, 1999). In this case gypsum builds around the spherically shaped ore particle and reduces surface area available to reactants. For a spherical particle where ash diffusion controls the conversion time expression is represented by Equation 3.1. In this model '*k*' is the rate constant, '*t*' is time and '*α*' is conversion.

$$kt = 1 - \frac{2}{3}\alpha - (1 - \alpha)^{2/3} \quad (3.1)$$

Olanipekun also evaluated the scenario where the chemical reaction controls are represented by Equation 3.2; however, this model was not a good fit to his data in comparison to Equation 3.1.

$$kt = 1 - (1 - \alpha)^{1/3} \quad (3.2)$$

Note that both equations are the same as the Crank-Ginstling-Brounshtein model and the two-thirds-order model where there is three dimensional advance of the reaction interface presented in Chapter 2. Since the generation of solids should be negligible in the ore pre-reaction process, thereby reducing the potential for a coating effect, the appropriate fit of model should be opposite to Olanipekun's findings. In theory we should expect the chemical reaction to be the rate controlling step.

In the 1990's the Florida Institute of Phosphate Research (FIPR) focused a considerable portion of their research on reducing phospho-gypsum and pond water associated with the phosphoric acid production process. As a result multiple research studies focused on removing dolomite, also known as calcium magnesium carbonate ( $\text{CaMg}(\text{CO}_3)_2$ ), from the ore prior to acidulation. By reducing dolomite content in the ore, the primary source of carbonate, it was believed that a proportional reduction in sulfuric acid consumption and phospho-gypsum generation would be realized on a per ton of  $\text{P}_2\text{O}_5$  production basis.

Clifford's floatation process study 'Enhanced removal of Dolomite ( $\text{CaMg}(\text{CO}_3)_2$ ) Pebble Concentrate by  $\text{CO}_2$  Generation' found that separate treatment of the large and fine fractions,  $\pm 400$  mesh, from the mill discharge was ineffective. The carbonate tends to report to the fine fraction,  $-400$  mesh, so it was thought that this material could be treated separately which turned out to be ineffective. However, they successfully achieved a reduction in dolomite by treating the combined size fractions. This process also benefited from the addition of pond water as a pH adjustment alternative (Clifford, 2009).

In theory this improved performance from pond water addition supports the argument that the acidity of pond water reacts with excess carbonate, aiding with the liberation of  $\text{CO}_2$  in the floatation process. In Clifford's study this was confirmed through analysis of the cell water;  $\text{P}_2\text{O}_5$ , F and CaO precipitated out of solution and some MgO was dissolved from the rock. Based on carbonate reduction this process demonstrated the potential to reduce sulfuric acid consumption in the PAP digester by  $\sim 3\%$ . In their evaluation they also determined that this improves the life of the mine. This is a result of increased recovery of phosphate and processing of lower grade apatite than traditionally acceptable throughout industry.

## POND WATER MANAGEMENT & TREATMENT

Cameron's study 'Phosphoric Acid by Wet Process: Pond Water Management' emphasizes the importance of maintaining gyp stack pond water levels within acceptable limits in order to handle seasonal swings (Cameron, 1994). Typically pond water inventories rise in the colder winter months due to reduced evaporation and decrease in the summer months when evaporation is greater. However, it is important to note that evaporation is heavily impacted by wetted surface area which is dictated by pond level. Given the option it is preferential to operate on the negative side of the water balance. Finding additional make up water, as opposed to treating excess pond water, is much preferred in a situation where the balance is out of hand.

The three primary methods recommended by Cameron for keeping pond water balance in control are 1) reducing plant watershed such as CT blow down, rain water collection, etc. 2) eliminating pumps requiring seal water and replacing them with mechanical seals and 3) using a portion of the pond water in the mill circuit for crushing, grinding and floatation. The third option; however, does not apply to this study since this scenario does not involve a mill located in close proximity to the processing plant. It does, however, imply that introduction of pond water with the ore prior to acidulation will not have a detrimental impact on downstream processes.

In a joint study done by FIPR and the Tennessee Valley Authority (TVA), McFarlin evaluated the chemistry of gypsum systems and how it impacts the processing plant and the surrounding environment (McFarlin, 1992). In their study they found that the chemistry of pond water varies considerably from one processing plant to the next. In the first step McFarlin focused on the composition of solid and liquid phase fractions and what variables impact distribution of elements between to the two phases. In the second step they evaluated methods for reducing the composition of low solubility elements such as P and F in the liquid phase.

One concern or hypothesis was that fluoride emissions from gypsum systems are heavily impacted by small changes in pond water concentration (i.e. increasing acidity through evaporation increases emissions). However, it was found that changes in concentration by evaporating up to 75% of a solution had little to no impact on fluoride evolution. In this case evaporating up to 75% of a pond water sample did not change the total

mass of fluoride in the liquid phase. A majority of the fluoride evolution occurs as  $\text{SiF}_4$  when the surface of the gypsum dries. Therefore, it is important to keep gyp stack surfaces wetted in order to reduce fluoride emissions.

It is known that limestone will reduce soluble P and F concentrations in pond water so the McFarlin study evaluated the use of low grade dolomite or carbonate containing mill rejects such as phosphate slimes and clays to treat the pond water. The carbonaceous containing reagents were successful in reduced soluble P and F in the pond water which present a lower cost alternative to lime or limestone. Conversely non-dolomitic containing ore did not reduce F concentrations in the liquid phase.

Although pond water treatment with ore could potentially reduce soluble fluoride it is difficult to argue that it will reduce potential emissions. According to Prayon fluoride is re-liberated from the solid phase during PAP acidulation as shown in Equation 3.3.



However, by shifting a portion of the fluoride load away from the pond water system and reducing the cycles of concentration the opposing argument could be made that potential for emissions are reduced.

Alternative treatment options exist such as reverse osmosis which was evaluated in another joint study done by FIPR and Mosaic (Jardine, 2005). Although quite costly at \$14/1,000 gallons of pond water treated, it represents a good alternative to liming if the goal is to generate clean water rather than just “treat” pond water. In the case of gyp stack closure this may be applicable but for an operating process plant the need for “fresh water” quality is less of a concern. A majority of the makeup water only needs to meet pH requirements dictated by regulatory agencies in order for it to be readily introduced back into a phosphoric acid processing plant. Although also regulated to a certain degree, the presence of minor impurities in water is less of a concern and has negligible impacts on process performance.

## PHOSPHATE DEWATERING

It is common to ‘dewater’ phosphate ore slurry in industry prior to acidulation if it is transported to the processing facility via pipeline, yet very little literature or research exists on

the behavior and the mechanism of dewatering of phosphate ore slurries. The studies that do exist focus on the dewatering of phosphatic clays, also known as tailings from the milling or beneficiation process (Pittman, 1983). Unfortunately this research, although interesting, does not necessarily apply to the dewatering of phosphate ore after the pre-reaction process. The particle size and chemical composition of the mill product behaves in a considerably different manner than that of the mill tailings in terms of dewatering and/or thickening. As a result there is a need for additional research and understanding of phosphate dewatering systems.

#### LITERATURE REVIEW CONCLUSIONS

The carbonate in sedimentary phosphate rock present in the Western United States is problematic due to increased sulfuric acid consumption and reduced production rates from foaming. However, there is an opportunity for phosphoric acid producers to use excess carbonate to their advantage and reduce the potential environmental impact and processing challenges associated with phospho-gypsum handling systems. Previous work with dolomitic phosphate has shown that ore carbonate could be a cost effective alternative to existing treatment options which may also improve phosphate recovery and reduce reagent consumption. As opposed to treating and disposing of potentially hazardous bi-products such as pond water associated with phospho-gypsum handling there is an opportunity to re-introduce these streams back into the process in a cost effective manner that can be beneficial to process operations in a safe and environmentally responsible manner. There is also an opportunity to broaden the scope of options available to producers for pond water management best practices. Keeping pond water system inventories within manageable levels and in balance is critical to the operation of a phosphoric acid processing plant. In order for a full scale ore pre-reaction system to be implemented, a deeper understanding of the mechanisms behind the pond water reaction with ore carbonate and the dewatering/sedimentation of phosphate ore slurry is required.

Materials and methods used to test the hypothesis and objectives of this study are presented in chapter 4.

## CHAPTER 4: MATERIALS & METHODS

### BENCH SCALE BATCH TESTS

Bench scale batch testing was the first step in evaluating the ore pre-reaction process. Tests were split into two categories which involved 1) reaction kinetics and 2) ore slurry dewatering. Results from bench scale test work were then used for the design of both lab pilot and plant pilot continuous test units.

### CONSTANT VOLUME BATCH REACTOR

In order to evaluate the reaction kinetics associated with the neutralization of  $\text{H}_3\text{PO}_4$ ,  $\text{H}_2\text{SO}_4$  and  $\text{HF}$  in pond water, a constant volume batch reactor was utilized. The set up consisted of a 4,000 ml glass beaker, a hot plate to control temperature, a thermocouple to monitor temperature, a pH meter, and a mixer to keep the slurry mixture agitated during the reaction. Figures 7 and 8 are a depiction of the bench scale equipment set up. The reactions were carried out in a fume hood and left open to the atmosphere in order to allow proper ventilation of  $\text{CO}_2$  gas generated during the reaction.

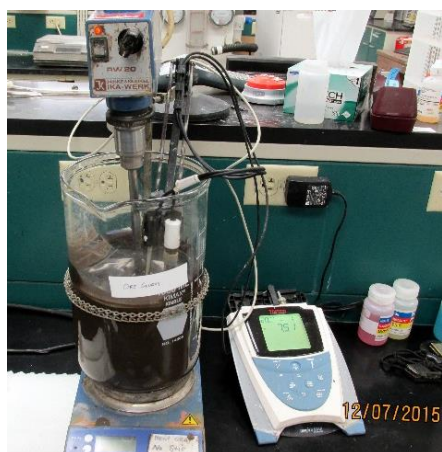


Figure 7 - Constant Volume Batch Reactor

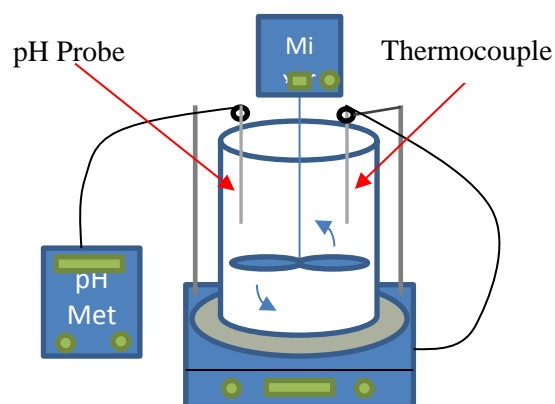


Figure 8 - Batch Reactor Schematic

Table 3 is a summary of the bench scale test parameters. In total there were 42 separate parameters and each experiment was carried out in duplicate for a total of 84 tests. Synthetic solutions of  $\text{P}_2\text{O}_5$  and  $\text{SO}_4$  were tested for comparison against Pond Water in order to individually evaluate each of the reaction mechanisms.

Table 3 - Bench Scale Test Parameters

Parameter	Neutralizing Agent	
	Phosphate Ore Slurry	Limestone
Temperature:	75°F	75°F
Solution 1	P <sub>2</sub> O <sub>5</sub> a) 0.75% b) 1.50% c) 3.00%	P <sub>2</sub> O <sub>5</sub> a) 0.75% b) 1.50% c) 3.00%
Solution 2	SO <sub>4</sub> a) 0.25% b) 0.50% c) 1.00%	SO <sub>4</sub> a) 0.25% b) 0.50% c) 1.00%
Solution 3	Pond Water	Pond Water
Temperature:	100°F	100°F
Solution 1	P <sub>2</sub> O <sub>5</sub> a) 0.75% b) 1.50% c) 3.00%	P <sub>2</sub> O <sub>5</sub> a) 0.75% b) 1.50% c) 3.00%
Solution 2	SO <sub>4</sub> a) 0.25% b) 0.50% c) 1.00%	SO <sub>4</sub> a) 0.25% b) 0.50% c) 1.00%
Solution 3	Pond Water	Pond Water
Temperature:	120°F	120°F
Solution 1	P <sub>2</sub> O <sub>5</sub> a) 0.75% b) 1.50% c) 3.00%	P <sub>2</sub> O <sub>5</sub> a) 0.75% b) 1.50% c) 3.00%
Solution 2	SO <sub>4</sub> a) 0.25% b) 0.50% c) 1.00%	SO <sub>4</sub> a) 0.25% b) 0.50% c) 1.00%
Solution 3	Pond Water	Pond Water

These ‘synthetic’ solutions were made up by dosing tap water with reagent grade phosphoric acid and sulfuric acid until the target concentration was achieved. Testing with HF solutions was avoided for this study due to concerns with safe handling. Table 4 lists the dosing parameters for each of the tests carried out with phosphate ore and limestone. For each test, concentration vs. time data were generated by collecting homogeneous slurry samples from the overall solution at intermediate time intervals. 10 to 15 samples total were collected for each test at time intervals ranging anywhere from 5-20 minutes. Sampling intervals

depended on reaction speed which was found through trial and error and each sample was ~ 100 ml. Although this method of sampling changed the total volume of the reaction it did not change the concentration of reactants and products in relation to one another.

Table 4 - Bench Scale Test Dosing Parameters

	Phosphate Ore	Limestone
Slurry wt (grams)	2,000	2,000
% solids by weight	62%	8%
Process Water wt (grams)	1,500	1,500
Total wt (grams)	3,500	3,500
% solids by weight	35%	5%

The liquid and solid fractions were then separated using a combination of centrifugation followed by vacuum filtration as shown in Figure 9-12. Once the remaining solids were dried, a liquid and solid fraction could be analyzed to evaluate the concentration of each component.



Figure 9 - Lab Centrifuge



Figure 10 - Sample after Centrifuging



Figure 11 - Vacuum Filtration Apparatus



Figure 12 - Vacuum Filtration of Supernatant

## HYDRO-CYCLONE TEST WORK

In order to re-thicken the ore slurry post pre-reaction, one option was to use hydro-cyclones in combination with high-rate thickening. The hypothesis was that hydro-cyclones could relieve the load on a gravity-thickener while being much less capittally intensive. Additionally, they would take up a much smaller foot print than a large thickener that would be required to handle the increased volume of material from the ore pre-reaction process. Therefore, an existing plant thickener used to thicken pipeline ore slurry from 62% solids up to 68% solids prior to PAP digester feed could be repurposed for thickening hydro-cyclone overflow. In this scenario the diluted pre-reacted ore slurry would be fed directly to hydro-

cyclones from the continuously stirred tank reactor (CSTR), the underflow would be recovered as slurry suitable for PAP digester feed (+68% solids) and the overflow would report to a thickener to dewater the slurry further and recover the remainder of the solids. In practice the thickener underflow could then be blended back with the hydro-cyclone underflow solids and thickener overflow could be used as makeup water elsewhere in the PAP plant.

Hydro-cyclone testing had two objectives 1) maximize underflow solids concentration and 2) maximize underflow solids recovery. In order to determine optimum performance the feed solids concentration and pressure were varied for each test. The solids concentration was adjusted by adding tap water for dilution and the feed pressure was adjusted using a centrifugal pump equipped with a variable frequency drive (VFD) which made it possible to adjust pump speed. The test parameters are shown in Table 5, only one variable was changed at a time resulting in the evaluation of 35 separate feed conditions.

Table 5 - Lab Scale Hydro-Cyclone Test Matrix

Feed Solids Concentration (% wt)	Feed Pressure (psig)
10%	10
15%	15
20%	20
25%	25
30%	30
	35
	40

Figure 13 is a schematic of the lab scale hydro-cyclone test loop. For this evaluation two 4" urethane hydro-cyclones from different manufacturers were utilized. Each hydro-cyclone was placed under the same operating conditions and then evaluated in a side by side comparison.

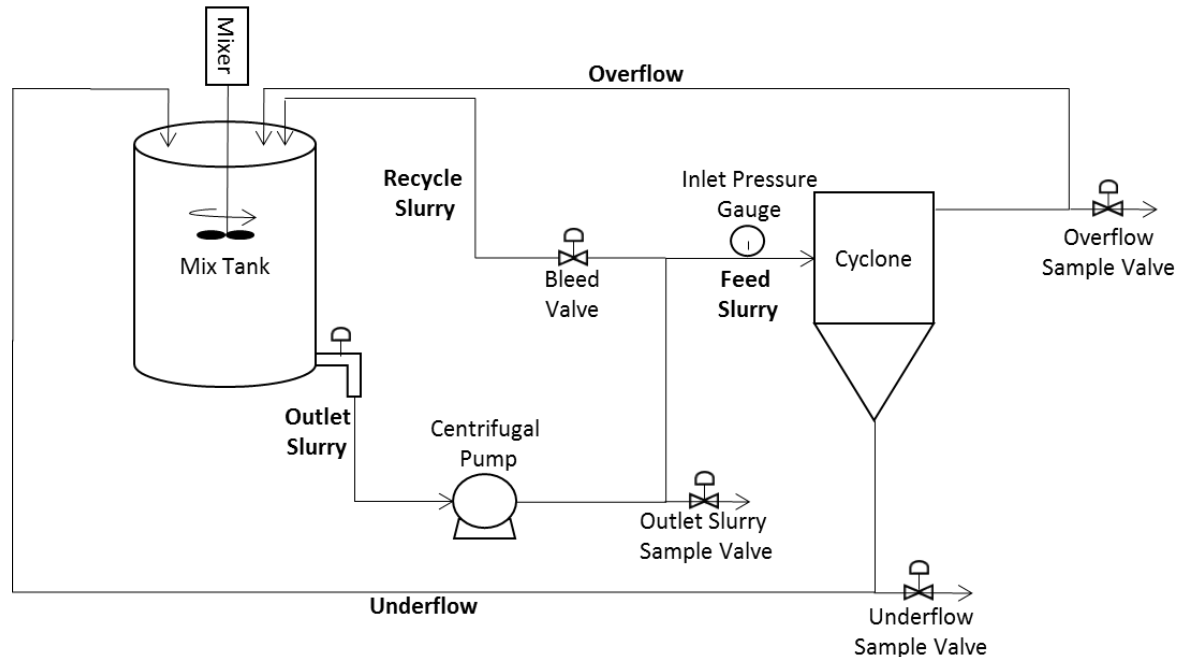


Figure 13 - Hydro-Cyclone Batch Test Equipment Schematic

#### HYDRO-CYCLONE OVERFLOW SEDIMENTATION TEST WORK

Once the optimum performance was achieved with the hydro-cyclone, enough overflow material was collected to determine the settling characteristics of the solids. The objective with bench scale sedimentation testing was to evaluate design criteria for a thickener which included determining flocculate type and dose, feed dilution requirements, rise rate, bed compaction and supernatant (overflow) quality. Optimum performance would maximize underflow solids and minimize supernatant total suspended solids (TSS). For this study a combination of the Kynch and Coe & Clevenger (CC) test methods were utilized for determining the settling characteristics of the hydro-cyclone overflow slurry (Seidel, 1995).

The Kynch method utilizes a cylinder fitted with a rake mechanism spinning at 6 revolutions per hour (RPH), the rake reduces the impacts of wall effects present in a narrow test cylinder which impede settling and simulates the rake mechanism in a full scale thickener. The CC method is based on the premise that the settling rate is function of the solids concentration and there is a critical controlling concentration. For these tests the solid-liquid interface was monitored as a function of time as well as the clarity of the supernatant liquid via turbidity measurement and TSS. In order to complete tests quickly while varying flocculent dosage, flocculent type and solids concentration; multiple tests were conducted

simultaneously using 500 ml settling cylinder as shown in Figure 14. Each cylinder was equipped with a rubber stopper to allow for gentle agitation after flocculent addition without introducing excessive air bubbles, the solid-liquid interface was then monitored by marking the flask at intermediate time intervals. The settling test variables are shown in Table 6 and included flocculent screening and feed dilution determination.



Figure 14 - Sedimentation Cylinders

Table 6 - Settling Test Matrix

Control Point	Test Variable
1. Flocculent	a) No Flocculent
	b) Anionic
	c) Cationic
	d) Cationic & Anionic
2. Feed Dilution	a) 1.5%
	b) 2.0%
	c) 2.5%
	d) 3.0%
	e) 3.5%
	f) 4.0%
	g) 4.5%

## PILOT TESTING

Using data from batch pre-reaction and sedimentation testing as feed design criteria, further testing of the ore pre-reaction and dewatering process was carried out in two phases: 1) a semi-batch continuous lab pilot and 2) a continuous plant pilot. It is important to note that the objective of pilot testing was to review process viability as opposed to re-evaluate reaction kinetics. Both processes consisted of a CSTR to pre-react the ore and a hydro-cyclone and ore thickener to dewater the ore slurry. Turndown capacity of the hydro-cyclone did not allow for continuous operation of a lab pilot without using feed tanks for the thickener and pulling intermittent samples of hydro-cyclone over flow and under flow at short fixed time intervals. A simplified process schematic is shown in Figure 15, the key difference between the two processes were semi-batch continuous vs. continuous processes, equipment size and throughput.

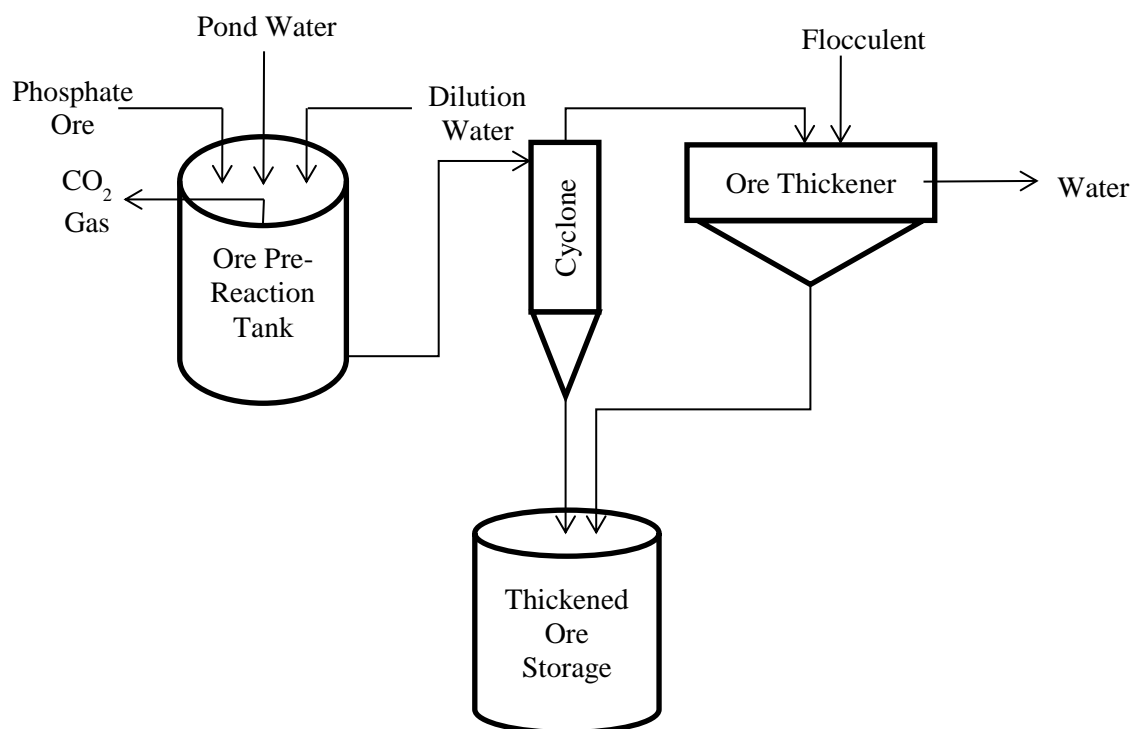


Figure 15 - Continuous Pilot Process Schematic

## PROCESS EQUIPMENT

Actual equipment used in lab pilot and plant pilot testing are shown in Figures 16 and 17. Scale-up from the lab pilot to plant pilot was required to avoid many of the inherent issues

encountered with small scale slurry systems (i.e. line plugging) and to move to a truly continuous process. This was mainly a result of higher flow rates which kept solids suspended due to higher line velocities and turbulent flow and avoided the issues with equipment turn down capacity. This allowed for much greater process control and steady throughput.

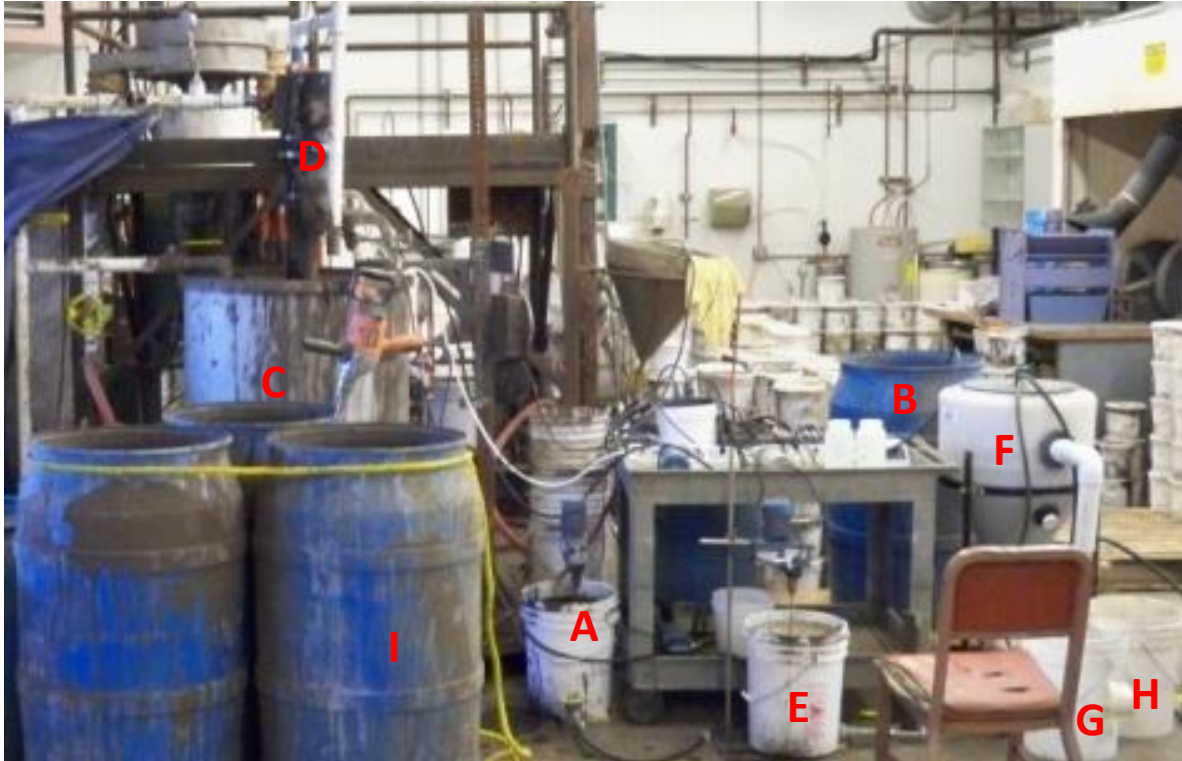


Figure 16 - Lab Pilot Process Equipment

Table 7 - Lab Scale Pilot Process Equipment List

Label	Description
A	Phosphate Ore Slurry Feed Tank
B	Decant Water Feed Tank
C	Ore Pre-Reaction Tank
D	Hydro-Cyclone
E	Thickener Feed Tank
F	Thickener
G	Thickener Overflow Tank
H	Thickener Underflow Tank
I	Thickened Ore Storage



Figure 17 - Plant Pilot Process Equipment

#### MISCELLANEOUS DEWATERING TEST WORK

Additional dewatering test work was carried out with Derrick dewatering equipment using product slurry generated from the plant pilot CSTR and hydro-cyclone overflow. The objective was to evaluate alternative equipment options for hydro-cyclones that could potentially load relieve and/or replace a high rate thickener while taking up a much smaller foot print in a full scale process. The two additional options evaluated were a 4' x 8' Derrick dewatering screen fitted with various panel sizes and a Sharples P-660 decanter centrifuge. Both pieces of equipment used for pilot testing are shown in Figures 18 and 19, respectively. The screen is preferentially designed to be used in combination with hydro-cyclones where the underflow is fed to the screens and the solids are further dewatered. The mesh size of the screens and dewatering capability is heavily dictated by the particle size distribution of the solids. The decanter centrifuge has a wider range of applications but performance is also dictated by particle size which usually can be enhanced with the use of settling aids.



Figure 18 - Dewatering Screen



Figure 19 - Decanter Centrifuge

## ANALYTICAL TECHNIQUES

For the pre-reaction kinetic evaluation elemental analysis primarily focused on the  $P_2O_5$ ,  $SO_4$ , and F concentrations in the liquid phase and  $CO_2$  in the solid phase. For this testing Ca analysis of the ore was of little interest since there was no way of differentiating between carbonate calcium and fluorapatite calcium. Therefore  $CO_2$  analysis was relied on for determining total carbonate content in the ore solids phase. For  $CO_2$  analysis of the ore, a Chittick Gasometric apparatus was utilized. In this method the ore sample is reacted with an acid such as HCl or  $HNO_3$  and the volume of carbon dioxide gas evolved is measured. The  $CO_2$  concentration by weight is then calculated from the gas volume using factors dependent on temperature and barometric pressure. However,  $CO_2$  analysis is relatively time consuming so this method was used sparingly throughout the course of testing. The liquid samples from testing were analyzed using a combination of X-Ray Fluorescence (XRF) and Inductively Coupled Plasma (ICP) Techniques. The XRF instrument was a Rigaku ZSX Primus 3 and the ICP instrument was a Perkin Elmer Optima 5300DV. Fluoride which is outside the capability range of this equipment was measured using an Orion fluoride ion selective probe with model # 9409BN. Figure 20 – 22 is a depiction of the XRF, ICP and Fluoride ion selective probe, respectively.



Figure 20 - Rigaku XRF Analyzer

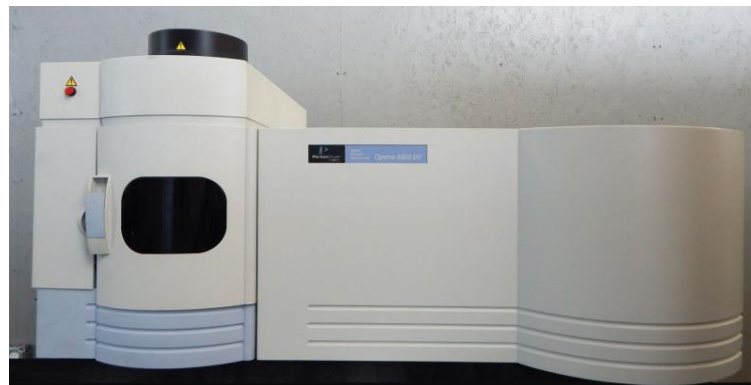


Figure 21 - Perkin Elmer ICP



Figure 22 - Thermo/Orion Fluoride Probe

For dewatering test work the primary analytical tool used was a Malvern Mastersizer 3000 for particle size analysis (PSA). The PSA was important for evaluating dewatering performance and particle size split for the various process equipment tested. The particle size

distribution typically dictates sedimentation behavior and is a critical component used for correct selection and sizing of dewatering equipment. This instrument uses laser diffraction to measure the size of particles which is achieved by measuring the intensity of light scattered as a laser beam passes through a dispersed particulate sample (Mastersizer 3000: Malvern, 2016). These data are then analyzed to calculate the size of the particles that created the scattering pattern. Figure 23 depicts the Malvern PSA equipped with both a wet and dry dispersion unit. Turbidity measurement expressed as Nephelometric Turbidity Units (NTU's) was also important in evaluating dewatering performance. Although somewhat subjective, NTU's are an indication of whether or not fine particles are settling out of solution or remaining suspended in the supernatant. Figure 24 is the Lamotte 2020we Turbidimeter used for measurement.



Figure 23 - Malvern Particle Size Analyzer



Figure 24 - Lamotte NTU Meter

The following chapters 5 through 7 present the results and discussion in the same order as the aforementioned tests in this chapter. Bench scale batch reaction kinetics are discussed in chapter 5, hydro-cyclone and sedimentation test results in chapter 6, lab pilot and plant pilot testing in chapter 7.

## CHAPTER 5: REACTION KINETIC RESULTS & DISCUSSION

This chapter is an analysis of the concentration vs. time data and how it relates to rate parameters associated with converting acids in the pond water to their insoluble salts. Data collection was described previously in chapter 4 and consisted of monitoring the liquid phase concentrations using the following acid/carbonate/ore combinations:

1. Synthetic acid solutions with limestone (carbonate)
  - a. Phosphoric Acid ( $P_2O_5$ )<sup>2</sup>
  - b. Sulfuric Acid ( $SO_4$ )<sup>3</sup>
2. Synthetic acid solutions with phosphate ore
  - a. Phosphoric Acid ( $P_2O_5$ )
  - b. Sulfuric Acid ( $SO_4$ )
3. Pond water with limestone
4. Pond water with phosphate ore

As mentioned in chapter 4 the synthetic solutions included only sulfuric and phosphoric acid and did not include hydrofluoric acid due to safe-handling concerns. Therefore concentration vs. time data for fluoride could only be evaluated using pond water.

### $P_2O_5$ EVALUATION

Figures 25 through 27 show the normalized concentration & pH vs. time data at constant temperatures of 75°F, 100°F and 120°F when synthetic solutions of phosphoric acid were reacted with limestone. The normalized concentration is found by dividing the instantaneous molar concentration,  $C_A$ , at a given time 't' by the initial molar concentration,  $C_{A0}$ , given at time  $t = 0$ . The relationship between concentration and conversion, which will be referenced throughout the chapter, is shown in equation 5.1 below.

$$Conversion = 1 - \frac{C_A}{C_{A0}} \quad (5.1)$$

---

<sup>2</sup> In this discussion the terms  $P_2O_5$  and phosphoric acid ( $H_3PO_4$ ) are used interchangeably.

<sup>3</sup> In this discussion the terms  $SO_4$  and sulfuric acid ( $H_2SO_4$ ) are used interchangeably.

It can be seen that all of the reactions consistently reached completion at ~80% conversion and a terminal pH of ~6.0. There also appeared to be a slight time delay before any measurable change in concentration occurred in the liquid phase. This time delay which is denoted on figures 25 and 26, decreased as the reaction temperature increased. At ambient temperatures the time delay was ~10 minutes, at 100°F ~5 minutes and at 120°F it was almost non-existent.

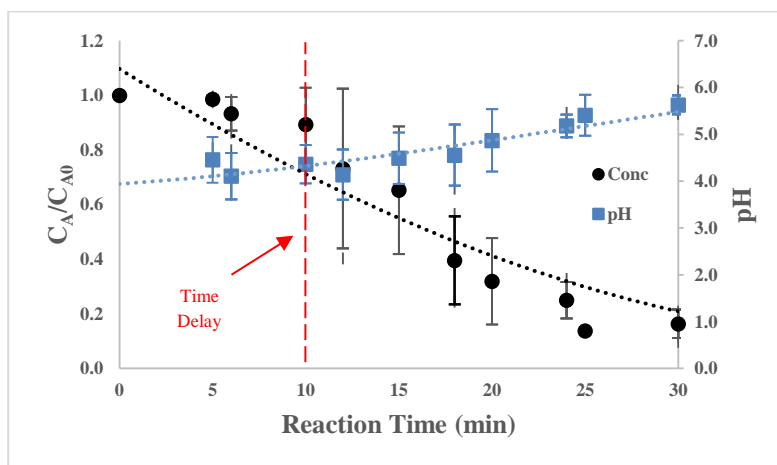


Figure 25 - 75°F P<sub>2</sub>O<sub>5</sub> Solution Concentration & pH vs. Time w/Limestone

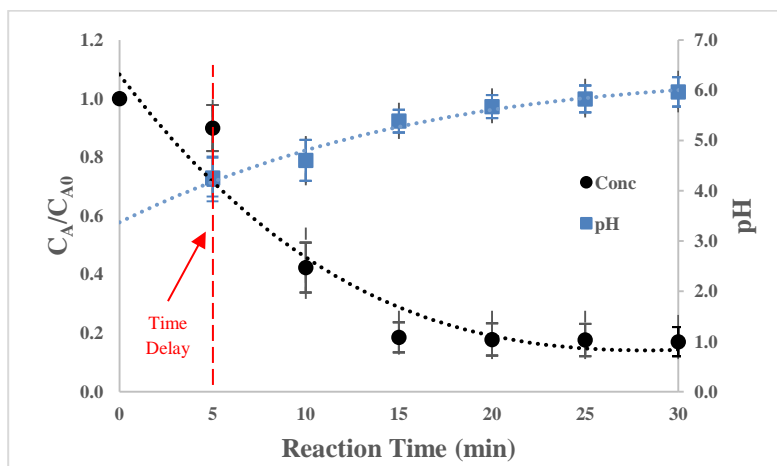


Figure 26 - 100°F P<sub>2</sub>O<sub>5</sub> Solution Concentration & pH vs. Time w/Limestone

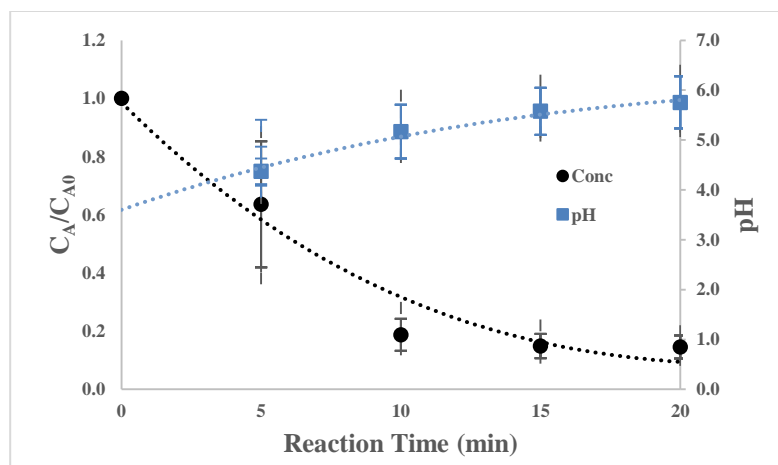


Figure 27 - 120°F P<sub>2</sub>O<sub>5</sub> Solution Concentration & pH vs. Time w/Limestone

Comparatively the normalized concentration and pH data are also shown for reactions of synthetic phosphoric acid solutions with phosphate ore. Here we saw two separate behaviors: the first which is shown in figures 28 through 30 and the second which is shown in figures 31 through 33. Again normalized concentration is shown on the primary axis and pH on the secondary axis. The first set of behavior was observed when initial acid concentrations were greater than or equal to 1.5% P<sub>2</sub>O<sub>5</sub> (0.106M) and exhibited similar characteristics to the reactions with limestone in that 1) they both had a time delay followed by 2) a convex decline in concentration. However, they also had the following distinctions: On average these reactions had a time delay 4 to 6 times longer than with limestone, as shown in Table 8, and took 3 to 4 times longer to reach completion at ~80% conversion. The terminal pH at completion was also lower at ~ 4.5.

Table 8 - Reaction Time Delay

Reactant/Temperature:	75°F	100°F	120°F
Limestone	10 min	5 min	-
Ore	40 min	30 min	15 min

The first set of behavior is labeled with a “2<sup>nd</sup> proton” notation to differentiate between the second set of behavior which is labeled with a “1<sup>st</sup> proton” notation. The reasoning behind this has to do with the 1<sup>st</sup> and 2<sup>nd</sup> proton dissociation of the triprotic phosphoric acid, H<sub>3</sub>PO<sub>4</sub>,

which is believed to dictate the behavior of the concentration profile as function of time. More on this will be discussed later in the chapter.

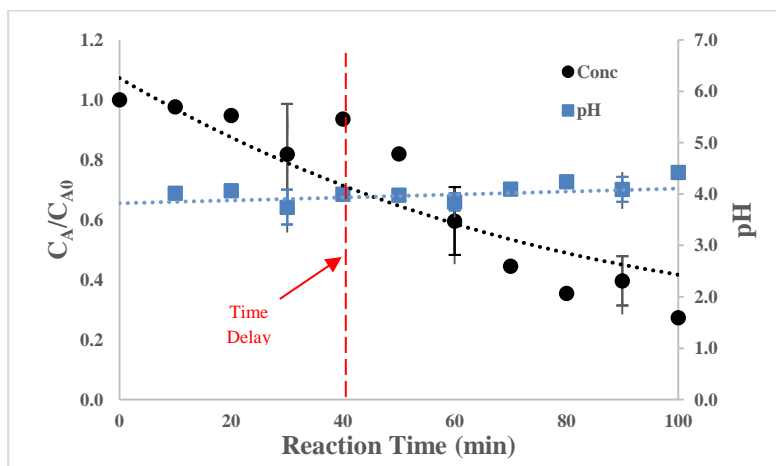


Figure 28 – 75°F  $P_2O_5$  Solution Concentration vs. Time w/Ore (2<sup>nd</sup> Proton)

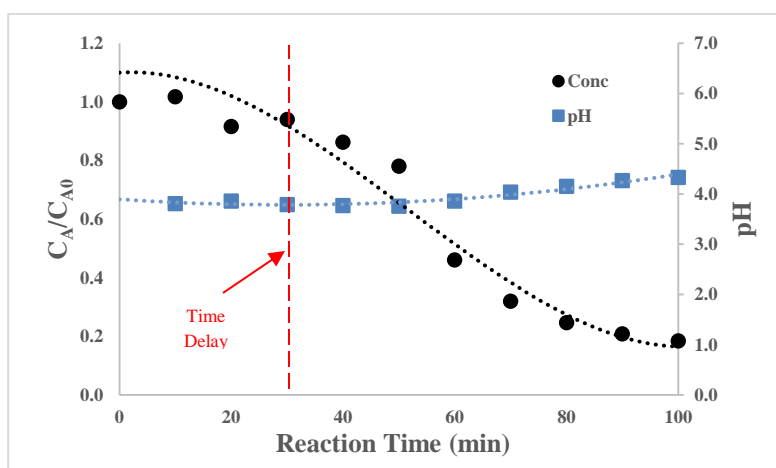


Figure 29 - 100°F  $P_2O_5$  Solution Concentration vs. Time w/Ore (2<sup>nd</sup> Proton)

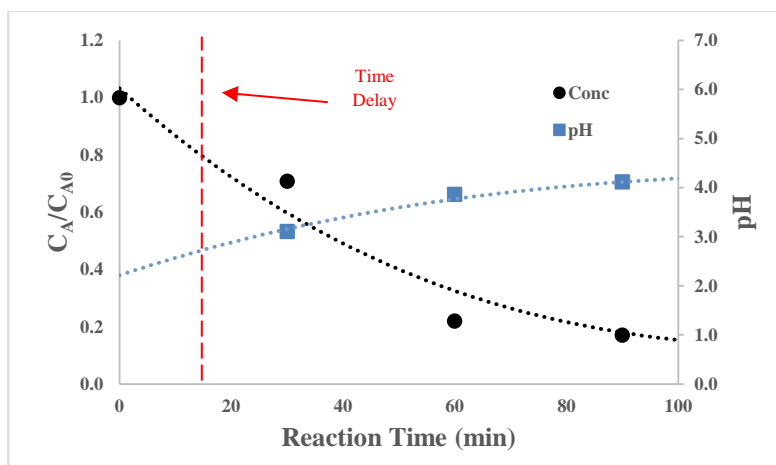


Figure 30 - 120°F  $P_2O_5$  Solution Concentration vs. Time w/Ore (2<sup>nd</sup> Proton)

The second set of behavior was seen when starting concentrations of the phosphoric acid solution were below 1.5%  $P_2O_5$ . Here the concentration as a function of time exhibited very different behavior than what was seen previously for the three reaction temperatures. The concentration decreased very slowly with linear behavior and reached a terminal conversion of only 20%. Also note that the pH remained relatively unchanged at ~4.0 over the course of the reaction, whereas the pH increased in the previous data sets.

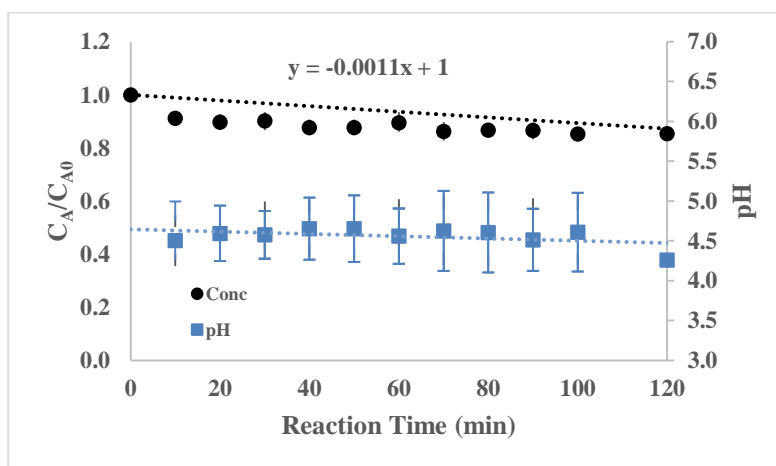


Figure 31 - 75°F  $P_2O_5$  Solution Concentration vs. Time w/Ore (1<sup>st</sup> Proton)

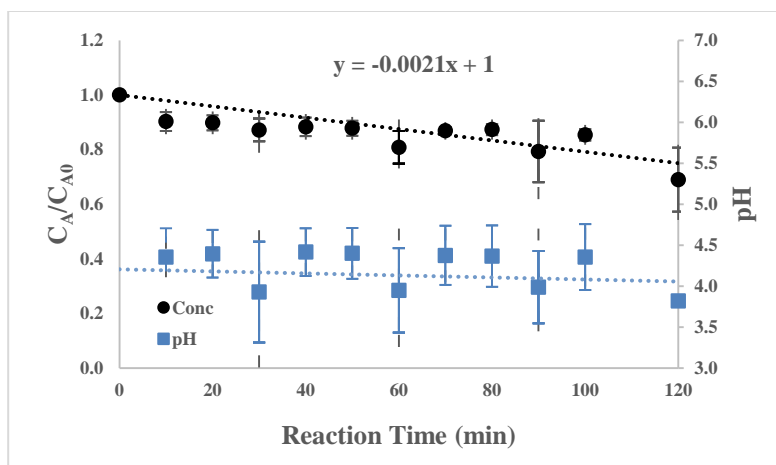


Figure 32 - 100°F P<sub>2</sub>O<sub>5</sub> Solution Concentration vs. Time w/Ore (1<sup>st</sup> Proton)

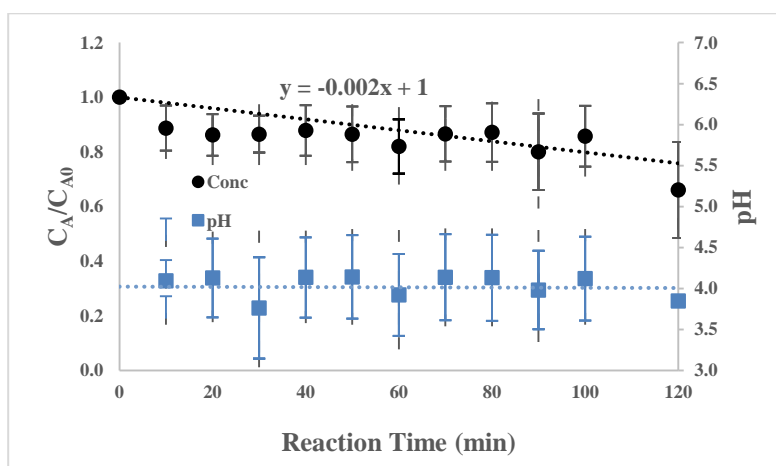


Figure 33 - 120°F P<sub>2</sub>O<sub>5</sub> Solution Concentration vs. Time w/Ore (1<sup>st</sup> Proton)

From the first two sets of data with limestone and phosphate ore we observe that there is a clear relationship between increased rate of reaction and increased temperature. Incremental increases in temperature decreased the observed time delay and reduced the amount of time required for the reaction to reach completion at ~80% conversion. This relationship with temperature is less clear in the second set of behavior seen with phosphate ore in figures 31 through 33.

In order to determine the rate constant and rate order both linear and non-linear regression software from Polymath were used to evaluate the data. From chapter 2 we assumed the rate law took the following form.

$$R = k[A]^m[B]^n \quad (2.7)$$

However, because the concentration of carbonate, the solid reactant (B), is in excess of the liquid reactant (A) the assumption was made that the concentration of the solid reactant would be relatively unchanged throughout the course of the reaction. Since the molar ratio of reactant B to A was greater than 10:1 this allows equation 2.7 to be simplified by considering  $k'$  as a constant as shown in equation 5.2. Measurement of the initial and final carbonate concentration of the solid reactant indicated this assumption was valid.

$$k[B]^N = k' \quad (5.2)$$

The simplified rate law can then be written as

$$R = k'[A]^m = k'C_A^m \quad (5.3)$$

Which allows us to express the change in concentration over time as

$$-\frac{dC_A}{dt} = R = k'C_A^m \quad (5.4)$$

Integrating this equation using the initial condition  $t = 0$  and  $C_A = C_{A0}$  for  $m \neq 1$  gives Equation 5.5.

$$t = \frac{1}{k'} \frac{C_{A0}^{(1-m)} - C_A^{(1-m)}}{(1-m)} \quad (5.5)$$

For  $m = 1$ , the equation would take the following form

$$C_A/C_{A0} = C_{A0} e^{-k't} \quad (5.6)$$

Taking the natural log of both sides gives

$$\ln \left[ \frac{C_A}{C_{A0}} \right] = -k't + \ln[C_{A0}] \quad (5.7)$$

Equation 5.5 allowed the use of Polymath non-linear regression software to iteratively solve for values of  $k'$  and  $m$  by minimizing the sum of squares of differences between measured and calculated time values. However, it must be noted that when the reaction is first order this method will not work since  $m \neq 1$ , a plot of  $\ln[C_{A0}/C_A]$  vs time must be used instead. For  $N$  data points the software uses the following Equation 5.8 to calculate sum of squares.

$$S^2 = \sum_{i=1}^N (t_{mi} - t_{ci})^2 = \sum_{i=1}^N \left( t_{mi} - \frac{C_{A0}^{1-m} - C_A^{1-m}}{k'(1-m)} \right)^2 \quad (5.8)$$

The issue with this method is the curvature of the concentration vs. time data as shown previously in the  $P_2O_5$  with limestone data sets, Figures 25 through 27, and the first set of  $P_2O_5$  with phosphate ore data sets, Figures 28 through 30. At the start of the reaction and at lower temperatures there was an evident time delay in the reaction. Including this time delay in the non-linear regression data resulted in a negative reaction order, which implies that  $P_2O_5$  concentration in the liquid phase has an inverse effect on the rate of reaction. However, since  $P_2O_5$  in itself is a normalized value for phosphoric acid,  $H_3PO_4$ , as well as its dissociated form  $H_2PO_4^-$  or  $HPO_4^{2-}$  it is believed that multiple steps occurred involving intermediates which increased the complexity of the reaction. Therefore the solubility of the likely intermediates and products may have given a false indication of the extent of reaction since there was a steady increase in pH over the course of the reaction. With the exception of the second set of  $P_2O_5$  with phosphate ore data sets, Figures 31 through 33, where pH was unchanged this issue was common across all  $P_2O_5$  reaction rate data.

By re-zeroing the time scale to the end of the time delay caused by the first proton dissociation it was found that the rate law was most accurately represented by first order reaction kinetics for the two similar data sets of behavior seen with limestone and phosphate ore. This was determined by plotting the natural log of normalized concentration,  $\ln[C_A/C_{A0}]$ , vs time and then using linear regression to find the rate constant,  $k'$ . Initially the sum of squares method discussed earlier in the chapter was used to converge on a solution, however,

since the sum of squares method should not be used for first order reactions the natural log technique was used instead to find a more accurate representation. Since the data is expressed as percent conversion the last term in Equation 5.7 goes to zero and the  $k'$  term can be determined using simple linear regression. Figure 34 and 35 shows the natural log plot of conversion as function of time. Here the slope of the line represents the negative value of the rate constant,  $k'$ .

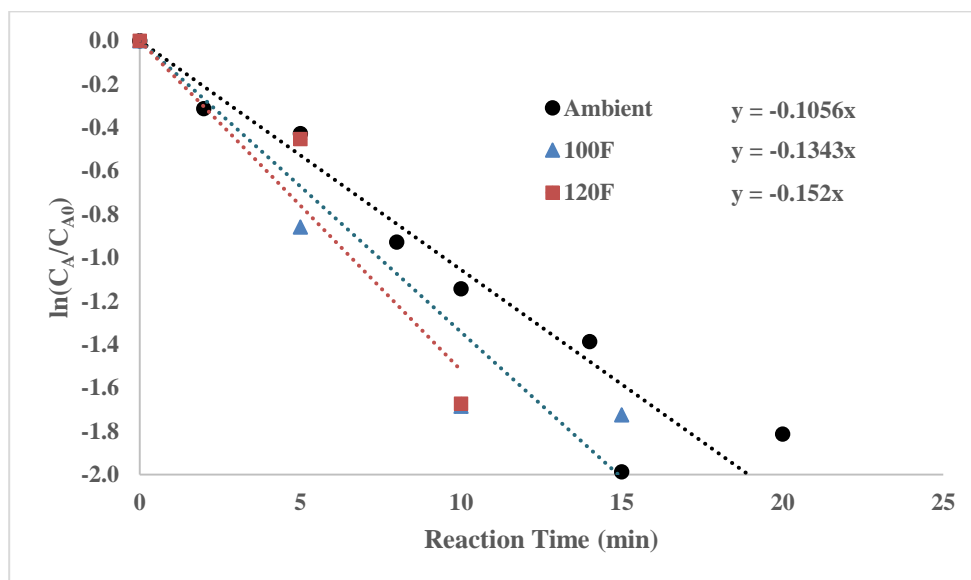


Figure 34 -  $P_2O_5$  w/Limestone Natural Log of Concentration vs Time

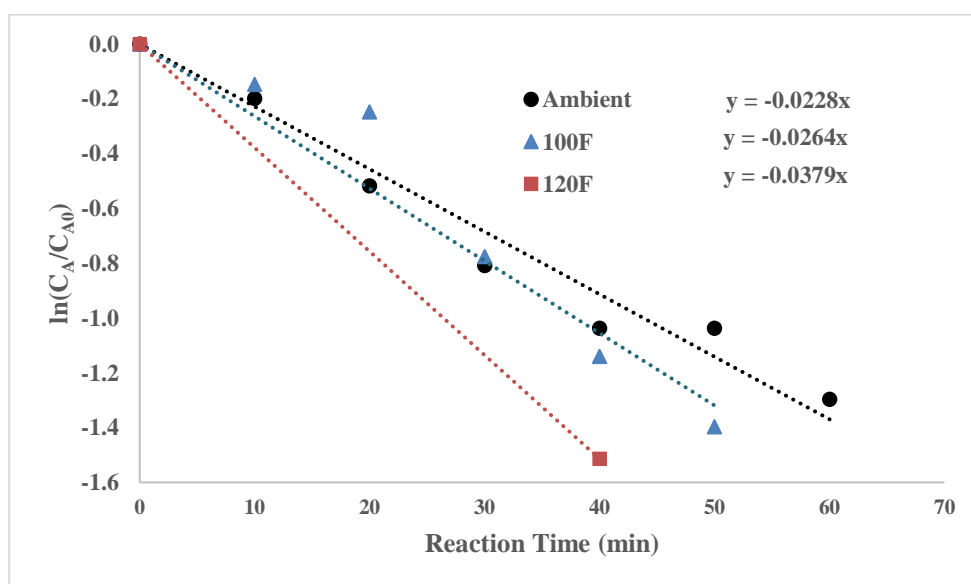


Figure 35 -  $P_2O_5$  w/Ore (2<sup>nd</sup> Proton) Natural Log of Concentration vs Time

Since the third set of  $P_2O_5$  data dominated by the 1<sup>st</sup> proton dissociation, Figures 5.7 through 5.9, had a linear normalized concentration-time relationship the reaction was represented by zero order kinetics as shown in equation 5.9. Here the rate constant  $k'$  is simply the slope from the regression line.

$$\frac{C_A}{C_{A0}} = C_{A0} - k't \quad (5.9)$$

In order to find the relationship between temperature and reaction kinetics, we know from chapter 2 that the Arrhenius temperature equation takes the following form.

$$k(T) = Ae^{-E/RT} \quad (2.8)$$

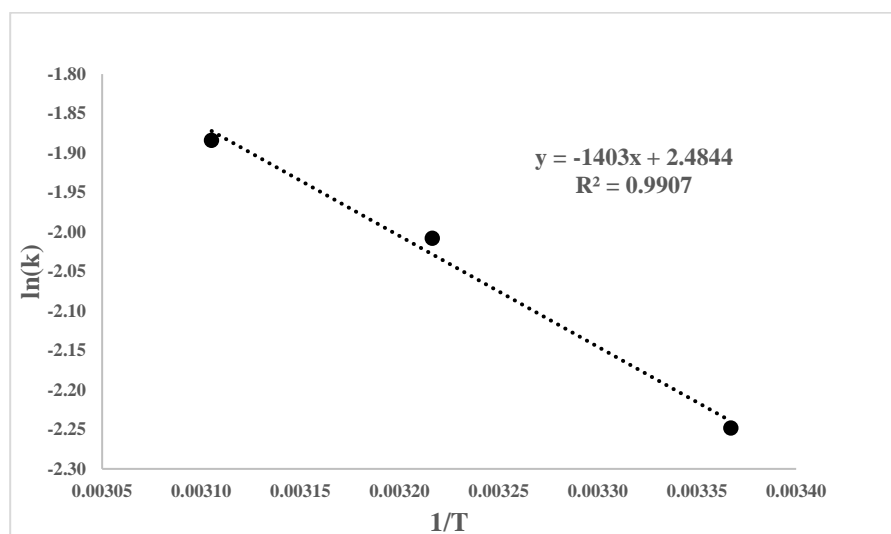
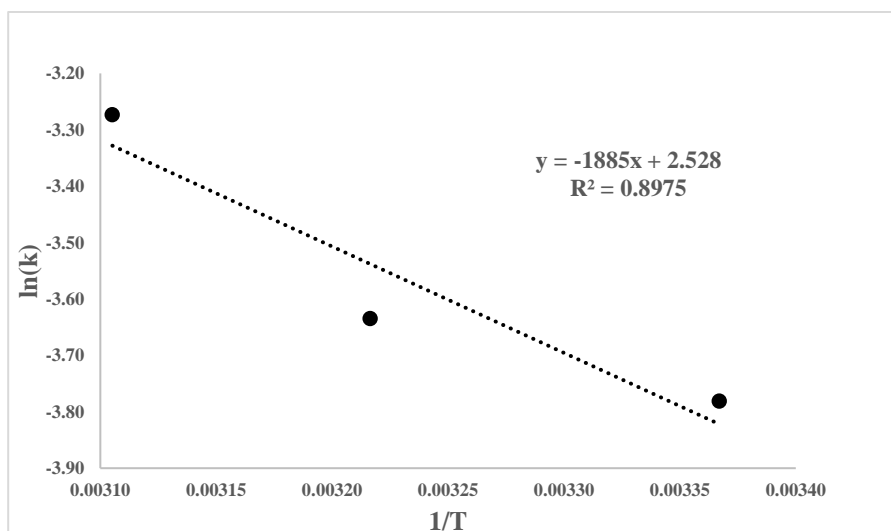
We can convert this to equation 5.10 by taking the natural log of both sides of the equation.

$$\ln(k) = \ln(A) - \frac{E}{R} \left( \frac{1}{T} \right) \quad (5.10)$$

Plotting the rate constant data generated from the three different  $P_2O_5$  reaction data sets in Table 9, we see that  $\ln(k')$  vs.  $1/T$  can be predicted using a linear model as shown in figure 5.14 through 5.16. These represent the reactions of  $P_2O_5$  with limestone,  $P_2O_5$  with phosphate ore dominated by the 2<sup>nd</sup> proton dissociation and  $P_2O_5$  with phosphate ore dominated by the 1<sup>st</sup> proton dissociation, respectively. Using the regression model, values for  $\ln(A)$  and  $\frac{E}{R}$  are predicted. The values for  $k'$  ( $min^{-1}$ ),  $A$  ( $min^{-1}$ ) and  $E$  ( $J/mol$ ) are shown in Table 5.2. Note that these units apply to a first order reaction, shown in the 2<sup>nd</sup> and 3<sup>rd</sup> columns. For a zero order reaction, shown in the final column, the units change to ( $M * min^{-1}$ ) for both  $k'$  and  $A$ .

Table 9 - Arrhenius Temperature Dependence for P<sub>2</sub>O<sub>5</sub> w/Limestone & Phosphate Ore

Reaction Temperature (K)		Limestone		Phosphate Ore (2 <sup>nd</sup> Proton)		Phosphate Ore (1 <sup>st</sup> Proton)	
T	1/T	k' (min <sup>-1</sup> )	ln(k')	k' (min <sup>-1</sup> )	ln(k')	k' (M*min <sup>-1</sup> )	ln(k')
297	0.0034	0.106	-2.25	0.0228	-3.78	0.0011	-6.81
311	0.0032	0.134	-2.01	0.0264	-3.63	0.0021	-6.17
322	0.0031	0.152	-1.88	0.0379	-3.27	0.0020	-6.21
		A = 11.9	E = 11,660	A = 12.5	E = 15,680	A = 3.86	E = 19,940

Figure 36 - P<sub>2</sub>O<sub>5</sub> w/Limestone Arrhenius Temperature DependenceFigure 37 - P<sub>2</sub>O<sub>5</sub> w/Ore Arrhenius Temperature Dependence (2<sup>nd</sup> Proton)

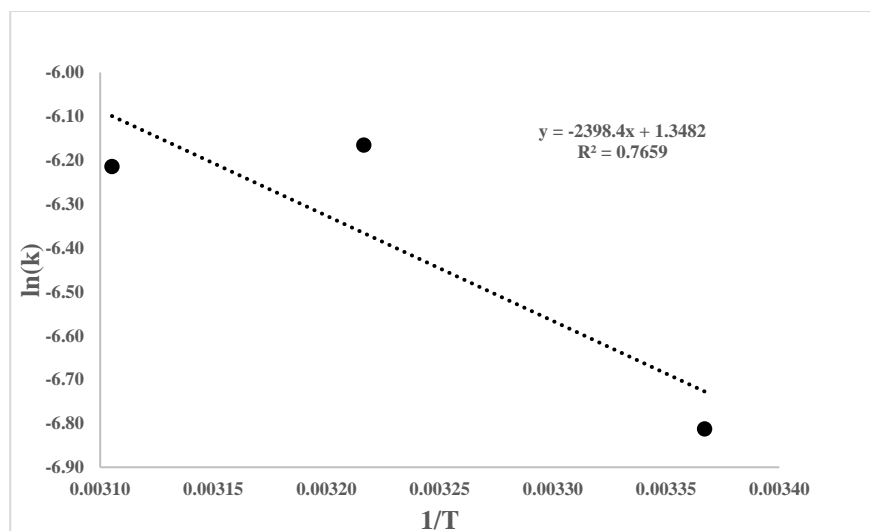


Figure 38 - P<sub>2</sub>O<sub>5</sub> w/Ore Arrhenius Temperature Dependence (1<sup>st</sup> Proton)

All three data sets appear to exhibit Arrhenius temperature dependence in the range from ambient (75°F) to 120°F. The R<sup>2</sup> values for the regression line in Figures 36 and 37 showed very good agreement at or above 0.90. Although the R<sup>2</sup> value was slightly less in Figure 38 at 0.76 the behavior was still consistent with Arrhenius temperature dependence. From the experiments using synthetic phosphoric acid solutions and the P<sub>2</sub>O<sub>5</sub> concentration-time data we are able to draw three important conclusions:

1. 80% conversion of phosphoric acid to insoluble dibasic calcium phosphate is achievable with starting concentrations at or ~1.5% P<sub>2</sub>O<sub>5</sub> using phosphate ore and/or limestone.
2. Reaction time can be reduced by increasing reaction temperature and ranges from 100 to 60 minutes based on temperatures from ambient (75°F) to 120°F.
3. Impurities in the phosphate ore matrix likely reduce the availability carbonate because of the observed increase in reaction time requirements compared to limestone.

#### EXPLANATION OF TIME DELAY & REACTION INTERMEDIATE SOLUBILITY

In order of reaction, we expected the sulfuric acid to react first followed by phosphoric acid and then hydrofluoric acid. The basis being pK<sub>a</sub> values and the relationship between pH and conjugate acid-base pairs expressed by the Henderson-Hasselbalch equation 5.11.

$$pH = pK_a + \log \frac{[base]}{[acid]} \quad (5.11)$$

A review of reaction intermediates, solubilities and  $pK_a$  values proved that this could be a problem as indicated in Table 10. Here the data is presented in order of expected reaction occurrence based on  $K_a$  and corresponding  $pK_a$  values. Also included is the intermediate ionization reaction occurring at a given  $pK_a$  value, the salt product formed and its solubility in mg/ml. The pH stays well above 3 during the reaction so sulfuric acid should have completely dissociated in solution to form  $CaSO_4$  (gypsum), however; with phosphoric acid we likely only saw the first and second proton dissociate to form  $Ca(H_2PO_4)_2$  (mono-calcium phosphate) and  $CaHPO_4$  (dibasic calcium phosphate) since the pH of the reaction only ranged from 3 to 5. The original hypothesis ignored reaction intermediates and made the assumption that all phosphoric acid would be converted to  $Ca_3(PO_4)_2$ . Yet the  $pK_a$  required for this to happen is 12.34, so in the acid pH range of the reaction this product never could have formed, only the first and second salt products mono and dibasic calcium phosphate.

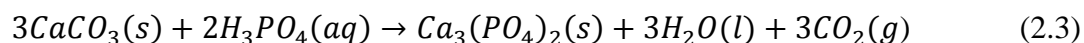
Table 10 - Reaction Order, Solubility and Salts Formed (*Masterton & Hurley, 2009*)

Reaction Order	Acid	$K_a$	$pK_a$	Ionization Involved	Salt Formed	Solubility (mg/mL)
1 <sup>st</sup>	$H_2SO_4$	$2.40 \times 10^6$	-6.38	$H_2SO_4 \rightarrow H^+ + HSO_4^-$	$Ca(HSO_4)_2$	-
2 <sup>nd</sup>	$HSO_4^-$	$1.00 \times 10^{-2}$	2.00	$HSO_4^- \rightarrow H^+ + SO_4^{2-}$	$CaSO_4$	2.1
3 <sup>rd</sup>	$H_3PO_4$	$7.10 \times 10^{-3}$	2.15	$H_3PO_4 \rightarrow H^+ + H_2PO_4^-$	$Ca(H_2PO_4)_2$	16.7
4 <sup>th</sup>	HF	$6.60 \times 10^{-4}$	3.18	$HF \rightarrow H^+ + F^-$	$CaF_2$	0.016
5 <sup>th</sup>	$H_2PO_4^-$	$6.20 \times 10^{-8}$	7.21	$H_2PO_4^- \rightarrow H^+ + HPO_4^{2-}$	$CaHPO_4$	0.2
6 <sup>th</sup>	$HPO_4^{2-}$	$4.60 \times 10^{-13}$	12.34	$HPO_4^{2-} \rightarrow H^+ + PO_4^{3-}$	$Ca_3(PO_4)_2$	0.02

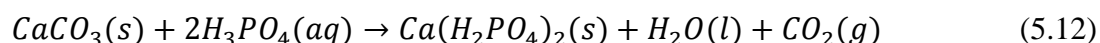
Mono-calcium phosphate has a very high solubility at 16.7 mg/ml. At the highest experimental starting concentration, 3%  $P_2O_5$  or 0.142 M of equivalent salt, 50% of the salt would remain in solution if 100% of the  $P_2O_5$  present as phosphoric acid were converted to mono-calcium phosphate. At or below starting concentrations of 1.5%  $P_2O_5$  or 0.071 M of equivalent salt, 100% of the salt would remain in solution because of the high solubility of mono-calcium phosphate. Therefore even if the phosphoric acid present in solution were reacting with the carbonate in the phosphate ore it would be difficult to accurately measure percent conversion based on the liquid concentration alone.

Dibasic calcium phosphate, the second ionization product which starts to dominate the reaction as the pH nears 4 and above, has a much lower solubility at 0.2 mg/ml. At the highest experimental starting concentration, 3% P<sub>2</sub>O<sub>5</sub> or 0.284 M of equivalent salt, only 1.0% of the salt would remain in solution if 100% of the P<sub>2</sub>O<sub>5</sub> present as phosphoric acid were converted to dibasic calcium phosphate. At or below starting concentrations of 1.5% P<sub>2</sub>O<sub>5</sub> or 0.142 M of equivalent salt, 0.5% of the salt would remain in solution and at 0.75% or 0.072M of equivalent salt, 0.25% would remain in solution. Therefore if the second ionization step dominates the reaction then analysis of the liquid fraction alone is a relatively accurate method for determining the extent of phosphoric acid conversion due to the low solubility of dibasic calcium phosphate.

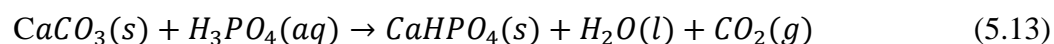
Based on the pH of the reacting solution when phosphoric acid is pre-reacted with ore slurry, the base chemical reaction likely takes the form of equation 5.12 and 5.13 as shown below instead of equation 2.3 as predicted in chapter 2.



1. Mono-calcium phosphate – up to pH 4.7



2. Dibasic calcium phosphate – between pH 4.7 and 9.8



Since phosphoric acid is a triprotic acid, all three protons do not dissociate simultaneously within the solution; they have different degrees of dissociation, and the protons are lost through several stages, with one dissociation at each stage. Now, if we note that the acid ionization constant,  $K_a$ , decreases at each stage (i.e.  $K_{a1} > K_{a2} > K_{a3}$ ) or the  $pK_a$  increases at each stage then we can predict how many protons are lost in a reaction based on the pH and  $pK_a$  values of the reacting solution using equation 5.11 presented earlier. The fractional degree of dissociation of each proton for phosphoric acid, in terms of pH of the

reacting solution, is shown in the Figure 39 below. Note that each  $pK_a$  value corresponds to the pH when 50% of the conjugate acid and 50% of the conjugate base are present in solution. If the pH is below the  $pK_a$  then more than 50% of the conjugate acid is present in solution, if the pH is above the  $pK_a$  then more than 50% of the conjugate base is present in solution.

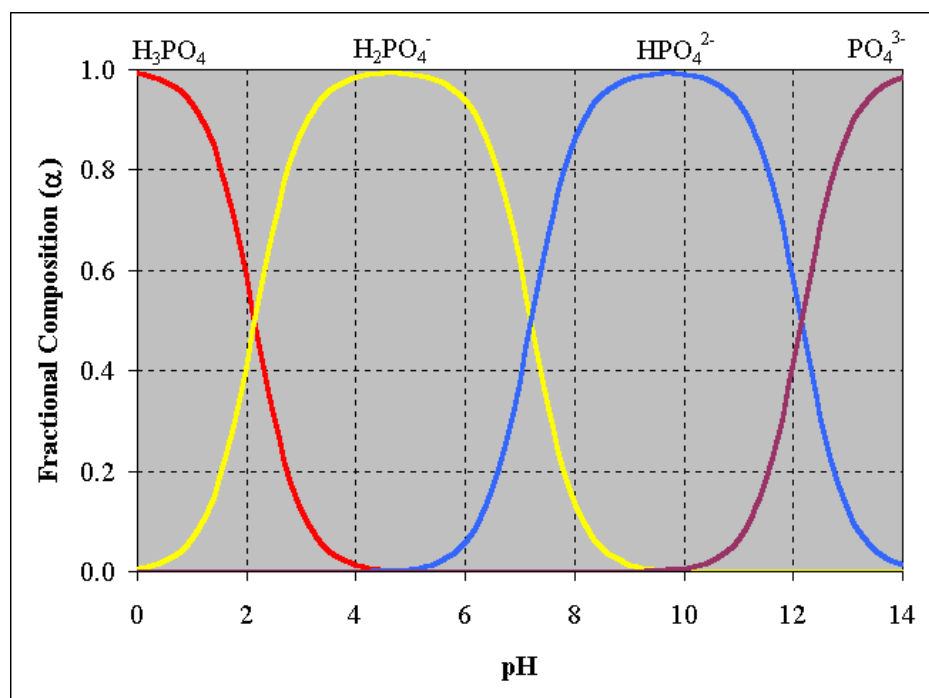


Figure 39 - Proton Dissociation for Phosphoric Acid

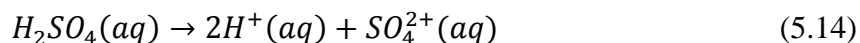
Since the pH of the reacting solution is always in the range of 3 to 5 in the ore pre-reaction process, phosphoric acid is never completely void of all protons. In fact in our range, less than  $\frac{1}{2}$  of the second proton is dissociated from the triprotic acid. However, since monocalcium phosphate,  $\text{Ca}(\text{H}_2\text{PO}_4)_2$ , is highly soluble in water, whereas dibasic calcium phosphate,  $\text{CaHPO}_4$ , is not, the chemical reaction doesn't reach a reversible equilibrium when we reach the pH range of 4 to 5. As dibasic calcium phosphate precipitates out from the reacting body, the reaction is driven to the right until a majority of the phosphoric acid reacts with calcium carbonate,  $\text{CaCO}_3$ , to form dibasic calcium phosphate,  $\text{CaHPO}_4$ . And even though the carbonate is in great excess to the stoichiometric amount required to neutralize all of the phosphoric acid in solution it is plausible that the reaction only reaches an apparent

80% conversion based on liquid phase concentrations because the remaining 20% of  $P_2O_5$  is dissolved in solution as mono-calcium phosphate,  $Ca(H_2PO_4)_2$ .

#### SO<sub>4</sub> EVALUATION

In the next set of data we examine the behavior of synthetic sulfuric acid solutions when reacted with limestone and phosphate ore. Here we also saw two sets of behavior irrespective of temperature which is believed to be driven by the solubility of the reaction products introduced in the previous section. At low starting concentrations, below 0.5% SO<sub>4</sub>, the reaction showed no change in liquid phase concentrations. This occurred when synthetic sulfuric acid solutions were reacted with both limestone and ore as shown in Figures 40 and 41. However, we saw a steady increase in pH over the course of the reaction indicating that the acid neutralization reaction was in fact happening. In these figures concentration is shown in the primary axis and pH on the secondary axis as a function of time. The solubility of CaSO<sub>4</sub> is 2.1 mg/ml, so at starting concentrations below 0.5% SO<sub>4</sub> or 0.017M of equivalent salt, 88% of the ionization salt product will remain in solution if 100% of the sulfuric acid were converted to the calcium sulfate. This explains why little to no change in concentration was seen in the liquid phase.

Although because a pure solution of sulfuric acid was used it was possible to predict the concentration of SO<sub>4</sub> present as H<sub>2</sub>SO<sub>4</sub> in the liquid phase using pH. From stoichiometry in equation 5.14 we know that there are twice as many  $H^+$  ions in solution as H<sub>2</sub>SO<sub>4</sub> or SO<sub>4</sub> when the acid completely dissociates. We also know that the pH and hydrogen ion concentration,  $[H^+]$ , are related by equation 5.15. As a result a “predicted concentration” is also shown in Figures 40 through 43.



$$[H^+] = 10^{-pH} \quad (5.15)$$

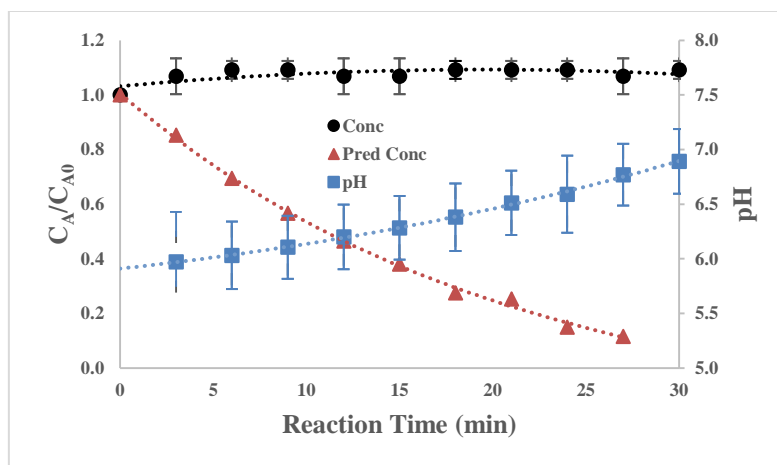


Figure 40 -  $\text{SO}_4$  Solution Concentration & pH vs Time w/Limestone (Low Concentration)

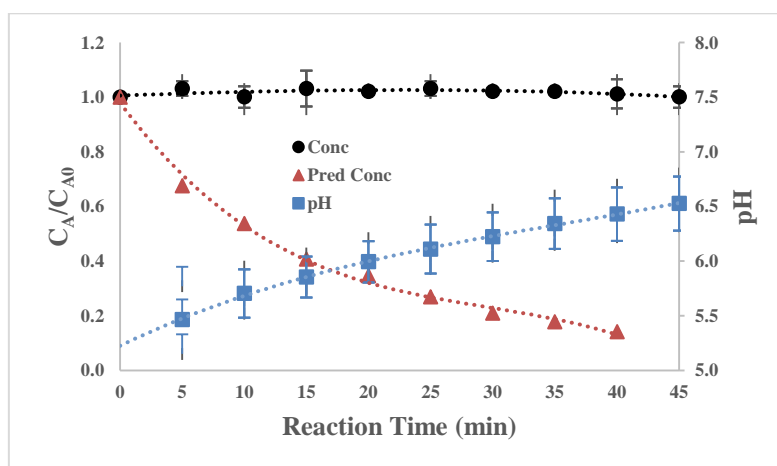


Figure 41 -  $\text{SO}_4$  Solution Concentration & pH vs Time w/Ore (Low Concentration)

At starting concentrations above 0.5% we did see a drop in liquid phase concentration as shown in Figures 42 and 43 for reactions with both limestone and phosphate ore. However, the reactions happened so quickly that it was not possible to measure any intermediate data. 5 minutes was the shortest possible sample interval and by the time the second sample was taken the reaction had already reached apparent completion based on the liquid phase analysis.

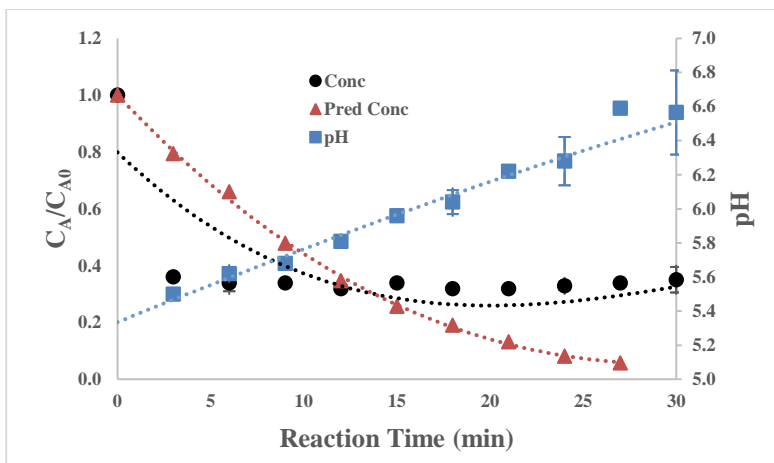


Figure 42 -  $\text{SO}_4$  Solution Concentration & pH vs Time w/Limestone (High Concentration)

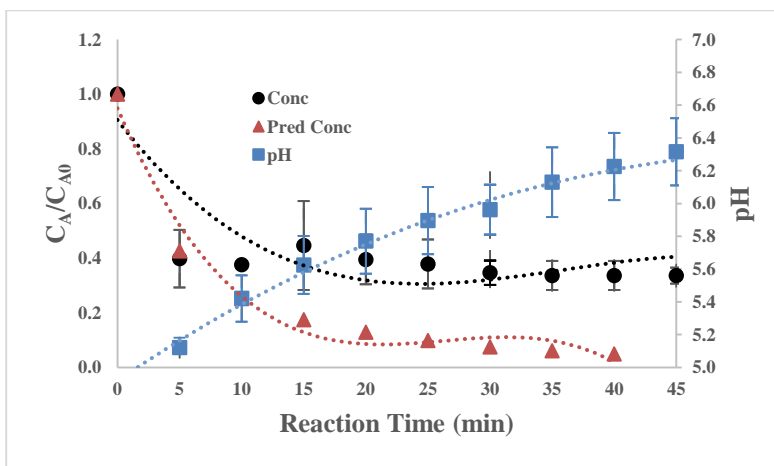


Figure 43 -  $\text{SO}_4$  Solution Concentration & pH vs Time w/Ore (High Concentration)

The terminal concentrations also correlate to the solubility of the reaction product, above 0.5%  $\text{SO}_4$  or 0.07M of equivalent salt, 22% of the ionization salt product would remain in solution if 100% of the sulfuric acid were converted to calcium sulfate,  $\text{CaSO}_4$ . Therefore with analysis of the liquid fraction alone it was not feasible to generate meaningful concentration vs time data that would allow for any type of kinetic modeling. However, the predicted concentrations based on pH exhibited first order reaction kinetic as shown by taking the natural log of concentration in Figure 44.

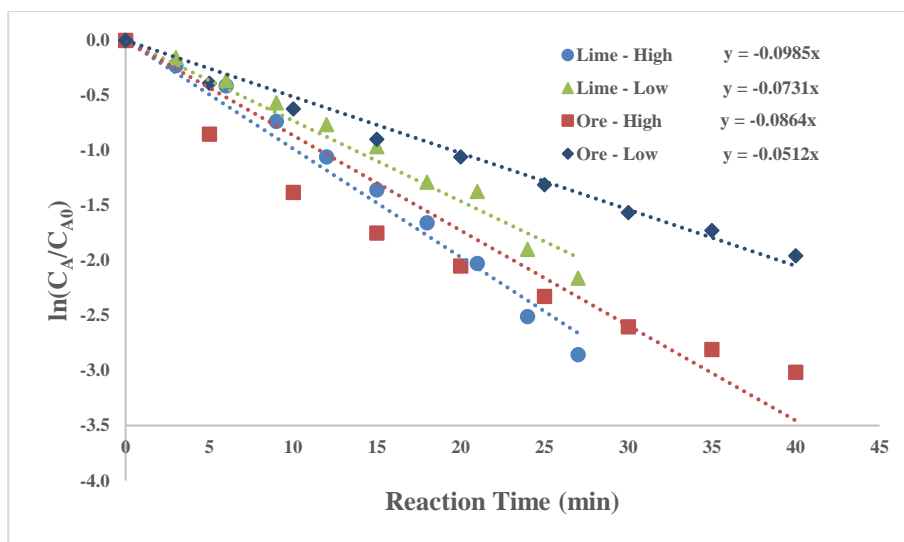


Figure 44 -  $\text{SO}_4$  Natural Log of pH Predicted Concentration vs Time

The following conclusions can be drawn from the batch test data generated using synthetic solutions of sulfuric acid:

1. 70% conversion of sulfuric acid to insoluble calcium sulfate is achievable with starting concentrations above 0.5%  $\text{SO}_4$  using phosphate ore and/or limestone as a neutralizing agent. At or below a starting concentration of 0.5%  $\text{SO}_4$ , conversion to the solid phase is not measurable.
2. At high starting concentrations ( $> 0.5\% \text{SO}_4$ ) the reaction reaches apparent completion in less than 5 minutes.
3. Impurities in the phosphate ore matrix have no apparent impact on the observed reaction rate in comparison to limestone.

## POND WATER EVALUATION

Moving on to the evaluation of pond water reacted with phosphate ore and limestone we see similar behavior compared to what was seen with the synthetic solutions as shown in Figure 45 and 46. Concentration is shown in the primary axis and reaction pH on the secondary axis as a function of time, each trends are labeled respectively. Starting with  $\text{P}_2\text{O}_5$  there is the same time delay in concentration change due to the first proton dissociation. Again we see a sudden drop on concentration occurring as the pH inflects upwards which is consistent with the 2<sup>nd</sup> proton dissociation of phosphoric acid dominating the reaction.

Comparing the time scale we also see that the reaction takes 2-3 times as long with ore to reach completion. Additionally all reactions only achieved a 40% conversion of  $P_2O_5$  to its insoluble salt when using pond water. With synthetic solutions 80% conversion was achieved which leads us to believe there must be interference with the competing side reactions.

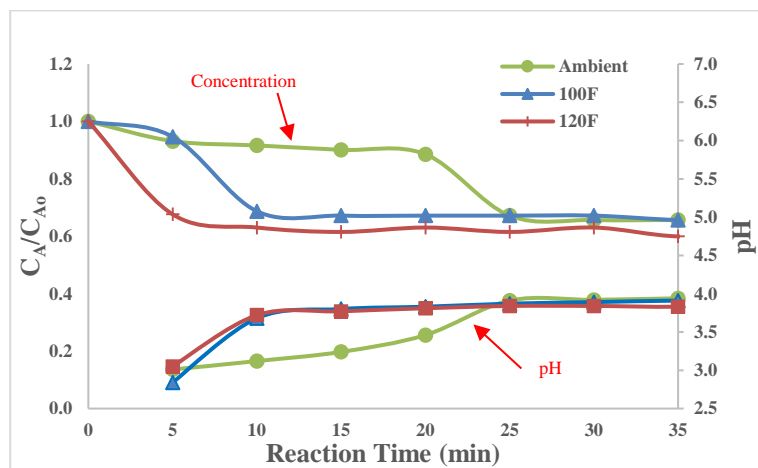


Figure 45 - Pond Water  $P_2O_5$  Concentration & pH vs Time w/Limestone

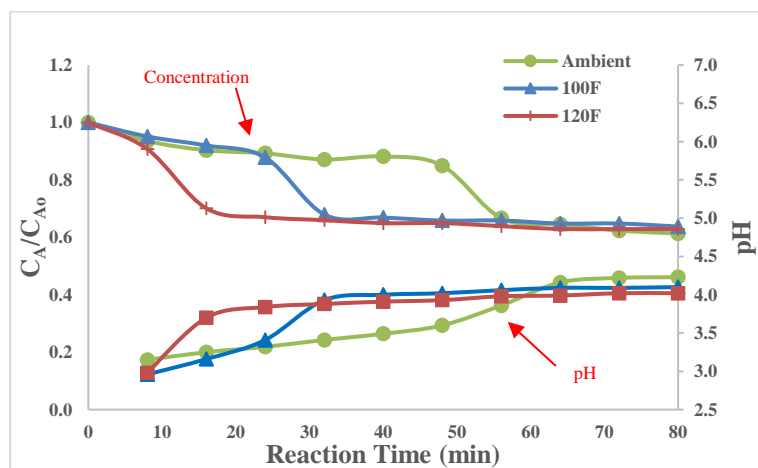
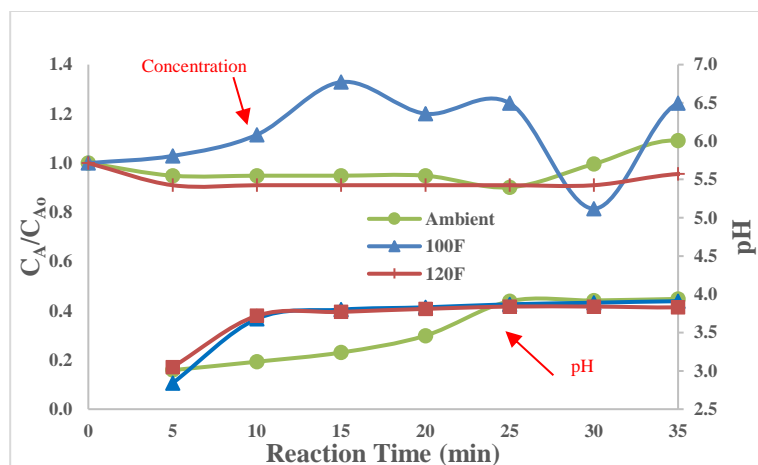
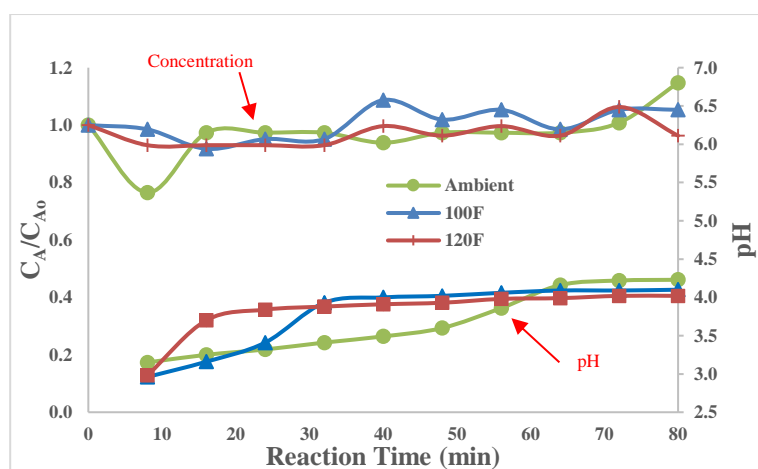


Figure 46 - Pond Water  $P_2O_5$  Concentration & pH vs Time w/Ore

$SO_4$  also exhibited the same behavior as the synthetic solutions as shown in Figure 47 and 48. The starting concentration was  $\sim 0.5\%$  so we expected to see very little/if any change in concentration due to the solubility of the product. The data shows that this was in fact the case, indicating again that liquid concentration data alone is not adequate for kinetic modeling, especially in the case of sulfuric acid.

Figure 47 - Pond Water SO<sub>4</sub> Concentration vs Time w/LimestoneFigure 48 - Pond Water SO<sub>4</sub> Concentration vs Time w/Ore

Fluoride concentration vs time data from pond water is shown in Figure 49 and 50 for reactions with limestone and phosphate ore. Concentration is shown on the primary axis and pH on the secondary axis as a function of time with each labeled respectively. The fluoride exhibited similar behavior to P<sub>2</sub>O<sub>5</sub>, but solubility of the reaction product should not have had an effect. CaF<sub>2</sub> has a solubility of 0.016 mg/ml, at a starting concentration of 0.75% F or 0.133M of equivalent salt, only 0.15% of the solids would remain in solution if 100% of the fluoride were converted to the ionization salt product. There is also only one proton dissociating from HF, so unless the fluoride is in the form of fluorosilicic acid, H<sub>2</sub>SiF<sub>6</sub>, and not HF, we would not have expected any type of time delay as seen with phosphoric acid. However, the fact that we did see this delay suggest that the conversion of fluoride is

controlled by the reaction kinetics of  $P_2O_5$ . What we mean by this is that the reaction of fluoride will only go to completion once the 2<sup>nd</sup> proton dissociation of phosphoric acid dominates the reaction. To verify this we would have to use a synthetic solution of hydrofluoric acid which again is beyond the scope of this study for safety reasons. Both experiments showed that > 98% conversion of fluoride is possible. This may have been even higher due to the lower detection limit readings of the analytic equipment.

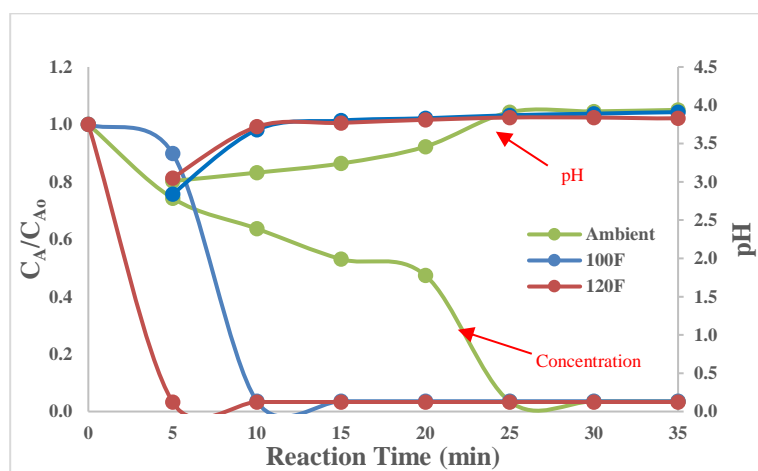


Figure 49 - Pond Water F Concentration & pH vs Time w/Limestone

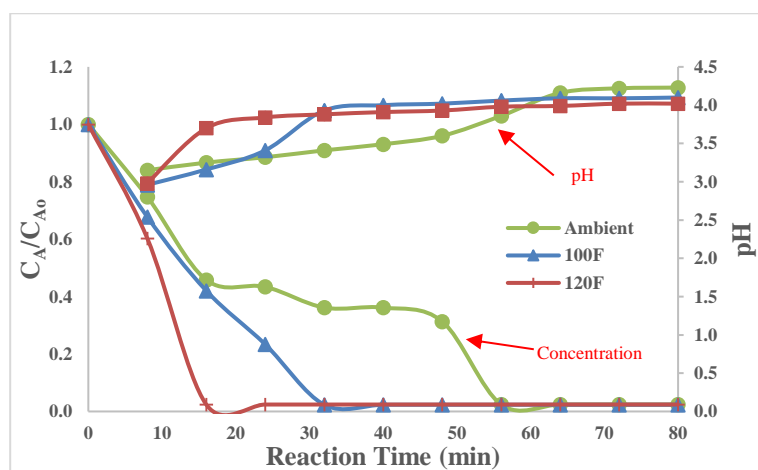


Figure 50 - Pond Water F Concentration & pH vs Time w/Ore

If the fluoride were present as fluorosilicic acid,  $H_2SiF_6$ , in solution then in water this converts to silicon dioxide and hydrofluoric as shown in equation 5.16. This may explain the

brief plateau of the reaction at lower temperatures before it went to completion. If the molar ratio of F:Si is 6:1 in solution then it is very likely that the fluoride is present in the form of fluorosilicic acid and not HF. Checking the pond water concentrations the ratio was 4:1 by weight which translates to a 6:1 molar ratio. Therefore it is very feasible that the assumption that fluoride was solely in the form of HF was incorrect. It is recommended that additional concentration vs time data be generated using synthetic solutions of fluorosilicic acid reacted with limestone and phosphate ore to verify this hypothesis.



It is also important to note that change in particle size distribution before and after the reaction was negligible as shown in Figures 51 and 52. This validates the assumption that diffusion through the ash layer was not a rate limiting step.

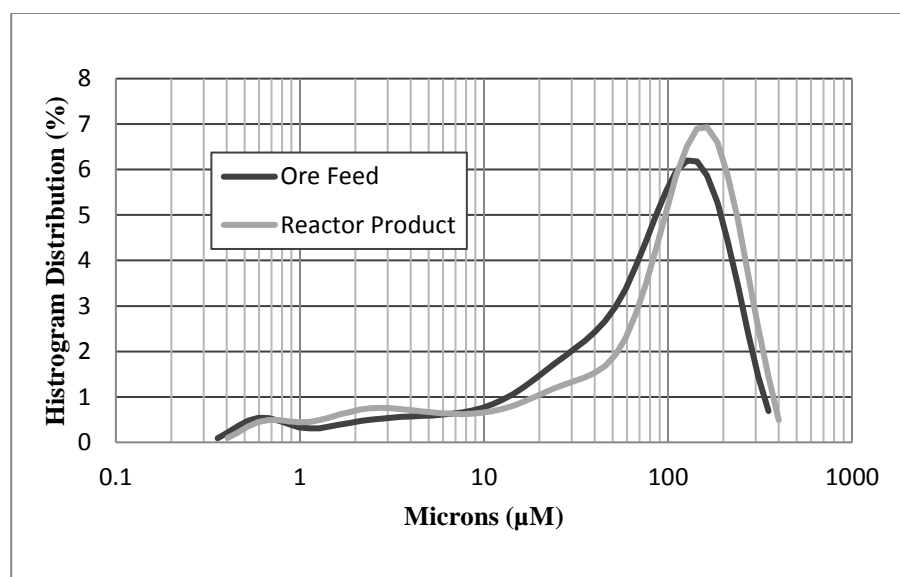


Figure 51 - Pre/Post Reaction Histogram PSD

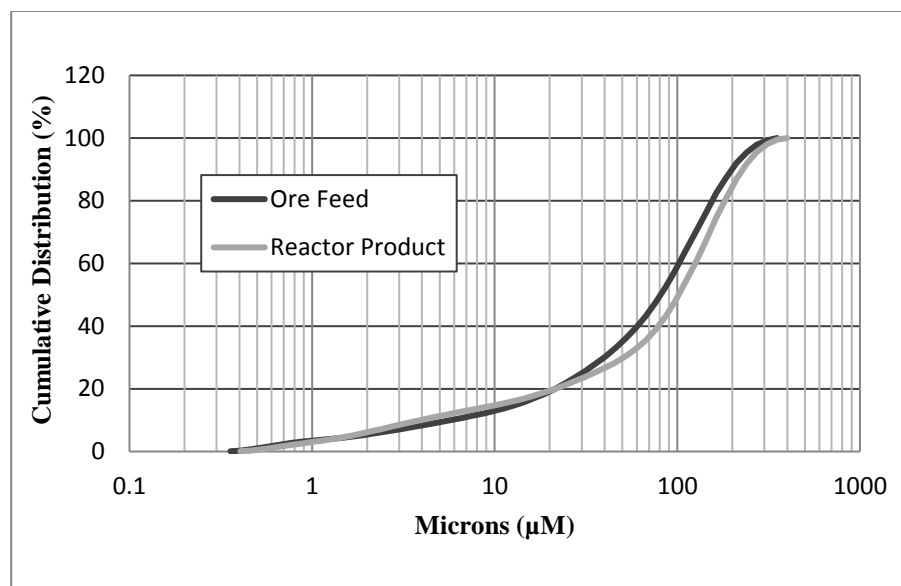


Figure 52 - Pre/Post Reaction Cumulative PSD

## REACTOR DESIGN CONSIDERATION

If we recall from chapter 1 that the pond water analysis is approximately 1.5%  $P_2O_5$ , 0.4%  $SO_4$  and 0.8% F as shown in table 11, the constant volume batch reactor data can be used to predict final liquid phase analysis. At the worst case temperature scenario, ambient (75°F), a continuously stirred tank reactor (CSTR) would need be sized to accommodate a minimum of 1 hour residence time.

Table 11 - Predicted Liquid Phase Analysis for CSTR

Constituent	Pond Water Starting Analysis	Expected Conversion	Final Liquid Phase Analysis
$P_2O_5$	1.47%	40%	0.88%
F	0.83%	98%	0.02%
$SO_4$	0.44%	0%	0.44%
pH	< 2.0	-	4.0-5.0

## CONCLUSIONS

Aside from a delayed reaction due to impurities in the matrix, the excess carbonate in phosphate ore is equally effective as limestone at neutralizing pond water acidity. The concentration vs time data were useful in determining time required for each reaction to reach

completion, with the exception of  $\text{SO}_4$ , Arrhenius temperature dependence for  $\text{P}_2\text{O}_5$  and the percent conversion of soluble reactants to their corresponding insolubility salts for  $\text{P}_2\text{O}_5$ ,  $\text{SO}_4$  and F. Monitoring liquid phase concentrations alone was reliable for some species, but overall proved to be a challenging technique for generating an accurate kinetic model for all liquid reactants. Because of interference from competing side reactions and/or false indications from unexpected reaction intermediates and high solubility of reaction ionization salt products further refinement is required in the measurement of liquid phase concentrations. pH analysis is also a useful tool for checking the extent of reaction and the state of reaction intermediates but can prove challenging due to inconsistencies in pH measurement and the need for frequent calibration. Future work should avoid over simplification of the reaction mechanism, take a closer look at intermediate reactions and focus on refining the overall kinetic model. Ore slurry dewatering test results via hydro-cyclones and sedimentation will be discussed in Chapter 6.

## CHAPTER 6: DEWATERING RESULTS & DISCUSSION

Preliminary dewatering test work after pre-reaction and dilution of the ore slurry evaluated the use of hydro-cyclones in combination with gravity thickening. In this processing step, pre-reaction product slurry at approximately 25-35 wt% solids is first sent through a hydro-cyclone followed by gravity thickening of the fine particle size fraction containing overflow. The underflow from the thickener is then blended with the coarse underflow from the hydro-cyclone and sent on for further processing in PAP.

### HYDRO-CYCLONE TEST WORK

The original test matrix was quickly modified from that discussed in chapter 4 to focus on feed concentrations within the 25 to 35% range due to unacceptable performance above or below that solids window. Target performance was a minimum of 68% solids concentration by weight in the underflow and 80% solids recovery. Recoveries were well above 80% for feed containing less than 25% solids, but the solids concentration in the underflow dropped below 60%. Above 35% solids in the feed the recoveries dropped below 70%, but the solids concentration was well above 68%. By varying feed pressure it was possible to generate multiple performance curves within the 25 to 35% feed solids range and evaluate the total underflow solids concentration and underflow solids recovery. Figure 53 shows the solids recovery performance curve, which indicates how much of the total solids in the feed reports to the underflow of the cyclone based on feed pressure and feed concentration. The curve was generated by plotting solids recovery test data at constant pressures and describes how solids recovery drops as feed concentration increases and feed pressure decreases. Here we are focused on finding the minimum feed pressure and highest feed solids concentration that will maximize underflow solids recovery and concentration. Excessive pressure requires greater pump energy and low solids results in over dilution or the requirement for greater dewatering capacity. Figure 54 is the underflow solids performance curve which indicates how feed pressure and feed solids impact the concentration of the underflow. This curve was also generated by plotting solids recovery test data at constant pressures and describes how underflow solids concentration increases by increasing feed concentration and pressure.

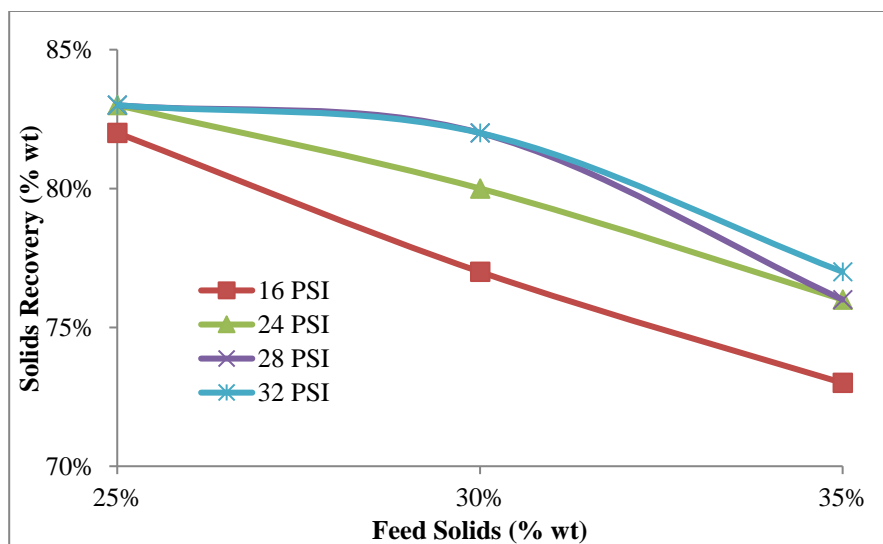


Figure 53 - Krebs Hydro-Cyclone Underflow Solids Recovery Performance

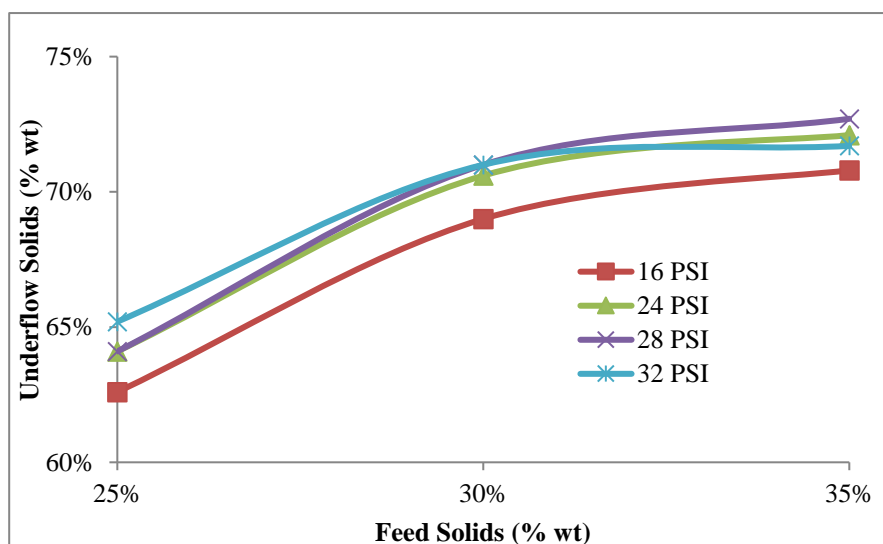


Figure 54 - Krebs Hydro-Cyclone Underflow Solids Performance

Using the performance curve information from figures 53 and 54 it was determined that the optimum cyclone performance was achieved with 30% feed solids and a feed pressure of 28 psi using a Krebs urethane gMax 4" hydro-cyclone. Under these conditions >80% solids recovery and >68% solids concentration in the underflow was achieved. The combined performance curve at 28 psig feed pressure is shown in figure 55 where the dashed lines represent the desired performance objective for solids recovery and underflow concentration, respectively.

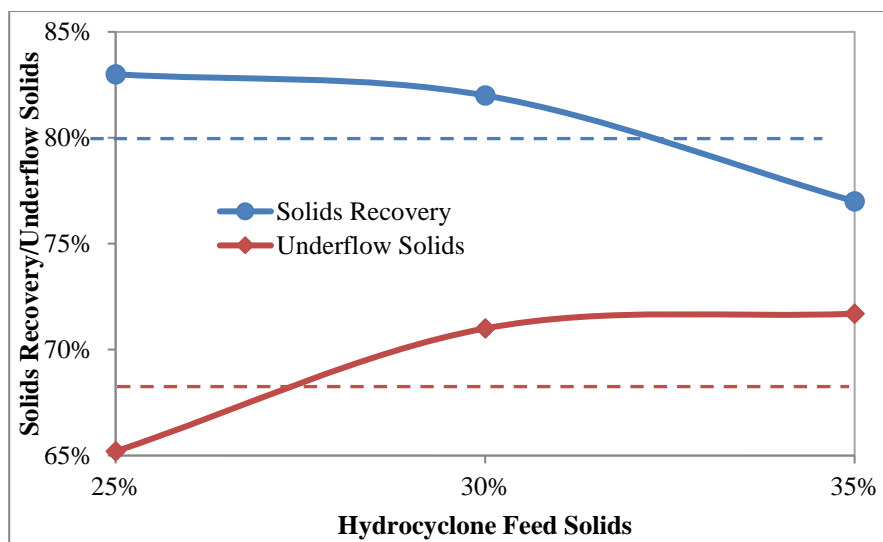


Figure 55 - Krebs Hydro-Cyclone Performance Curves @ 28 PSIG

A second 4" urethane hydro-cyclone from Derrick Corporation was also evaluated early on in testing but quickly abandoned due to poor performance across all test parameters. Figure 56 is a cutaway schematic showing the primary components of a typical hydro-cyclone. Here the ratio of the apex diameter to vortex finder diameter is an important component of correctly sizing and/or selecting a hydro-cyclone. For the Derrick cyclone the apex to vortex finder ratio was too small for the solid particle size distribution (PSD) resulting in a phenomena called roping.

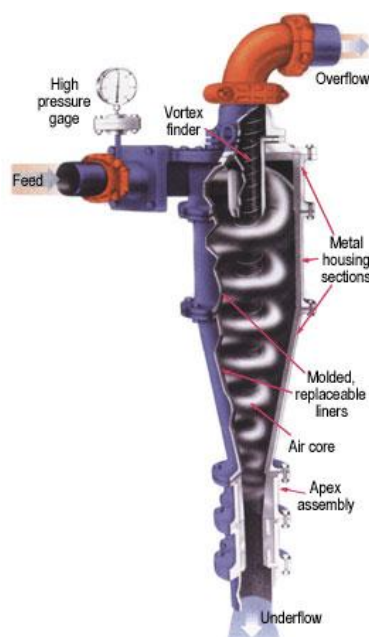


Figure 56 - Krebs Hydro-Cyclone Cut Away (Arterburn, 1982)

Underflow slurry is supposed to fan or spray out of the bottom of the cyclone but if the apex is incorrectly sized a phenomena called roping occurs as shown in figure 57. If the apex is too small for a given slurry PSD it becomes overloaded which can significantly reduce solids recovery in the underflow, increase wear on internal components and even lead to plugging of the apex. Derrick did not have the option to increase apex diameter so testing with the cyclone was abandoned early on.

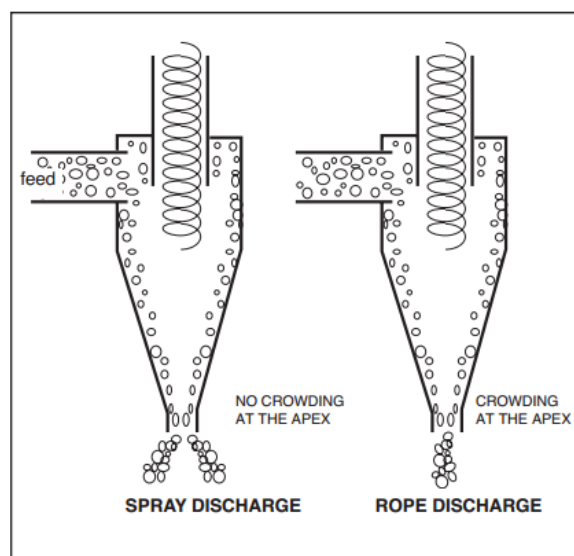


Figure 57 - Hydro-Cyclone Spray vs Rope Discharge (*GN Solids Control, 2016*)

#### HYDRO-CYCLONE OVERFLOW SEDIMENTATION TEST WORK

Using ore slurry generated from the optimal hydro-cyclone performance testing discussed in the previous section a series of settling test were conducted with the overflow material. Table 12 shows the initial slurry characteristics of the cyclone overflow including the PSD which is described by the D20, D50 and D80% values. D50 is considered the median particle size value by volume, therefore 50% of the particles have a diameter above this value and 50% below. The D20 and D80 values can be described in a similar manner. 20% of the particles by volume fall below the D20 diameter value and 20% fall above the D80 value.

Table 12 - Cyclone Overflow Slurry Characteristics

pH	TSS, wt%	D20%	D50%	D80%
7.0	8.5	1.5 $\mu\text{m}$	3.9 $\mu\text{m}$	11.4 $\mu\text{m}$

Figure 58 is a graphical depiction of the particle size distribution. The cumulative distribution or the percentage by volume (0-100%) under a given diameter is shown on the primary axis. The histogram distribution or instantaneous volume percentage at a given particle size is shown on the secondary axis.

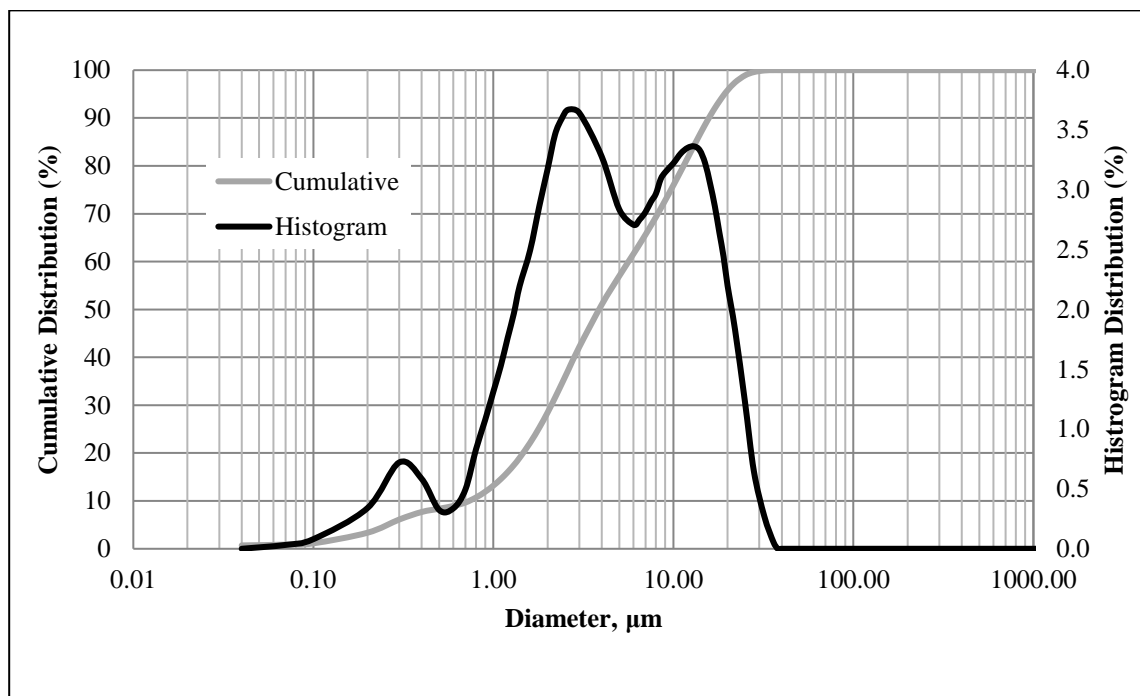


Figure 58 - Hydro-Cyclone Overflow Particle Size Distribution

Table 13 shows the impact of varying flocculent type on supernatant quality after a 24 hour settling period. For these tests the slurry was used ‘as is’ from the hydro-cyclone without any feed dilution. For each test a 1% neat/liquid flocculent solution by weight was made up from dry flocculent and then each slurry sample was dosed with a ratio of 1:1,000 by volume of neat floc solution to slurry. For the final test with anionic and cationic floc the slurry had a combined dose ratio of 2:1,000.

Table 13 - Settling Test Supernatant Water Quality

Test Variable	TSS (g/L)	TDS (g/L)	TS (g/L)	NTU's
No Flocculent	0.16	2.8	3.0	46.1
Anionic	0.08	2.9	3.0	37.2
Cationic	0.00	3.0	3.0	5.0
Anionic & Cationic	0.02	1.9	2.0	4.9

Table 14 shows the final bed compaction height from a starting 500 mL cylinder and the weight percent solids of the bed after a 24 hour period.

Table 14 - Final Bed Compaction and Weight % Solids

Test Variable	Bed Compaction (mL)	Percent Solids
No Flocculent	230	19
Anionic	225	20
Cationic	255	18
Anionic & Cationic	190	24

Figure 59 and 60 show the NTU's of the supernatant and solid-liquid interface as a function of time. It is clear that the cationic floc had very clear supernatant, but very poor settling rate. The opposite was true for the anionic floc. However, by combining the anionic and cationic flocculent the benefits of both were seen with increased settling rate and clear supernatant. The combination of flocculent also improved the solid bed compaction as shown in Table 14. Figures 61 through 68 show pictures of the various settling tests at intermediate time intervals and at final bed compaction after 24 hours of settling time.

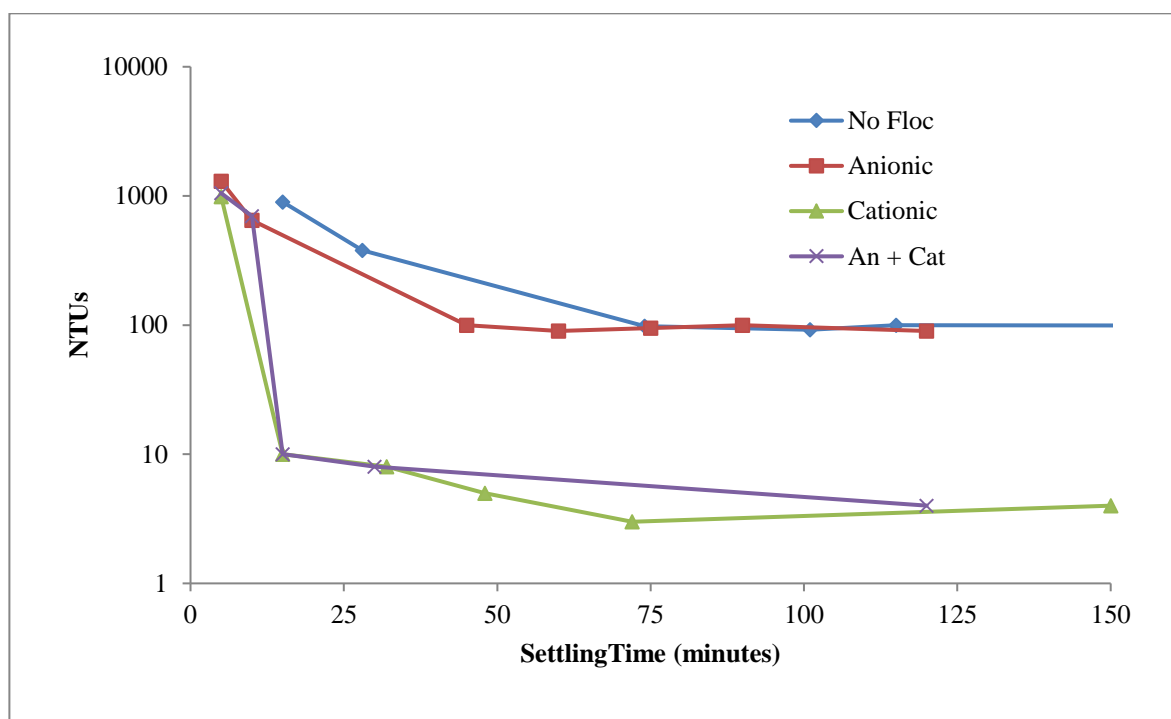


Figure 59 - Settling Test Supernatant NTU's

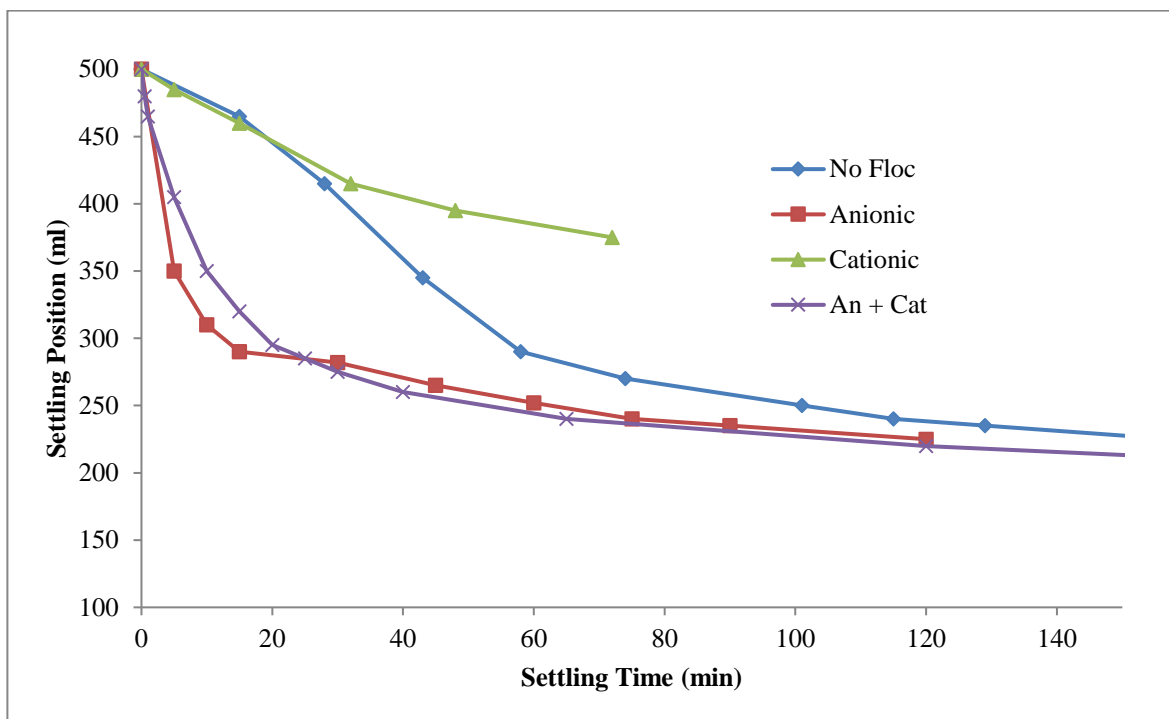


Figure 60 - Settling Test Solid-Liquid Interface Position



Figure 61 - No Floc @ 60 min

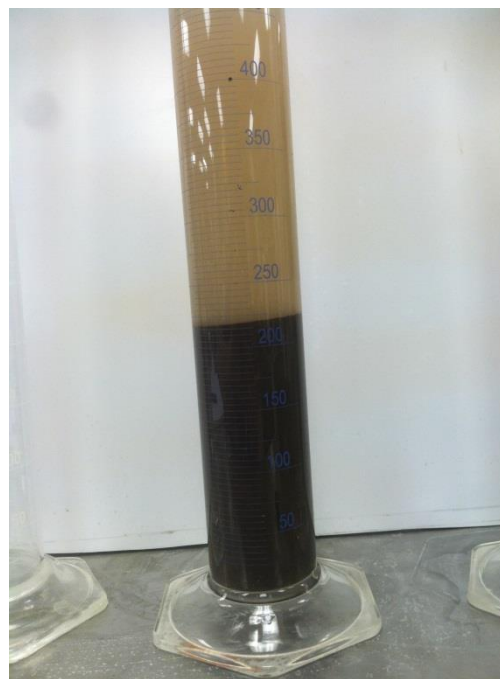


Figure 62 - No Floc @ 24 hrs



Figure 63 - Anionic @ 60 min



Figure 64 - Anionic @ 24 hrs



Figure 65 - Cationic @ 75 min



Figure 66 - Cationic @ 24 hrs

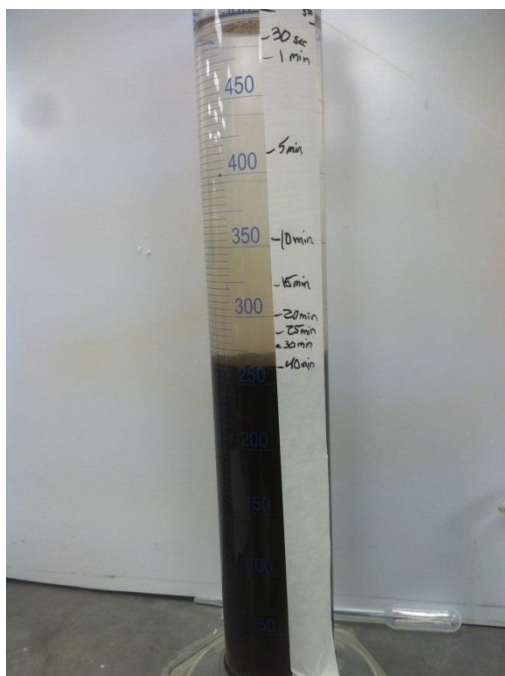


Figure 67 - An &amp; Cat @ 40 min

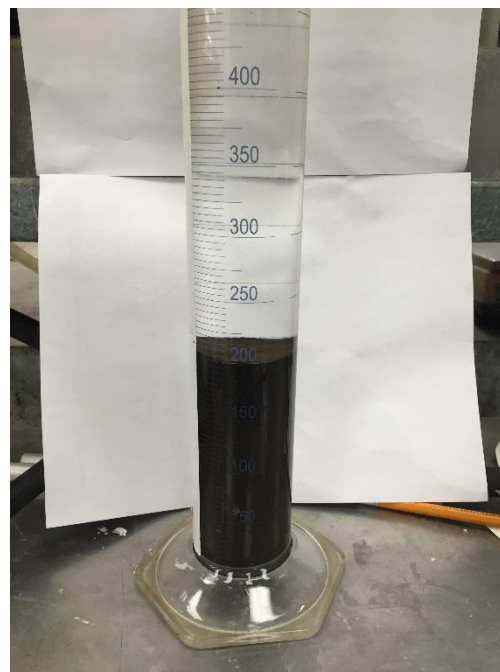


Figure 68 - An &amp; Cat @ 24 hrs

Achieving tight bed compaction in a gravity thickener is an important component of maintaining a high underflow solids concentration. Based on a hydro-cyclone performance of 72% solids in the underflow and 81% solids recovery this would require that the thickener maintain 53.5% solids at a minimum in order to achieve 68% solids when blending the thickener underflow back with the cyclone underflow. 68% is the minimum acceptable solids concentration of ore slurry for PAP feed. Therefore 24% solids in the thickener underflow is not high enough to be blended back with the hydro-cyclone underflow, additional means of dewatering and/or bed compaction are required.

#### THICKENER FEED DILUTION

For all slurries there is a narrow solids concentration range that provides the maximum solids settling flux. Concentrated feed slurries flocculate more efficiently when diluted to a lower solids concentration. A thickener operating within this concentration range will provide the maximum possible solids capacity and underflow concentration. This dilution can be accomplished internal to the thickener. Once the optimum floc concentration was found with a combination of cationic and anionic floc, flux settling tests were conducted at fixed polymer dosage over a range of solids concentrations. For each test a measured volume of the original

sample slurry was added to a 250 mL graduated cylinder and the appropriate amount of polymer was added to the cylinder and inverted several times, thus insuring a thorough mixing of polymer and solids. Interface settling data were taken so that the initial straight line settling rate (m/h) could be measured. Flux rate ( $\text{kg}/\text{m}^2\text{-h}$ ) was then calculated for each test by multiplying the suspended solids concentration ( $\text{kg}/\text{m}^3$ ) by the settling rate (m/h). Figure 69 shows the resulting flux rates as a function of slurry concentration and polymer dosage.

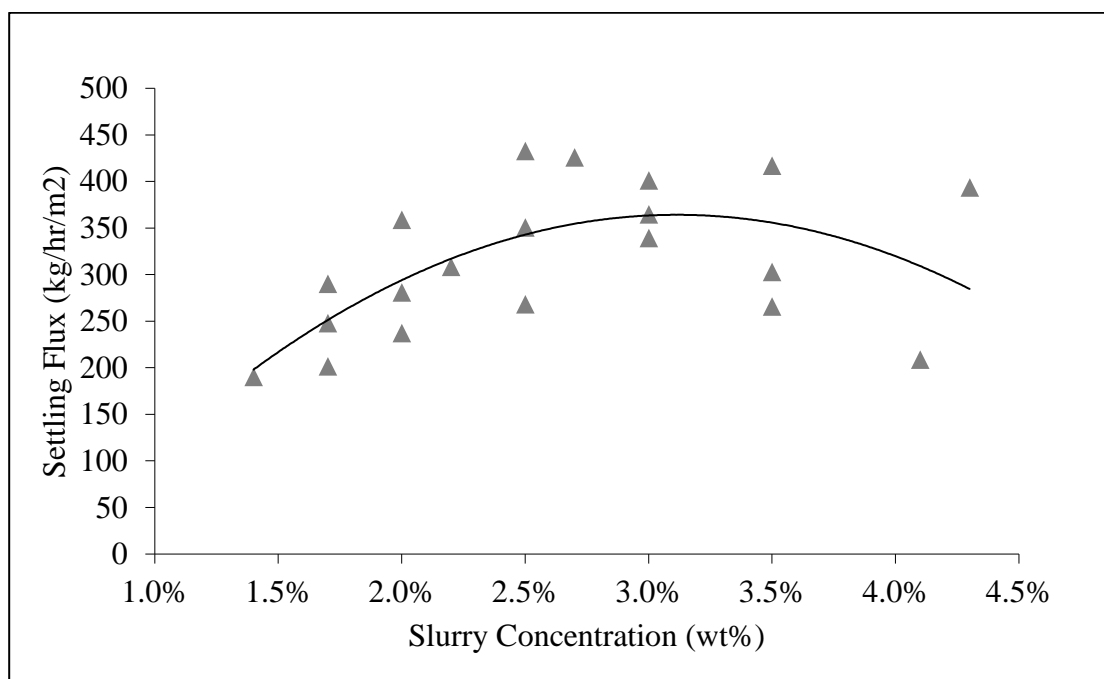


Figure 69 - Flux Settling Curve

As illustrated in Figure 69, the curves peaked at a solids concentration range of approximately 2 to 3.5 wt%. Given equal performance, less dilution is preferred to greater dilution. As such, a dilution of ~ 3% by weight should be targeted as part of the center well design in order to achieve maximum solids settling. Table 15 is a summary of the feed dilution test results and the design factors for rise rate and unit area.

Table 15 - Settling Test Results with Feed Dilution &amp; Polymer

Test #	1	2	3	4	5
Initial Feed Concentration – wt%	8.5	8.5	8.5	8.5	8.5
Diluted Feed Solids Concentration – wt%	3	3	3	–	–
Polymer Dose – lbs/ton	0.3	0.5	0.7	0.7	0.5
Supernatant TSS – mg/L	300	317	248	–	–
Rise Rate:					
Observed Settling Rate – gpm/ft <sup>2</sup>	1.8	4.3	7.2	–	–
Design Rise Rate – gpm/ft <sup>2</sup>	0.9	2.1	3.6	–	–
Unit Area:					
Design Unit Area – ft <sup>2</sup> /stpd	–	–	–	2.5	2.4
At UF Conc. – wt. %	–	–	–	33.6	35.1

## SETTLING SYSTEM DESIGN

Assuming a plant processes 5,000 TPD of dry ore through the pipeline and 80% of this is recovered in the cyclone underflow then 1,000 TPD of dry ore in the cyclone overflow would be fed to a thickener. This would require ~2,500 ft<sup>2</sup> of settling area which equates to a 28 ft diameter thickener. Also note here that tighter bed compaction was achieved than in the initial sedimentation tests which resulted in a solids concentration of ~33-35% in the underflow. This is much better than 24% but still not high enough to meet PAP feed requirements. When combining 35% slurry back with cyclone underflow this only reaches a combined concentration of 60% solids, which is unacceptable for PAP feed, again this needs to be 53.5% minimum to get 68% solids combined. Therefore an additional dewatering step is required which will be discussed later in chapter 7 of this study. However, for pilot testing discussed in chapter 7 this same setup of a hydro-cyclone in combination with gravity thickening was utilized knowing full well that an additional dewatering step would be required.

Using information from bench scale batch reaction data in chapter 5 and dewatering test work presented in this chapter, additional lab and plant pilot testing was conducted by combining the two steps into one continuous process. Results from those test will be presented in Chapter 7.

## CHAPTER 7: PILOT TESTING RESULTS & DISCUSSION

Upon completion of batch scale reaction and dewatering/sedimentation testing, viability testing of a continuous process was required. Pilot testing was carried out in two phases: 1) lab scale pilot and 2) plant scale pilot. Both processes had a similar flowsheet, shown in Figure 70, which consisted of a CSTR to pre-react the phosphate ore with gyp stack pond water and then a hydro-cyclone and gravity thickener for dewatering as discussed in chapter 4. The primary difference between the two systems was throughput, nominal design capacities which correspond with Figure 70 are outlined in Table 16 for each system. Some additional dewatering methods were also piloted which included screens and a decanter centrifuge.

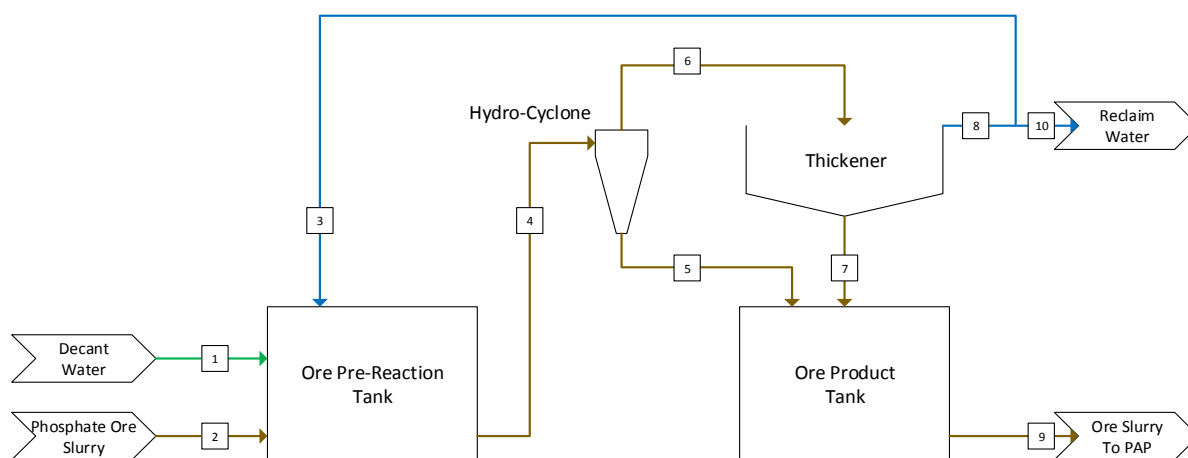


Figure 70 - Ore Pre-Reaction Pilot Flowsheet

Table 16 - Pilot Testing Nominal Design Capacities

Description	units	Pond	Phos	Dilution	Hydro-	Cyclone	Cyclone	Thickener	Thickener	Thickened	Reclaim
		Water	Ore	Water	Cyclone	Unders	Overs	Unders	Overs	Ore	Water
		Flow	Slurry Flow	Flow	Feed Flow	Flow	Flow	Flow	Flow	Flow	Flow
		1	2	3	4	5	6	7	8	9	10
Lab Pilot	gpm	0.07	0.05	0.03	0.15	0.03	0.11	0.01	0.10	0.04	0.07
	lbs/hr	33	43	15	91	31	60	9	51	40	36
Plant Pilot	gpm	1.7	1.4	0.8	3.8	0.9	2.9	0.3	2.7	1.1	1.9
	lbs/hr	858	1,118	390	2,366	806	1,560	234	1,326	1,040	936

## LAB PILOT

Based on previous hydro-cyclone and ore pre-reaction test work carried out separately, the two processes were combined to develop and test a continuous lab pilot ore pre-reaction and dewatering system. The benefits of the pre-reaction process were achieved through the removal of P<sub>2</sub>O<sub>5</sub>, Fluoride (F) and Sulfate (SO<sub>4</sub>) from the gyp stack pond water as shown in Table 17. Mass balance quantities were determined based on the nominal lab pilot feed rate of 33 lbs/hr of pond water.

Table 17 - Lab Pilot Feed/Product Analysis and Mass Balance

Description	P <sub>2</sub> O <sub>5</sub>	F	SO <sub>4</sub>	pH
<b>Pond Water Feed</b>				
Analysis (wt%, pH)	1.47%	0.83%	0.44%	1.5
Mass Balance (lbs/hr)	0.49	0.63	0.22	
<b>Thickener Overflow Effluent</b>				
Analysis (wt%, pH)	0.08%	<0.01%	0.15%	5.5
Mass Balance (lbs/hr)	0.03	0.00	0.05	
Recovery	5%	<1%	22%	
<b>Balance to Phos Ore Slurry</b>				
Mass Balance (lbs/hr)	0.46	0.63	0.17	
Recovery	95%	>99%	78%	

This translates to an improvement in overall P<sub>2</sub>O<sub>5</sub> recovery, fluoride removal and sulfate removal from the liquid phase. A complete breakdown of the stream analysis is shown in Table 18. Interestingly the liquid phase concentrations were much lower than what was achieved in bench scale testing even though treated at the same equivalent ratio of 1,000 gpm of pond water to 5,000 TPD of dry ore. This could have been explained by the high degree of recirculation and mixing which occurred during both phase of pilot testing.

Table 18 - Continuous Lab Pilot Stream Analysis

Sample Description	P <sub>2</sub> O <sub>5</sub>	F	SO <sub>4</sub>	Ca
<b>Pond Water Feed</b>				
Average	1.47%	0.83%	0.44%	0.18%
±Stdev	0.05%	0.01%	0.01%	0.01%
<b>Phosphate Ore Feed</b>				
Average	27.83%	2.92%	2.74%	30.32%
±Stdev	0.36%	0.02%	0.02%	0.32%
<b>Pre-Reacted Ore</b>				
Average	27.52%	3.52%	2.90%	29.41%
±Stdev	0.30%	0.07%	0.04%	0.17%
<b>Cyclone Underflow</b>				
Average	29.55%	3.20%	2.76%	31.27%
±Stdev	0.15%	0.06%	0.04%	0.24%
<b>Cyclone Overflow</b>				
Average	24.47%	4.56%	3.12%	26.77%
±Stdev	0.06%	0.28%	0.15%	0.14%
<b>Thickener Underflow</b>				
Average	24.83%	4.40%	2.91%	27.01%
±Stdev	0.15%	0.21%	0.09%	0.11%
<b>Thickener Overflow</b>				
Average	0.08%	<0.01%	0.15%	0.05%
±Stdev	0.01%	-	0.01%	0.01%

Because some of the equipment was oversized, specifically the hydro-cyclone, a large degree of recirculation was required. For both the lab and plant pilot systems a 4" hydro-cyclone was used which required a nominal feed rate of 80-90 gpm. However, both the lab and plant pilot throughput was only a small fraction of this rate as shown previously in Table 16. Scale down was not an option for the hydro-cyclone so recirculation of a large portion of the underflow and overflow back to the reactor was required in order to maintain system balance. The large amount of recirculation and agitation could have potentially eliminated any mass transfer limitations present during batch test work and increased the availability of the solid reactant, carbonate, present in the ore.

Table 19 results indicate that expected cyclone performance was also achieved. Although the thickener showed poor performance as shown in Table 20 and was only able to

increase the solids to 19% (>53.5% was desirable) the results were positive and consistent with initial sedimentation test work considering the design of the thickener.

Table 19 - Lab Pilot Cyclone Achieved Solids & Recoveries

Description	Flow	Solids		Recovery
	lbs/hr	wt %	lbs/hr	%
Hydro-cyclone Feed	91	31.0%	28.2	-
Underflow	29	72.0%	21.2	75%
Overflow	62	11.4%	7.1	25%

Table 20 - Lab Pilot Thickener Achieved Solids & Recoveries

Description	Flow	Solids		Recovery
	lbs/hr	wt %	lbs/hr	%
Thickener Feed	62	11.4%	7.1	-
Underflow	37	19.0%	7.1	100%
Overflow	24	0.0%	0.0	0%

The concern with this dewatering process was that the fine particles in the ore, which report to the cyclone overflow, would not settle in a thickener causing high total suspended solids (TSS) in the thickener overflow. However, with flocculent addition, this was not the case and effluent had good clarity (<30 NTUs) and low TSS (<200 ppm). The undesirable performance was more a result of an inadequately designed lab thickener.



Figure 71 - Lab Pilot Conical Thickener



Figure 72 - Plant Pilot Thickener Feed Well



Figure 73 - Plant Pilot Thickener Rake

The unit did not have a rake mechanism to steadily push solids to the cone discharge which made plugging an ongoing issue. The thickener used for lab testing is shown in Figure 71, the unit relied on a steep conical bottom and gravity to convey the solids to the discharge as opposed to a rake. Without a rake mechanism the solids bed does not compact as tightly which contributes to a decreased underflow solids content. The thickener also lacked any kind of feed dilution at the center well which reduced the settling flux rate of the solids. Both of these design flaws were accounted for and incorporated in the plant pilot thickener. The dilution feed well and rake mechanism are shown in Figure 72 and 73, respectively.

## PLANT PILOT

Because of some of the inherent issues with slurries and line plugging in small scale systems, scale up on the order of 26x was required to a plant pilot in order to achieve longer run time between process upsets and improve the reliability of the pre-reaction and dewatering test results. The plant pilot also incorporated an improved thickener design which included feed dilution at the center well along with a rake mechanism to help with bed compaction and transport of solids to the thickener discharge. Again, the same benefits were seen with the scaled up pilot as shown in Table 21. Mass balance quantities were determined based on the nominal lab pilot feed rate of 858 #/hr of pond water. A more detailed analysis of the process streams is also shown in Table 22.

Table 21 - Plant Pilot Process Feed and Product Water Analysis

Description	P <sub>2</sub> O <sub>5</sub>	F	SO <sub>4</sub>	pH
<b>Pond Water Feed</b>				
Analysis (wt%, pH)	1.32%	0.67%	0.44%	1.3
Mass Balance (lbs/hr)	11.33	5.75	3.78	
<b>Thickener Overflow Effluent</b>				
Analysis (wt%, pH)	0.19%	<0.01%	0.09%	4.6
Mass Balance (lbs/hr)	1.63	<0.09	0.77	
Recovery	14%	<1%	20%	
<b>Balance to Phos Ore Slurry</b>				
Mass Balance (lbs/hr)	9.70	>5.66	3.00	
Recovery	86%	>99%	80%	

Table 22 - Continuous Plant Pilot Stream Analysis

Sample Description	P <sub>2</sub> O <sub>5</sub>	F	SO <sub>4</sub>	Ca	CO <sub>2</sub>
<b>Pond Water Feed</b>					
Average	1.32%	0.67%	0.44%	0.12%	-
±Stdev	0.06%	0.01%	0.01%	0.00%	-
<b>Phosphate Ore Feed</b>					
Average	26.89%	2.50%	1.69%	29.48%	4.73%
±Stdev	0.54%	0.18%	0.01%	0.37%	0.13%
<b>Pre-Reacted Ore</b>					
Average	28.21%	2.95%	1.91%	29.61%	3.47%
±Stdev	0.49%	0.11%	0.05%	0.56%	0.14%
<b>Cyclone Underflow</b>					
Average	27.87%	2.76%	1.76%	30.55%	3.79%
±Stdev	0.51%	0.24%	0.06%	0.66%	0.33%
<b>Cyclone Overflow</b>					
Average	23.23%	4.07%	3.12%	25.37%	1.72%
±Stdev	0.58%	0.19%	0.13%	0.74%	0.22%
<b>Thickener Underflow</b>					
Average	21.81%	4.35%	2.00%	26.48%	2.00%
±Stdev	0.60%	0.58%	0.08%	0.68%	0.08%
<b>Thickener Overflow</b>					
Average	0.19%	<0.01%	0.09%	0.04%	-
±Stdev	0.02%	-	0.02%	0.01%	-

Table 23 results indicate that expected cyclone performance was also achieved with the larger pilot. The modified thickener did achieve much better performance than the lab system as shown in Table 24, but was still only able to increase the solids to 28% (>53.5% was desirable). Therefore additional means of dewatering was required.

Table 23 - Plant Pilot Cyclone Achieved Solids and Recoveries

Description	Flow	Solids		Recovery
	lbs/hr	wt %	lbs/hr	%
Hydro-cyclone Feed	2,366	31.0%	733.5	-
Underflow	846	72.0%	608.8	83%
Overflow	1,520	8.2%	124.7	17%

Table 24 - Plant Pilot Thickener Achieved Solids and Recoveries

Description	Flow	Solids		Recovery
	lbs/hr	wt %	lbs/hr	%
Thickener Feed	1,520	8.2%	124.7	-
Underflow	656	28.0%	124.7	100%
Overflow	864	0.0%	0.0	0%

## MISCELLANEOUS DEWATERING

From the results discussed in chapter 6 as well as lab and plant pilot testing it was found that hydro-cyclones in combination with gravity thickening alone were not enough to return the pre-reacted ore slurry back to a combined 68% solids. As a result there was additional interest in evaluating other means of dewatering that could either supplement hydro-cyclones and gravity thickening or act as a completely separate alternative.

## DEWATERING SCREENS

Testing was conducted using a Derrick 4' x 8' dual motor linear motion dewatering screen set on a fixed uphill bed angle of 5 degrees. The pilot test unit is shown on the following page in Figure 74 and 75. The screen is fixed with 3 interchangeable sections that can be changed out depending on performance. Ideally the first few panels are fixed with tighter mesh screens which allow a porous cake to form and then the last section is fixed with

a looser mesh to allow the cake to dewatering quickly before it is discharged off the end of the screen.



Figure 74 - Dewatering Screen Side View



Figure 75 - Dewatering Screen Solids Discharge

Two phases of testing were evaluated with the screens. The first was a direct replacement to the hydro-cyclones using reactor product slurry as feed at 31.5% solids. The second was a

supplement to the hydro-cyclones where underflow in the range of 59-72% solids was fed directly to the screens to further enhance dewatering. Table 25 shows the performance using pre-reacted ore slurry as direct feed. In the table the three number nomenclature indicates the panel micron size for the first, second and third interchangeable panel on the screen. In this case solids content off the end of the screen was very good at 75% + but the solids recovery was very poor. As a result this was considered an unacceptable alternative.

Table 25 - Reactor Product Dewatering Screen Performance

Test #	Panels ( $\mu\text{m}$ )	Slurry Feed (gpm)	Feed Solids (wt%)	Overs Solids (wt %)	Overs Recovery (wt %)
1	180-180-300	500	31.5%	75.2%	28.6%
2	100-100-180	150	31.5%	75.4%	51.5%
3	100-100-180	130	31.5%	77.1%	49.0%
4	100-100-180	125	31.5%	75.1%	52.7%

Table 26 shows the performance of the screens when fed with cyclone underflow. Test 6 and 9 showed the greatest enhancement in dewatering but the combined solids recovery (hydro-cyclone x screen) only resulted in 60-65% which was also viewed as unacceptable.

Table 26 - Hydro-Cyclone Underflow Dewatering Screen Performance

Test #	Panels ( $\mu\text{m}$ )	Slurry Feed (gpm)	Feed Solids (wt %)	Overs Solids (wt %)	Overs Recovery (wt %)
1	100-100-180	70	59.2%	73.3%	82.9%
2	300-300-300	130	59.2%	74.1%	54.2%
3	300-300-300	105	59.2%	76.3%	62.2%
4	300-300-300	115	64.5%	76.5%	43.4%
5	300-300-300	145	64.5%	76.5%	28.5%
6	300-300-300	120	70.0%	76.4%	80.6%
7	300-300-300	140	70.0%	75.8%	54.5%
8	300-300-300	135	72.0%	76.1%	67.0%
9	180-180-180	75	72.0%	77.9%	76.6%

## DECANTER CENTRIFUGE

The centrifuge was evaluated as a direct replacement to the hydro-cyclone and was conducted using a single Sharples 660 centrifuge with pre-reacted ore product slurry as feed.

Various conditions were evaluated while maintaining a constant bowl speed of 6,000 rpm. Table 27 is a summary of the test conditions and results. The data indicates that Test 5 produced the lowest moisture solids while maintaining the lowest solids content in the centrate or liquid fraction. This test was also conducted at the highest feed rate. Overall centrifuge dewatering performance was far superior to hydro-cyclones with over 99% + solids recovery. In combination with a clarifier the remaining suspended solids in the centrate could easily be recovered.

Table 27 - Decanter Centrifuge Dewatering Test Results

Test #	Conveyor RPM	Slurry Feed (gpm)	Feed Solids (wt %)	Centrate Solids (wt %)	Solids Moisture (wt %)
1	120	1.7	22%	0.81%	67%
2	80	1.7	32%	0.76%	85%
3	90	1.7	32%	0.76%	85%
4	90	2.1	29%	0.05%	85%
5	110	3.4	29%	0.09%	85%
6	120	3.4	29%	0.05%	83%

Another alternative may be to supplement the gravity thickening of the hydro-cyclone overflow using a decanter centrifuge in order to load relieve the thickener. However, this was not tested as part of this study and there is concern that this could unnecessarily increase the complexity of dewatering by having too much interdependency amongst equipment. Additional work is also need to understand the operating and maintenance costs associated with each process.

Chapter 8 is a summary of the ore pre-reaction and dewatering process results found in this study and recommendations for future work related to the understanding of reaction kinetics and phosphate ore slurry dewatering.

## CHAPTER 8: SUMMARY & CONCLUSIONS

### SUMMARY

In the manufacturing process of wet phosphoric acid there is a growing level of environmental scrutiny associated with phospho-gypsum byproduct stack management. As a result there is an increasing need to better understand best management practices and mitigate the risk associated with the handling of phospho-gypsum transport water and large pond water inventories.

This study evaluated the use of an alternative method to treatment – ore pre-reaction – where excess carbonate (i.e. limestone) in the phosphate ore was utilized to neutralize the acidity of pond water. This involved the non-catalytic heterogeneous solid-liquid reaction kinetics associated with carbonate in the ore and the acidic phosphate, fluoride and sulfate present in pond water. Because of the dilution from pond water addition, dewatering was also evaluated in order to understand process requirements associated with separating the treated effluent water and returning the ore slurry back to within an acceptable concentration range.

Literature review indicated that carbonate reduction in phosphate ore improves quality, process performance and reduces excess sulfuric acid consumption. It also indicated the importance of pond water management and emphasized that treatment of pond water is very costly. In addition, little information exists pertaining to phosphate ore dewatering even though it is common practice in industry to dewater phosphate ore slurry prior to acidulation. Therefore, dewatering test work was required to validate the proposed ore pre-reaction and dewatering process flowsheet.

Reaction kinetics and dewatering performance were evaluated through a series of bench scale, lab pilot and plant pilot testing. This involved generating numerous sets of concentration vs. time data from batch reactions as well as testing various dewatering equipment combinations including hydro-cyclones, dewatering screens, gravity thickening and centrifugation. Through pilot testing the continuous process flowsheet was checked for validity and used to identify gaps in preliminary process design.

## CONCLUSIONS & RECOMMENDATIONS FOR FUTURE WORK

Concentration – time data showed that the neutralization capability of excess carbonate in phosphate ore is likely hindered by impurities in the ore matrix due to lengthened reaction times, but is equally effective as limestone at neutralizing pond water acidity to the same degree. However, a better understanding of reaction intermediates is required. This holds true for both phosphoric acid,  $H_3PO_4$ , and sulfuric acid,  $H_2SO_4$ , whose intermediate and final salt products had varying degrees of solubility. As a result, the reliance on liquid phase concentrations alone proved to be challenging in terms of understanding the actual extent of reaction. That being said it was still possible to determine reactor size requirements to allow for adequate reaction time and determine expected conversion of acidic liquid phase constituents to their insoluble salts. The reaction kinetics between acidic process water and phosphate ore exhibited a combination of zero and first order dependence on the concentration of liquid phase reactant depending on the initial liquid phase concentration. By varying the reaction temperature it was also found that the reaction rate constant exhibited Arrhenius temperature dependence.

Dewatering test work proved that hydro-cyclones in combination with gravity thickening is a viable and cost effective option. However, additional work is required to optimize thickener performance and improve underflow solids concentration. This may include looking at deep bed or paste thickening to increase underflow solids concentration. Dewatering screens were inadequate as a result of the particle size distribution being below the effective range of the equipment, which suggests that vacuum filtration may be another more effective alternative to evaluate. The decanter centrifuge proved to be very effective at dewatering the overflow fines from the hydro-cyclone, however, these pieces of equipment can be very energy intensive and expensive to operate. It is suggested that this option be used only to supplement a small portion of the dewatering needs since a greater understanding of equipment longevity and full scale operating costs are required. A final dewatering equipment alternative that may be worth evaluating as future work is a filter press.

Overall the ore pre-reaction process is a promising alternative to traditional pond water treatment options as it can improve phosphate recovery, process performance and help to mitigate risks associated with phospho-gypsum handling and pond water management.

## REFERENCES

- Arterburn, R. A. (1982). The Sizing and Selection of Hydro-Cyclones. *Design and Installation of Communiton Circuits, 1*, 597-607.
- Becker, P. (1989). *Phosphates and Phosphoric Acid*. New York: Marcel Dekker, Inc.
- Cameron, J. E. (1994). Phosphoric Acid by Wet Process: Pond Water Management. In C. A. Hodge, & N. N. Popovici, *Pollution Control in Fertilizer Production* (pp. 225-236). New York: Marcel Dekker, Inc.
- Clifford, P. (2009). *Enhanced removal of Dolomite Pebble Concentrate by CO2 Generation*. Bartow: Florida Institute of Phosphate Research.
- EFMA. (2000). *Best Available Techniques for Pollution Prevention and Control in the European Fertilizer Industry*. Belgium.
- EPA. (2016, February 17). *Special Wastes: US Environmental Protection Agency*. Retrieved from US Environmental Protection Agency: <https://www.epa.gov/hw/special-wastes>
- GN Solids Control. (2016, June 6). *Hydrocyclone cut point for particle*. Retrieved from PRLOG: <https://www.prlog.org/12016620-hydrocyclone-cut-point-for-particle.html>
- Grenman, H., Tapio, S., & Murzin, D. (2011). Solid-liquid reaction kinetics - experimental aspects and model development. *Rev Chem Eng* 27, 53-77.
- Jardine, K. (2005). *Piney Point Pond Water Remediation Using Reverse Osmosis*. Bartow: The Mosaic Co. & Florida Institute of Phosphate Research.
- Levenspiel, O. (1999). *Chemical Reaction Engineer Third Edition*. New York: John Wiley & Sons.
- Mastersizer 3000: Malvern*. (2016, January 4). Retrieved from Malvern Instrument Website: <http://www.malvern.com/en/products/product-range/mastersizer-range/mastersizer-3000/>
- Masterton, W. L., & Hurley, C. N. (2009). *Chemistry: Principles and Reactions, 6th Edition*. Pacific Grove: Brooks, Cole.
- McFarlin, R. F. (1992). *Chemistry of Gypsum Systems*. Bartow: Tennessee Valley Authority & Florida Institute of Phosphate Research.

- Nielsson, F. T. (1987). *Manual of Fertilizer Processing*. Boca Raton: CRC Press.
- Olanipekun, E. (1999). Kinetics of Dissolution of Phosphorite in Acid Mixtures. *Chemical Society of Ethiopia*, 63-70.
- Partin, D. (2005). “*When Nameplate Is Not Enough*”—*Expanding Phos Acid*. Paris: ArrMaz Custom Chemicals.
- Pittman, W. (1983). *State-of-the-Art Phosphatic Clay Dewatering Technology and Disposal Techniques*. Bartow: Bureau of Mines & Florida Institute of Phosphate Research.
- Prayon. (2011). *Fundamentals of Weak Phosphoric Acid Production*. Belgium: Prayon Technologies S.A.
- Seidel, D. (1995). *Laboratory procedures for hydrometallurgical-processing and waste management experiments*. Pittsburg: U.S. Dept. of the Interior, Bureau of Mines.
- Siemens. (2009). *Treatment of Phosphate Fertilizer Plant Waste Water in Florida for Discharge and RE-use Purposes*. Jacksonville: Siemens Water Technologies Corp.
- Theys, T. (2003). *Influence of the rock impurities on the phosphoric acid process, products and some down stream uses*. Belgium: Prayon Technologies S.A.